Mode Locking and Mode Competition Phenomena in Lasers(Dissertation_全文)

AUTHOR(S):

Miyashita, Toyokatsu

MODE LOCKING AND MODE COMPETITION PHENOMENA IN LASERS

Toyokatsu Miyashita

MODE LOCKING AND MODE COMPETITION PHENOMENA IN LASERS

Toyokatsu Miyashita

February 1974

PREFACE

Lasers in general oscillate simultaneously in a large number of modes, since the optical wave length is extremly short compared with the resonator and the active medium. " Mode competition " denotes the competition among those modes for gain, and " mode locking " the phase locking of the beat notes produced from those modes. These two phenomena are, however, not always independent. An example of strong mode competition is a state in which every n-th mode oscillates and all the other modes are quenched. When the longitudinal modes are mode-locked, the amplitude, frequency, and phase of every mode become constant, and the total electric field makes a regular pulse train. Hence the mode locking is a necessary condition for various applications of multimode lasers in which the amplitude and phase of every oscillating mode are required to be constant or high peak power of optical pulses is required, for example, high-speed optical PCM communication system, holography, nonlinear optical effects, heating of plasma, and so on. Mode locking is also possible between the transverse modes. This transverse mode locking makes the transverse distribution of the total electric field vary periodically in time and space and the direction of the output beam sweep likewise. This is expected to be applied to an optical display. Mode locking is usually obtained by either of the following three methods: 1) a nonlinear property of the laser medium itself, 2) insertion of a saturable absorber into the resonator, and 3) internal loss- or phase-modulation. This thesis is limited to the mode competition and mode locking between the longitudinal modes caused by the two methods 1) and 3).

The phenomena investigated mainly in this thesis are " harmonic mode locking " and " mode-locked unidirectional traveling-wave oscillation." The former has much higher-speed mode-locked pulse trains than the conventional fundamental mode-locking. The laser with a very wide line width such as Nd:YAG laser is mode-locked by internal

modulation at a frequency which is several times as large as the fundamental cavity mode spacing. The latter has a more stable and much higher-peak pulse train than the conventional standing-wave oscillation. This is easily obtained by internal modulation in the gaseous ring lasers such as He-Ne laser. In contrast to the conventional mode locking, mode competition arises simultaneously in these two phenomena. In the former, mode competition occurs between mode groups each of which is composed of every n-th mode, and, in the latter, between the oppositely directed traveling-waves in a ring laser. This thesis investigates those phenomena in detail both theoretically and experimentally especilly in He-Ne lasers and demonstrates their possibilities, merits and demerits. The laser with a homogeneously broadened line is investigated only theoretically.

CONTENTS

CHAPTER 1

INTRODUCTION

The terms " mode competition " and " mode locking " are used naturally in the frequency domain. However, as far as periodic steady states are concerned, the representations of the oscillation in the frequency domain and in the time domain can be simply transformed to each other. Hence these phenomena may be investigated in either of the two domains. However the theories in the two domains have different merits and demerits, and then they have different quantitatively applicable scopes.

The analysis of the laser oscillation in the frequency domain requires an adequately small number of oscillating modes and weak oscillation intensity. There are almost no lasers except He-Ne laser that fulfil this requirement in the usual usage. Hence the frequency domain theory should be applied to lasers near threshold. He-Ne laser can be investigated almost satisfactory by this theory.

The analysis in the time domain generally requires the equation of motion of the laser action represented simply by the total macroscopic polarization, population inversion, and electric field. Hence its application is usually limited to the two-level atomic or molecular system with a homogeneously broadened spectral line. The obtained results, however, have been often applied to inhomogeneously broadened lasers.

This introductory chapter gives an explanation of the mechanism and a review of the study of the mode competition and mode locking phenomena viewed in both the frequency and time domains. The bidirectional traveling-wave laser is described in a separate section, since it has another unique characteristic.

1.1. Mode Locking and Mode Competition Phenomena Viewed in the Frequency and Time Domains

Lasers in general oscillate simultaneously in a number of modes. In the laser with an inhomogeneously broadened line, all the modes falling on the line may oscillate receiving gain independently from the laser medium. Although, by nature, only one mode can oscillate and saturate on a homogeneously broadened line, a number of modes which have different standing-wave patterns can oscillate simultaneously, since the spatial cross relaxation of the laser medium is usually very slow compared with any other relaxation. An instability of the laser action also causes multimode oscillation.

When a number of modes are oscillating, a large number of combination tones are generated near the modes through a nonlinear property of the laser medium. Through the interaction with these tones, the modes interact with each other. The interaction in energy is called mode competition and that in phase and frequency is mode locking. When the oscillating modes make free-running, the amplitude, frequency, and phase of each mode vary at random. When mode-locked, they become constant and the total electric field makes a sharp pulse train viewed in the time domain excluding the so-called FM locking.

Next let us consider about the mechanism of the mode locking. The laser medium has dispersion corresponding to its unsaturated gain curve. Due to this normal dispersion, the frequencies of the oscillating modes are pulled to the line center. Generally this dispersion is a nonlinear function of the frequency. Therefore the oscillating modes deviate from being equidistant. On the other hand, the nonlinear saturation of the laser medium makes amplitude and phase-dependent mode pushing. If the mode pushing can overcome the mode pulling, that is, if the nonlinear saturation is relatively strong compared with the unsaturated dispersion, the modes are able to become equidistant. This phenomenon is also explained from another

point of view as follows. The nonlinear saturation makes combination tones near the oscillating modes. The frequency differences between them come from the deviation of the modes from being equidistant due to the nonlinear frequency-dependence of the unsaturated dispersion. The relative amplitudes of the combination tones are larger as the nonlinear saturation is stronger. If the ratios of the relative amplitudes of the combination tones to the frequency differences are larger than a certain value, their frequencies are locked [82]. This phenomenon is called self-mode locking.

Even though the nonlinear saturation of the laser medium itself is weak, mode locking can be achieved with the aid of a saturable absorber or internal modulation. The strong nonlinear saturation of the absorber supplements the weak nonlinear saturation of the laser medium. The internal modulation makes side bands of each oscillating mode near other modes. The side bands play the same role as the combination tones. Hence a strong nonlinearity is generated equivalently.

For example, in ruby laser, the nonlinearity is adequate to lock the modes. In Nd:glass laser, the modes deviate substantially from being equidistant due to the large unsaturated dispersion and the nonlinearity is relatively weak. However a saturable absorber with a short radiative lifetime between the states in question has a strong tendency to lock the modes. In gas lasers such as He-Ne, Ar^+ and CO_2, the nonlinear terms are rather small and the modes deviate considerably from being equidistant. Therefore mode locking is achieved only under special favorable conditions.

The mode-locked states including mode competition may be classified into four groups. The first is the normal " 0-type " locking. The repetition rate of the pulse is equal to the fundamental mode spacing. The second may be called " quenched 0-type " locking. If, as a result of the competition between n mode groups each of which is composed of the every n-th mode, only a mode group can oscillate

being mode-locked, the total electric field makes a pulse train whose repetition rate is n times as large as the fundamental mode spacing. The third is called " π-type " locking. If the amplitudes and phases of the modes take such values that all the odd beat notes disappear, the repetition rate of the pulse become twice the frequency difference of the oscillating modes. The fourth may be called " quenched π-type " locking. The π-type locking may occur in the surviving mode group, then the frequency difference of the oscillating modes is n times as large as the fundamental mode spacing and the repetition rate of the pulse is $2n$ times as large.

Viewed in the time domain, the envelope and frequency of the total electric field is in a periodic steady state, when mode-locked. The mechanism of the mode locking viewed in this domain is identical with that of Cutler's regenerative pulse generator [82] in the radio-wave region. Its diagram is shown in Fig.1.1-1. A pulse is made sharp

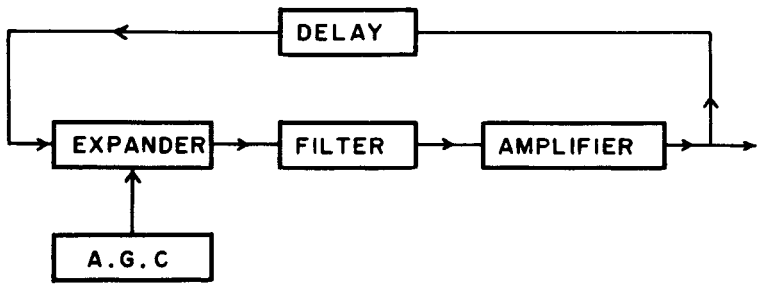

Fig.1.1-1. Block diagram showing the basic elements of the regenerative pulse generator circuit [82.b].

by the expander, broadened by the filter, and amplified without deformation by the amplifier. A.G.C. keeps one-loop gain unity. This cycle is repeated after the delay time required for one round trip along the resonator. If the two opposite effects of the expander and filter become in a stationary balanced state, the amplitude and frequency of the pulse become in a periodic steady state, *i.e.* mode locking is achieved. Various loop characteristics which might be inherent in the amplifier are represented as separate devices. An

intracavity modulator is an expander, and so is a saturable absorber.

1.2. Frequency Domain Theory (Coupled Mode Theory) of Normal Standing-Wave Lasers

As a basic concept for the mode competition " hole burning effect " was introduced by Bennett,Jr. [8] in 1962. According to his theory, a hole burns in the inhomogeneously broadened gain curve about each oscillating mode depending upon the oscillation intensity and the homogeneous broadening, if the homogeneous one is sufficiently narrow compared with the inhomogeneous one. Mode competition has been explained as a competition between the modes for gain due to the overlaps of the holes. The frequency pushing effect has been also explained from this effect.

Mode locking was achieved in 1964, for the first time, by Hargrove, Fork, and Pollack [27]. They applied the intracavity loss-modulation by an acousto-optic modulator to a He-Ne laser. Crowell made detailed experiments on the forced locking of He-Ne and Ar ion lasers [16]. He found also the condition for the self-mode locking. He has explained the mechanism of the mode locking by a coupled mode theory assuming the nonlinear property of the laser medium. Deutch obtained in 1965 a mode-locked pulse train from a ruby laser using the electro-optic (Pockel's) effect of KDP as an intracavity loss-modulator [57]. DiDomenico,Jr. and Yariv [32] have derived the following rather general results of the forced locking simply from coupled mode equations ignoring the nonlinear property and assuming a flat frequency characteristic of the laser medium: i) the form of an FM signal is obtained in the mode-locked state by intracavity reactive (phase) modulation, and ii) a pulse train is obtained by loss-modulation and the pulse length is approximately equal to the repetition period divided by the number of the oscillating modes.

The " theory of an optical maser " reported by Lamb,Jr. in 1964 [1] has given basic equations which can describe laser oscillations quantitatively. In his semiclassical theory, the electric field is described classically and expanded into the resonance modes of the resonator, and the laser medium is described quantum mechanically. The interaction between the laser medium and the electric field is described by a time-varying perturbation hamiltonian in the usual way. The quantum mechanical equation of motion is calculated by iterative method, and then the macroscopic polarization produced by the interaction is obtained. The obtained polarization is substituted into the source term of Maxwell's equations, and then the amplitude and phase determining basic equations are obtained. At high oscillation intensity, the number of modes and the order of the iterative calculation to be considered become large, then the basic equations become too complicated to be solved, which is a demerit of the theory. Usually the third order approximation of the iteration has been used, and, for He-Ne laser, this approximation gives fairly satisfactory results. In the paper, he solved graphically mode competition in the two-mode operation and also gave the condition for self-mode locking in the three-mode operation from the phase determining equations.

Based on Lamb's theory, various investigations have been made. McFarlane [9] calculated the frequency pushing and pulling effect in the two-mode operation and found the results to be in good agreement with the experimental results on a He-Ne laser. Fork and Pollack [10] made a detailed experiment of the mode competition effect in the two-mode operation of a He-Ne laser. Fitting the results to the theoretical ones, he decided the values of the relaxation constants including the collision effects. Fukui, Miyashita, and Ikenoue [12] investigated the mode competition analytically in the three- and four-mode operations, and obtained the result that the mode competition becomes stronger and the alternate modes become quenched

as the excitation becomes lower and the mode spacing narrower.

Uchida and Ueki [13] made a detailed experiment in a He-Ne laser and found the dependence of the self-locking on the excitation and cavity length. In their experiment, mode locked oscillation of the every adjacent mode, of the alternate modes, or of the every third mode was occured, as the excitation became lower and cavity length longer. With this result quanlitatively agrees the theoretical result by Fukui *et al.* [12]. Using modified Michelson-type resonator as a mode selector, Hirano and Kimura [34] obtained mode-locked pulse trains whose repetition rate is six times as large as the fundamental mode spacing (= 100MHz).

Investigations on the π-type locking were made for the first time by Statz and Tang [67]. They have given a method to decide the phases of the modes in a mode-locked state, appling the " maximum emission principle " to the phase-dependent combination tone terms of the coupled mode equations. They also confirmed the obtained results to agree with the experiment on a ruby laser. The condition for the π-type locking has been also given approximately from Lamb's equations by Sargent III [21] as well as by Bambini and Burlamacchi [22]. Miyashita, Mori, and Ikenoue [2] calculated the exact solutions of Lamb's equation numerically, which agree with the experimental results [23, 47].

A theory of the forced locking by intracavity loss- or phase-modulation has been developed by Harris and McDuff [33]. It includes the nonlinear saturation of the laser medium given in Lamb's theory and gives very exact solutions to this problem. Their results agree qualitatively with those of the simple theory by DiDomenico,Jr. and Yariv [32]. However it was derived that two kinds of mode locking occur by phase-modulation. About the central frequency of the mode-locked region, AM locking which has a pulse train occurs and, on the both sides of the region, FM locking which has the form of an FM signal occurs. On the boundaries of these two types of locking,

oscillation is quenched for high modulation indices. Ammann *et al.* [28] made a detailed experiment of the mode locking by phase-modulation on a He-Ne laser and confirmed that the theoretical results by Harris and McDuff agrees well with the experiment quantitatively. Although the AM locking by phase-modulation is of the same kind as that by loss-modulation, the relative phase of the obtained pulse train to the modulation signal takes either of the two values depending upon the initial condition or external turbulence. In some cases, this phase jump of π radian is controllable by the modulation frequency [30,31].

The " harmonic mode locking " by internal modulation has a practical utility, for a pulse train obtained by this mode locking has a high repetition rate. Hirano and Kimura [34] made internal phase-modulation of a He-Ne laser at frequencies which are three, four, and five times as large as the fundamental mode spacing, and obtained pulse trains of high repetition rate. Miyashita *et al.* [35] investigated in detail the second harmonic locking of a He-Ne laser by internal loss-modulation, and confirmed the following result experimentally as well as theoretically. About the central frequency of the locking region, fundamental mode locking occurs, and, on the lower frequency side or both sides, the repetition rate of the obtained pulse train is equal to the modulation frequency, *i.e.* twice the fundamental mode spacing.

1.3. Time Domain Theory of Unidirectional Ring Lasers

The time domain theory prefers dealing with the differential equations for the laser medium and Maxwell's equations described by the total electric field, total macroscopic polarization and total population inversion. Quantities which appears in the differential equations for the medium with an inhomogeneously broadened line are

functions of the parameter which describes the inhomogeneity. Hence the inhomogeneous laser is practically impossible to be treated by the time domain theory. The following review is all for homogeneous lasers. However those results have been applied to some inhomogeneous lasers.

In the most simple time domain theory, the so-called rate equation is solved on the assumption of π-pulse. Smith and Fox [19] obtained a relation between the intensity and the pulse width on this assumption, and confirmed that the relation agrees asymptotically at high excitation with the experimental results of a self-locked He-Ne laser. Smith [18] derived the condition for the multipulse oscillation which may be called self-harmonic mode locking and confirmed it in a He-Ne laser.

Tang and Statz [69], and Risken and Nummedal [70] solved the so-called matter equation for a two-level system and Maxwell's equation along the propagation of the electric field, and obtained as periodical steady state solutions mode-locked pulse trains including multipulse oscillation. Since one must solve differential equations numerically with a computer, their method requires that all the relaxations involved in the equations are fast enough for the calculation to arrive near a steady state in a short time enough for a computer. The longitudinal relaxation time T_1 is required not to be too long compared with the transverse relaxation time T_2 and with the one-round time T of the ring resonator. An application of this method to the forced locking with internal loss-modulation has been made by Cho *et al.* [78]. They obtained the cavity length-dependence of the mode-locked state restricting to the zero detuning. The detuning characteristics were obtained by Miyashita *et al.* [79] with a contrivance in the numerical calculation.

When $T_2 \ll T \ll T_1$, the laser medium is described by a Fourier transformed transmission function. It's gain is a saturable function of the oscillation intensity averaged over a time which is short compared with T_1 but long with T. Assuming that the spectral width of

the mode-locked pulse is sufficiently narrow compared with that of the gain curve and that the pulse shape and the gain function of the laser medium are all Gaussian, Kuizenga and Siegman [75] obtained analytically various locking characteristics for internal phase-modulation as well as for loss-modulation. The form of their results has a generality for application because of their analytical expressions, hence their results have been frequently applied especially to Nd:YAG or Nd:glass lasers.

1.4. Bidirectional Traveling-Wave Ring Lasers

The ring laser has been developed as a rotation rate sensor, and many areas of study have been made for its application [37]. The rotation sensing depends upon a frequency separation of the oppositely traveling (OT) waves in a ring laser which is proportional to the rotation rate. At low rotation rates, since the frequency separation of the OT waves is very small, phase locking occurs between them even with very small backscattering at the intracavity optical surfaces. Thus low rotation rates cannot be measured. To circumvent the locking, there have been some attempts. The mechanism of the phase locking due to backscattering has been analyzed by Aronowitz, Collins, and de Lang [48].

One of the other difficulties in using the ring laser as a rotation rate sensor is the mirror mode competition effect. The OT modes located symmetrically against the gain curve interact with the same velocity component of the gas laser medium. Thus a slight asymmetry causes suppression or extinction of one of the OT waves in case of small frequency separation. To reduce this effect, the modes should be located far enough from the center of the gain curve. This mode competition effect has been analyzed by Aronowitz [38,40] and Hutchings *et al.* [39].

The above mentioned ring lasers are all of He-Ne and in the single longitudinal mode operation, in which one clockwise (cw) traveling mode and one counter-clockwise (ccw) traveling mode oscillate.

Buholz *et al.* [50,51] have made an alternative approach to the problem. They have operated a ring laser in many longitudinal modes and phase-locked the OT waves with intracavity modulation. In this case, the OT waves travel in short pulses. Thus, if they pass the active medium alternately, good isolation between them will be achieved.

Some analyses have been made on the mode of the ring resonator [36]. Collins *et al.* have obtained the resonance frequencies. They are essentially identical to those of Fabry-Perot resonator, however they differ according as the number of mirrors of which the ring resonator is composed is odd or even. This is because the horizontal distribution of the laser beam is inverted after one-round trip of the ring resonator of an odd number of mirrors. Bagaev *et al.* and Watkins *et al.* have confirmed experimentally that the horizontally or vertically linearly polarized wave as well as the circularly polarized one can be a fundamental mode in the triangular ring resonator.

A unique characteristic of the ring laser comes from the fact that the cw and ccw traveling-waves exist as two independent modes and therefore the unidirectional traveling-wave oscillation is possible. These OT waves degenerate in the normal laser and make a standing wave. The unidirectional traveling-wave oscillation has several merits, for example: 1) there are no saturation effects due to the mirror mode competition nor due to the spatial hole burning, 2) the fundamental transverse mode TEM_{00} is easily obtainable because the spatial inhomogeneity of the resonator is somewhat averaged through the inversion of the horizontal distribution of the laser beam in a round trip, 3) satelite pulses hardly appear because the first backscatterings at optical surfaces in the resonator are injected to

the direction of the non-oscillating traveling-wave. The ring resonator itself is strong against the optical damage, if it is composed of prisms using the total reflection without a dielectric coated mirror.

Various methods for obtaining the unidirectional oscillation have been considered. In the oldest method, a Faraday isolator is inserted in the resonator. Although the unidirectional oscillation is achieved surely, it has rather large insertion loss and therefore this method is not practical. There is a simple method in which a traveling-wave is injected into the oppositely directed traveling-wave with an externally placed mirror. This method is useful when the energy coupling is strong enough between the OT waves in the laser medium. In an Ar ion laser [43], unidirectional oscillation has been achieved near the threshold of oscillation. In a He-Ne laser (6328Å) [44.a], the directionality ratio (ratio of the intensities of the OT waves) has become 5 - 7 : 1. In a dye laser [44.b], the ratio 40 : 1 has been achieved at maximum. Using the difference in the distribution of the beam radius between the OT waves over an unstable ring resonator, the ratio as high as 18 : 1 has been achieved in a CO_2 laser [44.c]. Finally, there is an interesting method in which mode-locked unidirectional traveling-wave oscillation is achieved dynamically by internal modulation. This oscillation has an output of a regular pulse train with high peak intensity and narrow pulse width. This phenomenon was discovered for the first time by Buholz *et al.* [50] and has been investigated in detail both theoretically and experimentally by Miyashita *et al.* [52,53].

Basic equations for a bidirectional multimode ring laser with an inhomogeneously Doppler-broadened line have been derived by Miyashita *et al.* [2] following Lamb's theory of a standing-wave laser [1]. Solving numerically those equations with internal loss-modulation, they obtained the results in which mode-locked unidirectional traveling-wave oscillation or bidirectional one arises depending on

modulation frequency and modulator position, and the unidirectional one has a pulse train whose peak intensity is twice as large as that of the bidirectional one. The results are in good agreement with the experimental results [52,53].

Basic equations for a bidirectional ring laser with a homogeneously broadened line have been also derived in the time domain by Miyashita *et al.* [79]. Numerically solving these equations, they have found that the internally loss-modulated homogeneous ring laser has a similar characteristic to the inhomogeneous one and that the unidirectional oscillation of the homogeneous laser has a pulse train of much higher peak intensity than that of the inhomogeneous one. However, this characteristic may be limited to the case in which the recovery time T_1 of the population inversion is on the order of the period T of the pulse train and the pulse width is not too short compared with T_1.

Basic equations for a bidirectional homogeneous ring laser are applicable to a standing-wave laser with the boundary condition for Fabry-Perot resonator. Miyashita *et al.* have calculated the fundamental and second harmonic mode locking of the homogeneous standing-wave laser with internal loss-modulation and compared the result with the experimental one in a Nd:YAG laser [81].

1.5. Outline of the Content

In Chapter 2, the quantum mechanical equation of motion of the two-level system with electric dipole transition is reviewed.

Chapter 3 deals with the laser with an inhomogeneously Doppler-broadened line. In Section 3.1, the amplitude and phase determining equations for a bidirectional traveling-wave ring laser are derived from the quantum mechanical equation of the laser medium and Maxwell's equation by iterative method to the third order approximation

following the procedure of Lamb's theory of a standing-wave laser. As a special case, the equations for a standing-wave laser are included. Section 3.2 shows how the coefficients of the equations should be modified in a mixed isotope case. Section 3.3 gives the additional polarization generated by internal loss-modulation. Section 3.4 deals with the normal standing-wave laser. In the first place, how the admixture of an isotope reduces the mode competition effect is shown in the disappearance of the Lamb dip. As an investigation of the mode competition, the amplitudes of the modes in the three-mode operation are calculated and various types of oscillation are shown versus relative excitation and cavity length. An experimental result on a He-Ne laser is shown being compared with the theoretical one. Self-mode locked states are numerically calculated in the three-mode operation and 0-type locking is shown to occur usually. In the latter half of the section, the second harmonic mode locking by internal loss-modulation is discussed. Theoretical calculation for a multimode operation and a detailed experiment on a He-Ne laser are shown. They prove to agree with each other quantitatively. Section 3.5 deals with the unidirectional traveling-wave ring laser. As in the standing-wave laser, self-mode locking is investigated theoretically in the three-mode operation and also experimentally on a He-Ne unidirectional ring laser. Mode locking by internal loss-modulation is considered only theoretically. An advantageous point of the ring laser is shown in the peak intensity of the mode-locked pulse train compared with the standing-wave one. Section 3.6 deals with the bidirectional traveling-wave ring laser. Self-mode locking is investigated analytically in the two-mode operation. Especially, the crossing point of the OT waves are considered. Main part of the section is for investigations on the phase locking and competition of the OT waves by internal loss-modulation. To begin with, an approximate analytical investigation is made for the most simple two-mode operation. From numerical calculations, the amplitude and phase of the output pulse

train are shown versus modulation frequency for the two- and five-mode operations. Occurrence of the mode-locked unidirectional traveling-wave oscillation and a comparison with the bidirectional one are shown. The results of a detailed experiment on a He-Ne ring laser are shown. They prove to agree with the theoretically expected results qualitatively and even quantitatively for certain modulator positions.

Chapter 4 deals with the laser with a homogeneously broadened line only theoretically. Section 4.1 gives basic equations for a bidirectional traveling-wave ring laser in the time domain. In Section 4.2, a contrivance in the finite difference calculation along the ring resonator to obtain the mode-locked pulses as stationary solutions even for nonzero detuning of the modulation frequency. Section 4.3 gives detuning characteristics of the forced locking of a unidirectional ring laser. Section 4.4 deals with a bidirectional ring laser. In the first place, the conditions for various CW oscillations and self-pulsing (self-mode locking) are considered and some numerical solutions of the basic equation are shown. Next, the wave forms of the mode-locked pulse train obtained by internal loss-modulation are calculated. Occurrence of the mode-locked unidirectional traveling-wave oscillation and a comparison with the bidirectional one are shown. Section 4.5 deals with a standing-wave laser. In the former part, the dependence of the types of the self-mode locked states on pumping parameter, normalized cavity length, and position of the active medium are given from the numerical solutions. In the latter half, second harmonic mode locking by internal loss-modulation is considered. The dependence of the mode-locked state on modulation frequency and positions of the active medium and the modulator are investigated. Some numerical results are shown being compared with the reported experimental results.

In Chapter 5, a brief summary of the results is given and some concluding remarks are made.

CHAPTER 2

INTERACTION BETWEEN LASER MEDIUM AND ELECTROMAGNETIC WAVE

The interaction between laser medium and intense electromagnetic wave will be described semiclassically, treating the medium quantum mechanically and the electromagnetic wave according to Maxwell's theory.

The quantum mechanical equation of motion of the particle (atom, molecule, ion, etc.) making the laser action is given by Schrödinger's equation [85]

$$i\hbar \frac{d}{dt} |\psi\rangle = H|\psi\rangle \quad , \tag{2-1}$$

where H is the total hamiltonian of the particle, and $|\psi\rangle$ is a Dirac's ket vector which describes the state of the particle. It should be noticed that time t is in the moving system with that particle. The total Hamiltonian H is composed of two parts. One is the Hamiltonian H_0 for the unperturbed particle, and the other is H' for the electromagnetic field perturbation. Thus

$$H = H_0 + H' \quad , \tag{2-2}$$

and

$$H_0|n\rangle = W_n|n\rangle \ , \quad n = 1,2,\ldots, \tag{2-3}$$

where W_n and $|n\rangle$ are, respectively, the eigenvalue and the eigen vector of the unperturbed Hamiltonian H_0. The perturbation H' is generally expanded as a sum of the electric dipole, magnetic dipole, electric quadrupole, and so on. The magnetic dipole term is dominant in the maser for radio wave and the electric one in the laser

from infrared to ultraviolet. We will treat the latter in the following part. Then

$$H' = - \boldsymbol{\mu}\cdot\boldsymbol{E} = - \mu E\cos\theta \tag{2-4}$$

where θ is the angle between the electric field $\boldsymbol{E}$ and the dipole operator $\boldsymbol{\mu}$. Thus the work to do in this section is reduced to a time-varying perturbation problem.

The state of the particle $|\psi\rangle$ is expanded in the eigen vectors at $t = 0$ of the unperturbed Hamiltonian in the Schrödinger picture.

$$|\psi(t)\rangle = \sum_n a_n(t)|n\rangle \tag{2-5}$$

We consider the most simple two-level particle, denoting the upper level by 2 and the lower level by 1. If $|n\rangle$ is also a eigen vector of the parity operator, then

$$\mu_{nn} = \langle n|\mu|n\rangle = 0 \ , \quad n = 1,2, \tag{2-6}$$

and μ_{21} and μ_{12} can be made real by a suitable choice of the phase of $|n\rangle$.

The component of the microscopic polarization produced by that particle parallel with the electric field $\boldsymbol{E}$ is given by

$$p = \langle\psi|\mu|\psi\rangle\cos\theta \ . \tag{2-7}$$

Substituting Eq.(5) into Eq.(7), we find

$$p = (a_1a_2^* + a_1^*a_2) \mu_{12}\cos\theta \ . \tag{2-8}$$

Now we introduce the density operator which is a hermitian operator,

$$\rho = |\psi\rangle\langle\psi| \ . \tag{2-9}$$

The matrix representation of the density operator over the base vectors $\{|n\rangle\}$ is given by

$$\rho_{nm} = \langle n|\rho|m\rangle = a_n^* a_m \ . \tag{2-10}$$

Then Eq.(8) becomes

$$p = (\rho_{12} + \text{c.c.})\mu_{12}\cos\theta \ . \tag{2-11}$$

Using this density operator, we obtain the following equation from Eq.(1).

$$i\hbar \frac{d}{dt}\rho = [\, H \,, \rho \,] \ , \tag{2-12}$$

which is the well-known equation of motion in the quantum mechanics. This equation does not include the spontaneous decay of the levels 1 and 2. To include it, we should introduce a operator Γ and modify Eq.(12) as follows:

$$i\hbar \frac{d}{dt}\rho = [\, H \,, \rho \,] - i\hbar \frac{1}{2}\{\Gamma(\rho - \rho^e) + (\rho - \rho^e)\Gamma\} \ , \tag{2-13}$$

where ρ^e is the density operator of the thermal equilibrium state of the particle without the electric field. Matrix representations of H and Γ are, respectively,

$$(H) = \begin{pmatrix} W_1 & -\mu_{12}E\cos\theta \\ -\mu_{21}E\cos\theta & W_2 \end{pmatrix} , \tag{2-14}$$

$$(\Gamma) = \begin{pmatrix} \gamma_1 & 0 \\ 0 & \gamma_2 \end{pmatrix} , \tag{2-15}$$

where γ_1 and γ_2 are the spontaneous decay rates of the levels 1 and 2 respectively.

Rewriting Eq.(13) in the matrix elements, we find

$$\frac{d}{dt}\rho_{11} = -\gamma_1(\rho_{11}-\rho_{11}^{e}) + \frac{i}{\hbar}(\rho_{21}-\rho_{12})E\mu_{12}\cos\theta \ , \qquad (2\text{-}16)$$

$$\frac{d}{dt}\rho_{22} = -\gamma_2(\rho_{22}-\rho_{22}^{e}) + \frac{i}{\hbar}(\rho_{12}-\rho_{21})E\mu_{12}\cos\theta \ , \qquad (2\text{-}17)$$

$$\frac{d}{dt}\rho_{21} = -i\omega\rho_{21}-\gamma'_{12}\rho_{21}-\frac{i}{\hbar}(\rho_{22}-\rho_{11})E\mu_{12}\cos\theta \ , \qquad (2\text{-}18)$$

where

$$\hbar\omega = W_2 - W_1 \ , \qquad (2\text{-}19)$$

and γ'_{12} is the natural line width of the transition between levels 1 and 2. This quantity is given as $(\gamma_1 + \gamma_2)/2$ from Eq.(13). However it becomes larger approximately proportionally to the pressure in the gaseous medium [10], *i.e.*

$$\gamma'_{12} = \gamma_{12} + (\text{const.})\times(\text{pressure}) \ , \qquad (2\text{-}20)$$

where

$$\gamma_{12} = \frac{1}{2}(\gamma_1 + \gamma_2) \ . \qquad (2\text{-}21)$$

This is the reason why a new independent quantity γ'_{12} was introduced in the above equation.

CHAPTER 3

MODE COMPETITION AND PHASE LOCKING IN THE LASER WITH AN INHOMOGENEOUSLY BROADENED LINE

(Coupled Mode Theory)

To begin with, let us consider the inhomogeneity of the line broadening. The inhomogeneous broadening of the laser medium can be classified into two groups. One is a superposition of various spectral lines of the stationary particles. In this type, the variety of the spectral lines comes from spatial inhomogeneity of the field around the particles. The other is a superposition of the various Doppler-shifted spectral lines of the moving particles. This broadening depends upon the velocity distribution of the particles in the gaseous medium. There is an essential difference between these two types. In the former type, a particle can interact only with a frequency component of the electric field. In the latter type, however, a moving particle interacts with two frequency components due to Doppler effect. The oppositely directed two traveling-wave modes whose frequencies are symmetrical about the transition frequency of the stationary particles, interact with the same velocity group of the particles. Hence they couple deeply with each other.

In this chapter, some investigations will be made of the oscillation characteristics of various types of the gaseous laser which has the second type of inhomogeneous broadening of the line.

3.1. Basic Equations -Pure Isotope Case-

The amplitude and phase determining equations will be derived for the most general bidirectional multimode ring laser [2].

A. Field Equations

Usually, the electric field is linearly polarized to a definite direction by Brewster windows. Hence the electric field and macroscopic polarization may be treated as scalar quantities. From Maxwell's equations, an approximate wave equation for the electric field $E(z,t)$ in the cavity is obtained as

$$\frac{\partial^2 E}{\partial z^2} - \mu_0\sigma \frac{\partial E}{\partial t} - \mu_0\varepsilon_0 \frac{\partial^2 E}{\partial t^2} = - \mu_0\nu^2 P \ . \qquad (3.1\text{-}1)$$

Here only the axial variation of E has been considered. Since the macroscopic polarization $P(z,t)$ will be very nearly monochromatic at an optical frequency ν, its second time derivative has been replaced by $- \nu^2 P$ in Eq.(1).

The total electric field in a ring laser is expanded in the traveling-wave-type eigenfunctions as follows:

$$E(z,t) = \frac{1}{2} \sum_n [\, E_n^{\ell}(t)\sin\{ \Phi_n^{\ell}(z,t)\} - E_n^{r}(t)\sin\{ \Phi_n^{r}(z,t)\}] \ , \qquad (3.1\text{-}2)$$

where

$$\Phi_n^{r}(z,t) = \nu_n^{r} t + \phi_n^{r}(t) - K_n^{r} z \ , \qquad (3.1\text{-}3)$$

$$\Phi_n^{\ell}(z,t) = \nu_n^{\ell} t + \phi_n^{\ell}(t) + K_n^{\ell} z \ . \qquad (3.1\text{-}4)$$

Here superscripts r and ℓ denote cw and ccw traveling-waves, respectively; E_n and ϕ_n are the slowly time-varying amplitude and phase of the nth mode; ν_n the angular frequency, and K_n the wave number given,from the resonance condition, as

$$K_n^{\alpha} = 2\,(\, n_0 + n\,)\,\pi/L^{\alpha} \qquad \alpha = r,\ell, \qquad (3.1\text{-}5)$$

where L^{r} and L^{ℓ} are the perimeters of the resonator experienced by the cw and ccw traveling-waves, respectively, including the effects of passive nonreciprocal elements such as a Faraday biasing element,

and n_0 is the number of spatial variations of a certain mode.

The macroscopic polarization is expanded also in the traveling-wave-type eigenfunctions

$$P(z,t) = \frac{1}{2} \sum_n \{ P_n^{\ell}(z,t) + P_n^{r}(z,t) \} , \qquad (3.1\text{-}6)$$

where

$$P_n^{\ell}(z,t) = S_n^{\ell}(t)\sin [\, \Phi_n^{\ell}(z,t)] - C_n^{\ell}(t)\cos [\, \Phi_n^{\ell}(z,t)] , \qquad (3.1\text{-}7)$$

$$P_n^{r}(z,t) = -S_n^{r}(t)\sin [\, \Phi_n^{r}(z,t)] + C_n^{r}(t)\cos [\, \Phi_n^{r}(z,t)] . \qquad (3.1\text{-}8)$$

Here the in-phase and quadrature coefficients S_n and C_n are slowly varying functions of t.

Substituting Eqs.(2) and (6) into Eq.(1) and equating the coefficients of $\sin [\, \Phi_n^{r}(z,t)]$, $\cos [\, \Phi_n^{r}(z,t)]$, $\sin [\, \Phi_n^{\ell}(z,t)]$, and $\cos [\, \Phi_n^{\ell}(z,t)]$ separately to zero, and further, neglecting small terms $\ddot{E}_n$, $(\sigma/\varepsilon_0)\dot{E}_n$, and $\ddot{\phi}_n E_n$, we find self-consistency equations which are in the same form as Lamb's [1],

$$\dot{E}_n^{\alpha} + \frac{1}{2} (\nu/Q^{\alpha})E_n^{\alpha} = - \frac{1}{2} (\nu/\varepsilon_0)C_n^{\alpha} , \qquad (3.1\text{-}9)$$

$$(\nu_n^{\alpha} + \dot{\phi}_n^{\alpha} - \Omega_n^{\alpha})E_n^{\alpha} = - \frac{1}{2} (\nu/\varepsilon_0)S_n^{\alpha} , \qquad \alpha = r,\ell . \qquad (3.1\text{-}10)$$

Here the resonance frequency Ω_n^{α} of the nth mode of the empty resonator is given by

$$\Omega_n^{\alpha} = cK_n^{\alpha} , \qquad (3.1\text{-}11)^*$$

and the passive Q^{α} is obtained from the fictional conductivity, including the nonreciprocal effects of the system, as

$$Q^{\alpha} = \varepsilon_0 \nu/\sigma^{\alpha} . \qquad (3.1\text{-}12)$$

---

*Since the dielectric property of the passive medium in the resonator is included in the effective optical length of the resonator, the velocity of light is always for vacuum.

B. Polarization of the Medium

In contrast with Lamb's method, the macroscopic polarization can be obtained, as follows, a little more simply without considering when and where a particle is excited.

The macroscopic polarization $P(z,t)$ is composed of the contributions of all particles which arrive at position z at time t and given by

$$P(z,t) = \int_{-\infty}^{\infty} dv \int_{0}^{\pi} d\theta \cdot n(\theta,v,z,t) \langle p(\lambda,\theta,v,z,t) \rangle_{\lambda}, \tag{3.1-13}$$

where

$$n(\theta,v,z,t) = \Theta(\theta) W(v) n(z,t) \ . \tag{3.1-14}$$

Here the parameter λ denotes a pure state which is involved in the mixed state with a certain probability, and $\langle \ \rangle_{\lambda}$ the ensemble average over λ; $\Theta(\theta)$ stands for the distribution of the angle θ between the dipole operator and the electric field, which may be assumed to be uniform, *i.e.*

$$\Theta(\theta) = \frac{1}{4\pi} 2\pi \sin\theta = \frac{1}{2} \sin\theta \ . \tag{3.1-15}$$

The number of particles per unit volume at position z at time t is represented by $n(z,t)$. The normalized velocity distribution function $W(v)$ is assumed to be a Maxwellian distribution

$$W(v) = \frac{1}{u\sqrt{\pi}} \exp\left(- \frac{v^2}{u^2} \right) \ . \tag{3.1-16}$$

The speed parameter u is related to an effective temperature T by the equation

$$\frac{1}{2} mu^2 = kT \ , \tag{3.1-17}$$

where m is the particle mass and k is the Boltzmann constant.

The microscopic polarization $p(\lambda,\theta,v,z,t)$ is given by Eq.(2-11),

and the density matrix elements ρ_{12} and ρ_{21} in Eq.(2-11) is given as solutions of the differential equations (2-16~18). It should be noticed that the coordinate system (z,t) in Chapter 2 is moving with the particles. To avoid confusion in the following part, we use the notation (z',t') for the coordinates moving with the particles with a velocity v, and the notation (z,t) for the laboratory system. Then Eqs.(2-16~18) are rewritten as

$$\frac{d}{dt'}\rho_{11} = -\gamma_1(\rho_{11}-\rho_{11}^{e}) + \frac{i}{\hbar}(\rho_{21}-\rho_{12})\tilde{E}(z',t')\mu_{12}\cos\theta \ , \tag{3.1-18}$$

$$\frac{d}{dt'}\rho_{22} = -\gamma_2(\rho_{22}-\rho_{22}^{e}) + \frac{i}{\hbar}(\rho_{12}-\rho_{21})\tilde{E}(z',t')\mu_{12}\cos\theta \ , \tag{3.1-19}$$

$$\frac{d}{dt'}\rho_{21} = -i\omega\rho_{21} - \gamma_{12}'\rho_{21} - \frac{i}{\hbar}(\rho_{22}-\rho_{11})\tilde{E}(z',t')\mu_{12}\cos\theta \ , \tag{3.1-20}$$

where

$$\tilde{E}(z',t') = E(z'+vt',t') \ , \tag{3.1-21}$$

$$\rho_{nm} = \rho_{nm}(\lambda,\theta,v,z,t) \ , \qquad n,m = 1,2, \tag{3.1-22}$$

$$\rho_{nn}^{e} = \rho_{nn}^{e}(\lambda,z,t) \ . \tag{3.1-23}$$

Relation between the moving and laboratory systems can be given by the Galilean transformation since $c >> |v|$.

$$z = z' + vt' \ , \quad t = t' \ . \tag{3.1-24}$$

Let

$$\rho_{nm}(\theta,v,z,t) = n(z,t)\langle\rho_{nm}(\lambda,\theta,v,z,t)\rangle_{\lambda} \ , \tag{3.1-25}$$

$$\Lambda_n(z,t) = n(z,t)\langle\rho_{nn}^{e}(\lambda,z,t)\rangle_{\lambda} \ , \tag{3.1-26}$$

then Eqs.(18~20) become

$$\frac{d}{dt'}\rho_{11} = -\gamma_1(\rho_{11}-\Lambda_1) + \frac{i}{\hbar}(\rho_{21}-\rho_{12})\tilde{E}(z',t')\mu_{12}\cos\theta \ , \tag{3.1-27}$$

$$\frac{d}{dt'}\rho_{22} = -\gamma_2(\rho_{22}-\Lambda_2) + \frac{i}{\hbar}(\rho_{12}-\rho_{21})\tilde{E}(z',t')\mu_{12}\cos\theta \ , \tag{3.1-28}$$

$$\frac{d}{dt'}\rho_{21} = -i\omega\rho_{21} - \gamma'_{12}\rho_{21} - \frac{i}{\hbar}(\rho_{22} - \rho_{11})\tilde{E}(z',t')\mu_{12}\cos\theta \ , \tag{3.1-29}$$

where

$$\rho_{nm} = \rho_{nm}(\theta,v,z,t) \ . \tag{3.1-30}$$

Here $n(z,t)$ has been assumed to be a slowly varying function compared with all the time constants involved in the equations and treated as a constant. It will be incorrect to say that the number of the particles excited to level 2 is Λ_2 and the number of the particles deexcited to level 1 is Λ_1 in the thermal equilibrium state. Generally we can not say whether a particle is at the upper level or at the lower level. A state of a particle is a superpostion of the excited and de-excited states. Λ_1 and Λ_2 stand for the statistical weights of the superposition. Let us solve the above equations in iterative method.

C. First-Order Polarization

We may choose the thermal equilibrium state with $\tilde{E} = 0$ as the zeroth-order solution. Then

$$\rho_{11}^{(0)}(\theta,v,z,t) = \Lambda_1(z,t) \ , \tag{3.1-31}$$

$$\rho_{22}^{(0)}(\theta,v,z,t) = \Lambda_2(z,t) \ , \tag{3.1-32}$$

$$\rho_{21}^{(0)}(\theta,v,z,t) = 0 \ . \tag{3.1-33}$$*

In the iterative method, the nth-order solution is given by the solution of Eqs.(27~29) with the up to $(n-1)$th-order solutions substituted into the right hand sides. However we should choose suitable values for the integration constants so that the higher-order

---

* We are treating incoherent excitation. If the excitation is coherent or partially coherent, the off-diagonal elements $\rho_{21}^{(0)}$ and $\rho_{12}^{(0)}$ are not zero.

solutions are less important. Here we make the order of a solution equal to the power of E involved in the solution. Thus the first-order contributions to ρ_{nm} are given by

$$\rho_{11}^{(1)} = \rho_{22}^{(1)} = 0 \ , \tag{3.1-34}$$

$$\rho_{21}^{(1)}(\theta,v,z,t) = -\frac{1}{\hbar}\{\Lambda_2(z,t) - \Lambda_1(z,t)\}\mu_{12}\cos\theta$$

$$\times \int_{-\infty}^{t'} i\tilde{E}(z',t_1')\exp[(\gamma_{12}' + i\omega)(t_1' - t')]dt_1' \ , \tag{3.1-35}$$

where

$$\tilde{E}(z',t_1') = E(z' + vt_1',\ t_1') \ . \tag{3.1-36}$$

Here $\Lambda_n(z' + vt_1',\ t_1')$ has been treated as a slowly varying function of t_1' and evaluated at t' *. With a change of variable of integration from t_1' to

$$\tau = t_1' - t' \ , \tag{3.1-37}$$

we find

$$\rho_{21}^{(1)}(\theta,v,z,t) = -\frac{1}{\hbar}(\Lambda_2 - \Lambda_1)\mu_{12}\cos\theta$$

$$\times \int_{-\infty}^{0} iE(z + v\tau,\ t + \tau)\exp[(\gamma_{12}' + i\omega)\tau]d\tau \ . \tag{3.1-38}$$

Here Eq.(24) has been used.

Substituting Eq.(2) into Eq.(38), we find the integrant of Eq.(38)

$$iE(z + v\tau, t + \tau)\exp[(\gamma_{12}' + i\omega)\tau]$$

$$= \frac{1}{4}\sum_n \left[E_n^{\ell}(t + \tau)\exp[i\{\nu_n^{\ell}t + \phi_n^{\ell}(t + \tau) + K_n^{\ell}z + (\nu_n^{\ell} + K_n^{\ell}v)\tau\}] - \text{c.c.}\right.$$

---

* Then $z' + vt_1'$ and t_1' are replaced by $z' + vt' = z$ and $t' = t$ respectively.

$$- E_n^{\gamma}(t+\tau)\exp[i\{\nu_n^{\gamma}t + \phi_n^{\gamma}(t+\tau) - K_n^{\gamma}z + (\nu_n^{\gamma} - K_n^{\gamma}v)\tau\}] + \text{c.c.}\Big]$$

$$\times \exp[(\gamma_{12}' + i\omega)\tau] \ . \qquad (3.1\text{-}39)$$

We make a rotating wave approximation by keeping only exponential factors like $\exp i\{(\nu_n - \omega)\tau\}$ which are able to have resonance and neglecting rapidly varying ones like $\exp i\{(\nu_n + \omega)\tau\}$ which make very little contributions* when Eq.(39) is integrated over τ. We also assume that the amplitudes $E_n^{\alpha}(t+\tau)$ and phases $\phi_n^{\alpha}(t+\tau)$ do not vary much in a time $1/\gamma_{12}'$, so that they can be evaluated at time t. Then Eq.(39) becomes

$$\frac{1}{4}\sum_n \Big[- E_n^{\ell}(t)\exp[-i\Phi_n^{\ell}(z,t)]\exp[\{\gamma_{12}' + i(\omega - \nu_n^{\ell} - K_n^{\ell}v)\}\tau]$$

$$+ E_n^{\gamma}(t)\exp[-i\Phi_n^{\gamma}(z,t)]\exp[\{\gamma_{12}' + i(\omega - \nu_n^{\gamma} + K_n^{\gamma}v)\}\tau]\Big] . \qquad (3.1\text{-}40)$$

Let us define $\rho_{21}^{(1)}(z,t)$ by

$$\rho_{21}^{(1)}(z,t) = \mu_{12}\int_0^{\pi}\Theta(\theta)\cos\theta\cdot d\theta\int_{-\infty}^{\infty}W(v)dv\cdot\rho_{21}^{(1)}(\theta,v,z,t) \ , \qquad (3.1\text{-}41)$$

then, from Eqs.(2-11) and (13), we find the first-order polarization

$$P^{(1)}(z,t) = \rho_{21}^{(1)}(z,t) + \text{c.c.} \qquad (3.1\text{-}42)$$

The integrations over θ and v may be profitably done on Eq.(41) before that over τ. With Eq.(15), the integration over θ is done as

$$\int_0^{\pi}\frac{1}{2}\sin\theta\cos^2\theta\cdot d\theta = \frac{1}{3} \ . \qquad (3.1\text{-}43)$$

---

* They are some 10^{-6} time as large as those of the reserved factors.

The integration over v is done with Eq.(16) as

$$\frac{1}{u\sqrt{\pi}}\int_{-\infty}^{\infty}\exp[\ -\frac{v^2}{u^2}\pm iKv\tau]dv\ =\ \exp[\ -\frac{1}{4}K^2u^2\tau^2\ ] \qquad (3.1\text{-}44)$$

where the subscript n and superscript α (α = l or r) of K_n^{α} have been dropped since all of the modes considered have very nearly the same wave number $K = \nu/c$ and the small differences between K_n^{α}'s will make here only negligible contributions.

With the above calculation, we find

$$\begin{aligned} P^{(1)}(z,t) &= \frac{i}{12}\{\mu_{12}^2/(\hbar Ku)\}N(z,t) \\ &\quad \times\sum_n[\ E_n^r(t)Z(\nu_n^r-\omega)\exp\{-i\Phi_n^r(z,t)\} \\ &\quad -E_n^l(t)Z(\nu_n^l-\omega)\exp\{-i\Phi_n^l(z,t)\}] \\ &\quad +\text{complex conjugate.} \end{aligned} \qquad (3.1\text{-}45)$$

Here the excitation density $N(z,t)$ has been defined by

$$N(z,t) = \Lambda_2(z,t) - \Lambda_1(z,t)\ , \qquad (3.1\text{-}46)$$

and $Z(\nu-\omega)$ is an abbreviation for the well-known plasma dispersion function

$$\begin{aligned} &Z(\nu-\omega,\gamma'_{12},Ku) \\ &\quad = iKu\int_0^{\infty}\exp[i(\nu-\omega)\tau-\gamma'_{12}-\frac{1}{4}K^2u^2\tau^2]d\tau\ . \end{aligned} \qquad (3.1\text{-}47)$$

Since $N(z,t)$ is a slowly varying function of t, the spectrum of $N(z,t)\exp\{-i\Phi_n^{\alpha}(z,t)\}$ is confined into a narrow band around ν_n^{α}, having no components around $\nu_m^{\alpha}(m\neq n)$. Thus $N(z,t)$ in Eq.(45) can be

replaced by

$$N_0(t) = \frac{1}{L}\int_0^L N(z,t)dz \ . \qquad (3.1\text{-}48)^*$$

Then the first order in-phase and quadrature coefficients of the polarization are given, from Eqs.(6~8) and (45), by

$$S_n^{\alpha(1)}(t) = -\{\mu_{12}^2/(3\hbar Ku)\}Z_r(\nu_n^\alpha - \omega)N_0(t)E_n^\alpha(t) \ , \qquad (3.1\text{-}49)$$

$$C_n^{\alpha(1)}(t) = -\{\mu_{12}^2/(3\hbar Ku)\}Z_i(\nu_n^\alpha - \omega)N_0(t)E_n^\alpha(t) \ , \qquad (3.1\text{-}50)$$

where Z_r and Z_i are the real and imaginary parts of $Z(\nu-\omega)$, respectively. The OT waves are naturally independent of each other in the first order.

D. Third-Order Polarization

The second contributions to ρ_{nm} are similarly given by

$$\rho_{21}^{(2)} = 0 \ , \qquad (3.1\text{-}51)$$

$$\rho_{11}^{(2)}(\theta,v,z,t) = \frac{1}{\hbar^2}N(z,t)\mu_{12}^2\cos^2\theta\int_{-\infty}^{t'}dt_2'\int_{-\infty}^{t_2'}dt_1'$$

$$\times\tilde{E}(z',t_1')\tilde{E}(z',t_2')[\exp\{(\gamma_{12}'+i\omega)(t_1'-t_2')+\gamma_1(t_2'-t')\} + \text{c.c.}] \ , \qquad (3.1\text{-}52)$$

$$\rho_{22}^{(2)}(\theta,v,z,t) = -\frac{1}{\hbar^2}N(z,t)\mu_{12}^2\cos^2\theta\int_{-\infty}^{t'}dt_2'\int_{-\infty}^{t_2'}dt_1'$$

$$\times\tilde{E}(z',t_1')\tilde{E}(z',t_2')[\exp\{(\gamma_{12}'+i\omega)(t_1'-t_2')+\gamma_2(t_2'-t')\} + \text{c.c.}] \ , \qquad (3.1\text{-}53)$$

while the third-order contributions are given by

---

* The superscript of L^α has been dropped for the same reason as for K_n^α. Consequently any difference between OT waves comes from Q_n^α and Ω_n^α.

$$\rho_{11}^{(3)} = \rho_{22}^{(3)} = 0 \ , \tag{3.1-54}$$

$$\rho_{21}^{(3)}(\theta,v,z,t) = \frac{1}{\hbar^3} N(z,t)\mu_{12}^3 \cos^3\theta \int_{-\infty}^{t'} dt_3' \int_{-\infty}^{t_3'} dt_2' \int_{-\infty}^{t_2'} dt_1'$$

$$\times i\tilde{E}(z',t_3')\tilde{E}(z',t_2')\hat{E}(z',t_1')[\exp\{(\gamma_{12}' + i\omega)(t_1' - t_2') + \gamma_1(t_2' - t_3')\}$$

$$+ \text{c.c.}]\exp[(\gamma_{12}' + i\omega)(t_3' - t')] + \text{same with } \gamma_1 \text{ and } \gamma_2 \text{ interchanged.} \tag{3.1-55}$$

Let us define $\rho_{21}^{(3)}(v,z,t)$ by

$$\rho_{21}^{(3)}(v,z,t) = \mu_{12} \int_0^{\pi} \Theta(\theta)\cos\theta \cdot \rho_{21}^{(3)}(\theta,v,z,t)d\theta \ . \tag{3.1-56}$$

The integration over θ in Eq.(56) is reduced to

$$\int_0^{\pi} \frac{1}{2} \sin\theta\cos^4\theta d\theta = \frac{1}{5} \ . \tag{3.1-57}*$$

With a change of variable of integration from t_3', t_2', and t_1' to

$$\tau_3' = t_3' - t', \quad \tau_2' = t_2' - t_3' \ , \quad \tau_1' = t_1' - t_2' \ , \tag{3.1-58}$$

we find

$$\rho_{21}^{(3)}(v,z,t) = (\mu_{12}^4/(5\hbar^3))N(z,t) \int_{-\infty}^{0} d\tau_3' \int_{-\infty}^{0} d\tau_2' \int_{-\infty}^{0} d\tau_1'$$

$$\times iE(z + v\tau_3', t + \tau_3')E(z + v(\tau_2' + \tau_3'), t + \tau_2' + \tau_3')$$

$$\times E(z + v(\tau_1' + \tau_2' + \tau_3'), t + \tau_1' + \tau_2' + \tau_3')[\exp\{(\gamma_{12}' + i\omega)\tau_1' + \gamma_1\tau_2'\} + \text{c.c.}]$$

$$\times \exp[(\gamma_{12}' + i\omega)\tau_3'] + \text{same with } \gamma_1 \text{ and } \gamma_2 \text{ interchanged.} \tag{3.1-59}$$

---

* Generally, the integration of the nth order polarization over θ is replaced by a factor $1/(n+2)$.

The triple product of E in Eq.(59) is rewritten, using Eq.(2), as

$$
\begin{aligned}
& iE(z+v\tau_3',t+\tau_3')E(\cdots,\cdots)E(\cdots,\cdots) \\
&= -\frac{1}{64}\sum_{\mu}[E_\mu^{\ell}(t)\exp i\{\Phi_\mu^{\ell}(z,t)+(\nu_\mu^{\ell}+K_\mu^{\ell}v)\tau_3'\} - \text{c.c.} \\
&\quad - E_\mu^{r}(t)\exp i\{\Phi_\mu^{r}(z,t)+(\nu_\mu^{r}-K_\mu^{r}v)\tau_3'\} + \text{c.c.}] \\
&\quad \times\sum_{\rho}[E_\rho^{\ell}(t)\exp i\{\Phi_\rho^{\ell}(z,t)+(\nu_\rho^{\ell}+K_\rho^{\ell}v)(\tau_2'+\tau_3')\} - \text{c.c.} \\
&\quad - E_\rho^{r}(t)\exp i\{\Phi_\rho^{r}(z,t)+(\nu_\rho^{r}-K_\rho^{r}v)(\tau_2'+\tau_3')\} + \text{c.c.}] \\
&\quad \times\sum_{\sigma}[E_\sigma^{\ell}(t)\exp i\{\Phi_\sigma^{\ell}(z,t)+(\nu_\sigma^{\ell}+K_\sigma^{\ell}v)(\tau_1'+\tau_2'+\tau_3')\} - \text{c.c.} \\
&\quad - E_\sigma^{r}(t)\exp i\{\Phi_\sigma^{r}(z,t)+(\nu_\sigma^{r}-K_\sigma^{r}v)(\tau_1'+\tau_2'+\tau_3')\} + \text{c.c.}],
\end{aligned}
\tag{3.1-60}
$$

where the amplitudes E_n^{α} and phases ϕ_n^{α} have been evaluated at time t as done in Eq.(40). We substitute Eq.(60) into Eq.(59). Again we keep only exponential factors in the time integration over τ_1',τ_2', and τ_3' which are able to have resonance. Then we find that the terms to be kept in the integrant of Eq.(59) have either of the two groups of exponential factors as shown below.

Group 1.

$$
\begin{aligned}
&\exp[\{\gamma_{12}'+i(\omega-\nu_\sigma)\}\tau_1'+\{\gamma_1+i(\nu_\rho-\nu_\sigma)\}\tau_2' \\
&\quad +\{\gamma_{12}'+i(\omega-\nu_\mu+\nu_\rho-\nu_\sigma)\}\tau_3'-i(\nu_\mu-\nu_\rho+\nu_\sigma)t]
\end{aligned}
$$

or the same with γ_1 and γ_2 interchanged.

Group 2.

$$
\begin{aligned}
&\exp[\{\gamma_{12}'-i(\omega-\nu_\sigma)\}\tau_1'+\{\gamma_1-i(\nu_\rho-\nu_\sigma)\}\tau_2' \\
&\quad +\{\gamma_{12}'+i(\omega-\nu_\mu-\nu_\rho+\nu_\sigma)\}\tau_3'-i(\nu_\mu+\nu_\rho-\nu_\sigma)t]
\end{aligned}
$$

or the same with γ_1 and γ_2 interchanged.

There are such terms of wave number $\pm 3K$ as well as those of $\pm K$. The polarizations of wave number $\pm 3K$, however, do not make phase-match at all with the eigen-modes of the resonator. Therefore those terms may be ignored *. Consequently the terms to be kept are 12×2 terms as shown in Table I.

Table I This table gives the information needed for Eq.(61).

		Superscripts to Subscripts μ ρ σ	(±)	Coefficients of z	Coefficients of Kv
Group 1	1	$r\ r\ r$	−	$K_\mu - K_\rho + K_\sigma$	$\tau_1' + \tau_3'$
	2	$l\ r\ r$	+	$-K_\mu - K_\rho + K_\sigma$	$\tau_1' - \tau_3'$
	3	$l\ l\ r$	−	$-K_\mu + K_\rho + K_\sigma$	$\tau_1' + 2\tau_2' + \tau_3'$
	4	$r\ r\ l$	+	$K_\mu - K_\rho - K_\sigma$	$-(\tau_1' + 2\tau_2' + \tau_3')$
	5	$l\ l\ l$	+	$-K_\mu + K_\rho - K_\sigma$	$-(\tau_1' + \tau_3')$
	6	$r\ l\ l$	−	$K_\mu + K_\rho - K_\sigma$	$-(\tau_1' - \tau_3')$
Group 2	1	$r\ l\ r$	+	$K_\mu - K_\rho - K_\sigma$	$-(\tau_1' + 2\tau_2' + \tau_3')$
	2	$l\ r\ r$	+	$-K_\mu + K_\rho - K_\sigma$	$-(\tau_1' + \tau_3')$
	3	$r\ r\ r$	−	$K_\mu + K_\rho - K_\sigma$	$-(\tau_1' - \tau_3')$
	4	$r\ l\ l$	−	$K_\mu - K_\rho + K_\sigma$	$\tau_1' + \tau_3'$
	5	$l\ l\ l$	+	$-K_\mu - K_\rho + K_\sigma$	$\tau_1' - \tau_3'$
	6	$l\ r\ l$	−	$-K_\mu + K_\rho + K_\sigma$	$\tau_1' + 2\tau_2' + \tau_3'$

Thus

$$\rho_{21}^{(3)}(v,z,t) = -\frac{1}{320}(\mu_{12}^4/\hbar^3)N(z,t)\sum_\mu\sum_\rho\sum_\sigma\int_{-\infty}^{0}d\tau_3'\int_{-\infty}^{0}d\tau_2'\int_{-\infty}^{0}d\tau_1'$$

$$\times\Big\{\sum_1(\pm)E_\mu E_\rho E_\sigma \exp i[-(\nu_\mu-\nu_\rho+\nu_\sigma)t-(\phi_\mu-\phi_\rho+\phi_\sigma)+(\cdots)z+(\cdots)Kv]$$

$$\times\exp[\{\gamma_{12}'+i(\omega-\nu_\sigma)\}\tau_1'+\{\gamma_1+i(\nu_\rho-\nu_\sigma)\}\tau_2'+\{\gamma_{12}'+i(\omega-\nu_\mu+\nu_\rho-\nu_\sigma)\}\tau_3']$$

* In the fifth-order approximation, interacting with the terms of wave number $\pm 2K$ which appear in $\rho_{11}^{(4)}$ and $\rho_{22}^{(4)}$, those terms may make those of wave number $\pm K$ also. They will not be missed, however, if the fifth-order calculation are made from the formula corresponding to Eq.(59) in a similar manner.

$$+ \sum_2(\pm)E_\mu E_\rho E_\sigma \exp i[-(\nu_\mu+\nu_\rho-\nu_\sigma)t-(\phi_\mu+\phi_\rho-\phi_\sigma)+(\cdots)z+(\cdots)Kv]$$

$$\times\exp[\{\gamma'_{12}-i(\omega-\nu_\sigma)\}\tau'_1+\{\gamma_1-i(\nu_\rho-\nu_\sigma)\}\tau'_2+\{\gamma'_{12}+i(\omega-\nu_\mu-\nu_\rho+\nu_\sigma)\}\tau'_3]$$

$$+ \text{ same with } \gamma_1 \text{ and } \gamma_2 \text{ interchanged.}\Big] \ , \qquad (3.1\text{-}61)$$

where ambiguous factors can be known from Table I, and $\sum_1$ stands for a summation over group 1 of Table I and $\sum_2$ over group 2. The subscript n and superscript α ($\alpha = l$ or r) of K_n^α have been dropped in the coefficients of v as done in the first-order calculation.

Next let us consider

$$\rho_{21}^{(3)}(z,t) = \int_{-\infty}^{\infty}\rho_{21}^{(3)}(v,z,t)W(v)dv \ . \qquad (3.1\text{-}62)$$

Substituting Eq.(61) into (62), we find the following integrations over v:

$$\int_{-\infty}^{\infty}\exp[\pm iK(\tau'_1+\tau'_3)v]W(v)dv = \exp[-\tfrac{1}{4}K^2u^2(\tau'_1+\tau'_3)^2] \ , \qquad (3.1\text{-}63)$$

$$\int_{-\infty}^{\infty}\exp[\pm iK(\tau'_1-\tau'_3)v]W(v)dv = \exp[-\tfrac{1}{4}K^2u^2(\tau'_1-\tau'_3)^2] \ , \qquad (3.1\text{-}64)$$

$$\int_{-\infty}^{\infty}\exp[\pm iK(\tau'_1+2\tau'_2+\tau'_3)v]W(v)dv = \exp[-\tfrac{1}{4}K^2u^2(\tau'_1+2\tau'_2+\tau'_3)^2] \ . \qquad (3.1\text{-}65)$$

Here $Ku >> \gamma'_{12}$, γ_1, γ_2*, thus we may assume that the right hand sides of Eqs.(63~65) act like delta function of $\tau'_1+\tau'_3$, $\tau'_1-\tau'_3$, and $\tau'_1+2\tau'_2+\tau'_3$, respectively, in the integration over τ'_1, τ'_2 and τ'_3. Then the integration over τ'_3 can be done in the form

$$\int_{-\infty}^{0}d\tau'_3\int_{-\infty}^{0}d\tau'_1 G(\tau'_3,\tau'_1)\exp[-\tfrac{1}{4}K^2u^2(\tau'_1-\tau'_3)^2] \simeq \frac{2\sqrt{\pi}}{Ku}\int_{-\infty}^{0}d\tau'_1 G(\tau'_1,\tau'_1) \ . \qquad (3.1\text{-}66)$$

---

* For example, $Ku/2\pi \simeq 1$GHz; $\gamma'_{12}/2\pi$, $\gamma_1/2\pi$, $\gamma_2/2\pi < 100$MHz for He-Ne laser(6328Å).

The other Gaussian factors (63,65) do not have their full peaks in the range of integration, and give contributions which we neglect because they lead to expressions with higher powere of Ku in the denominator. Then, after performing the simple integrations over τ_1', τ_2', we find the third-order polarization

$$
\begin{aligned}
P^{(3)}(z,t) &= \rho_{21}^{(3)}(z,t) + \text{c.c.} \\
&= -\frac{\sqrt{\pi}}{320}\{\mu_{12}^4/(\hbar^3 Ku)\}N(z,t)\sum_{\mu}\sum_{\rho}\sum_{\sigma} \\
&\Big[E_\mu^\ell E_\rho^\ell E_\sigma^\ell \exp[i\{-(\nu_\mu^\ell-\nu_\rho^\ell+\nu_\sigma^\ell)t-(\phi_\mu^\ell-\phi_\rho^\ell+\phi_\sigma^\ell)-(K_\mu^\ell-K_\rho^\ell+K_\sigma^\ell)z\}]\mathcal{D}(-\tfrac{1}{2}\nu_\mu-\tfrac{1}{2}\nu_\sigma+\nu_\rho) \\
&+E_\mu^\ell E_\rho^r E_\sigma^r \exp[i\{-(\nu_\mu^\ell-\nu_\rho^r+\nu_\sigma^r)t-(\phi_\mu^\ell-\phi_\rho^r+\phi_\sigma^r)-(K_\mu^\ell+K_\rho^r-K_\sigma^r)z\}] \\
&\quad\times\mathcal{D}(\omega-\tfrac{1}{2}\nu_\mu^\ell+\tfrac{1}{2}\nu_\rho^r-\nu_\sigma^r) \\
&-E_\mu^r E_\rho^r E_\sigma^r \exp[i\{-(\nu_\mu^r-\nu_\rho^r+\nu_\sigma^r)t-(\phi_\mu^r-\phi_\rho^r+\phi_\sigma^r)+(K_\mu^r-K_\rho^r+K_\sigma^r)z\}]\mathcal{D}(-\tfrac{1}{2}\nu_\mu-\tfrac{1}{2}\nu_\sigma+\nu_\rho) \\
&-E_\mu^r E_\rho^\ell E_\sigma^\ell \exp[i\{-(\nu_\mu^r-\nu_\rho^\ell+\nu_\sigma^\ell)t-(\phi_\mu^r-\phi_\rho^\ell+\phi_\sigma^\ell)+(K_\mu^r+K_\rho^\ell-K_\sigma^\ell)z\}] \\
&\quad\times\mathcal{D}(\omega-\tfrac{1}{2}\nu_\mu^r+\tfrac{1}{2}\nu_\rho^\ell-\nu_\sigma^\ell)\Big] \\
&\times\{\mathcal{D}_1(\nu_\rho-\nu_\sigma)+\mathcal{D}_2(\nu_\rho-\nu_\sigma)\} + \text{complex conjugate},
\end{aligned}
\tag{3.1-67}
$$

where

$$
\mathcal{D}(\omega) = 1/(\gamma_{12}' + i\omega)\ , \qquad \mathcal{D}_k(\omega) = 1/(\gamma_k + i\omega)\ , \tag{3.1-68}
$$

$$
\mathcal{D}_k(\nu_\rho - \nu_\sigma) = \mathcal{D}_k(\nu_\rho^\ell - \nu_\sigma^\ell) \simeq \mathcal{D}_k(\nu_\rho^r - \nu_\sigma^r)\ , \tag{3.1-69}
$$

$$
\mathcal{D}(-\tfrac{1}{2}\nu_\mu-\tfrac{1}{2}\nu_\sigma+\nu_\rho) = \mathcal{D}(-\tfrac{1}{2}\nu_\mu^\ell-\tfrac{1}{2}\nu_\sigma^\ell+\nu_\rho^\ell) \simeq \mathcal{D}(-\tfrac{1}{2}\nu_\mu^r-\tfrac{1}{2}\nu_\sigma^r+\nu_\rho^r)\ . \tag{3.1-70}
$$

Since $N(z,t)$ is a slowly varying function of t, the spectrum of $N(z,t)\exp(-i\nu_n t)$ is restricted within a narrow band around ν_n; on the contrary, the spatial variation of $N(z,t)$ is as fast as $\exp[\pm i(K_n - K_{n-1})z]$, thus the spatial spectrum of $N(z,t)\exp[\pm iK_n z]$ is distributed at $\pm K_n$, $\pm K_{n\pm1}$, $\pm K_{n\pm2}$, and so on. Thus $N(z,t)$ should be expanded as

$$N(z,t) = N_0 + \sum_{n=1}^{\infty} N_n \{\exp(i\frac{2n\pi}{L}z) + \exp(-i\frac{2n\pi}{L}z)\} \quad , \quad (3.1\text{-}71)$$

with

$$N_n = \frac{1}{L}\int_0^L N(z,t)\cos\frac{2n\pi}{L}z\,dz \quad , \quad n = 0, 1, 2, \ldots \quad (3.1\text{-}72)$$

Here an assumption have been made that the excitation density $N(z,t)$ is distributed symmetrically about z=0. Configurations of the ring and normal lasers and their periodical expansions are shown in Fig. 3.1-1.

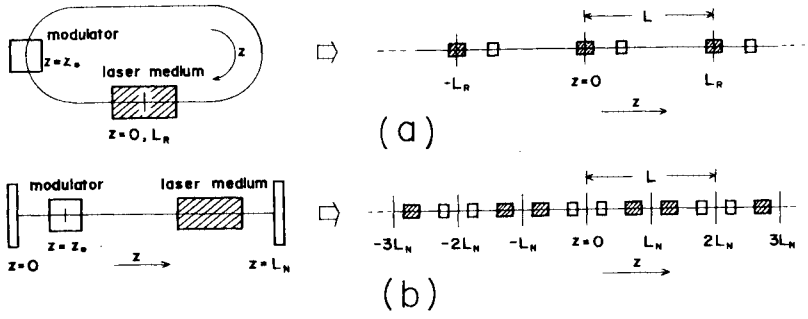

Fig.3.1-1. Configurations of the ring and normal lasers and their periodical expansions.
(a) ring laser ($L = L_R$), (b) normal laser ($L = 2L_N$).

Substitution of Eq.(71) into (67) gives the terms having the factors $\exp[-i\Phi_n^{\ell}(z,t)]$ and $\exp[-i\Phi_n^{r}(z,t)]$ as

$$P_n^{(3)}(z,t) = -\frac{\sqrt{\pi}}{320}\{\mu_{12}^4/(\hbar^3 Ku)\}\sum_{\mu}'\sum_{\rho}'\sum_{\sigma}'[\exp\{-i\Phi_n^{\ell}(z,t)\}$$

$$\times\{E_\mu^{\ell}E_\rho^{\ell}E_\sigma^{\ell}N_0\exp(-i\psi_{\mu\rho\sigma n}^{\ell\ell\ell})\mathcal{D}(-\frac{1}{2}\nu_\mu-\frac{1}{2}\nu_\sigma+\nu_\rho)$$

$$+ E_\mu^{\ell}E_\rho^{r}E_\sigma^{r}N_{2(\mu-n)}\exp(-i\psi_{\mu\rho\sigma n}^{\ell rr})\mathcal{D}(\omega-\frac{1}{2}\nu_\mu^{\ell}+\frac{1}{2}\nu_\rho^{r}-\nu_\sigma^{r})\}$$

$$- \text{same with } r \text{ and } \ell \text{ interchanged. }]\{\mathcal{D}_1(\nu_\rho-\nu_\sigma)+\mathcal{D}_2(\nu_\rho-\nu_\sigma)\}$$

$$+ \text{complex conjugate}, \quad (3.1\text{-}73)$$

where $\sum_{\mu}'\sum_{\rho}'\sum_{\sigma}'$ denote the summation over all the combinations which

satisfy the condition

$$\mu - \rho + \sigma = n \ , \tag{3.1-74}$$

and $\psi^{\alpha\beta}_{\mu\rho\sigma n}$ is defined as

$$\psi^{\alpha\beta}_{\mu\rho\sigma n} = (\nu^{\alpha}_{\mu} - \nu^{\beta}_{\rho} + \nu^{\beta}_{\sigma} - \nu^{\alpha}_{n})t + (\phi^{\alpha}_{\mu} - \phi^{\beta}_{\rho} + \phi^{\beta}_{\sigma} - \phi^{\alpha}_{n}) \ , \quad \alpha, \beta = r, \ell. \tag{3.1-75}$$

Then the third-order in-phase and quadrature coefficients of the polarization are given, from Eqs.(6~8) and (73), as

$$-\frac{1}{2}(\nu/\varepsilon_0)S^{\ell\,(3)}_{n} = \sum_{\mu}{}' \sum_{\rho}{}' \sum_{\sigma}{}' [(-\eta^{a}_{n,\mu\rho\sigma} \sin\psi^{\ell\ell}_{\mu\rho\sigma n} + \xi^{a}_{n,\mu\rho\sigma} \cos\psi^{\ell\ell}_{\mu\rho\sigma n}) E^{\ell}_{\mu} E^{\ell}_{\rho} E^{\ell}_{\sigma}$$

$$+ (-\eta^{b}_{n,\mu\rho\sigma} \sin\psi^{\ell r}_{\mu\rho\sigma n} + \xi^{b}_{n,\mu\rho\sigma} \cos\psi^{\ell r}_{\mu\rho\sigma n}) E^{\ell}_{\mu} E^{r}_{\rho} E^{r}_{\sigma}] \ , \tag{3.1-76}$$

$$-\frac{1}{2}(\nu/\varepsilon_0)C^{\ell\,(3)}_{n} = \sum_{\mu}{}' \sum_{\rho}{}' \sum_{\sigma}{}' [(-\xi^{a}_{n,\mu\rho\sigma} \sin\psi^{\ell\ell}_{\mu\rho\sigma n} - \eta^{a}_{n,\mu\rho\sigma} \cos\psi^{\ell\ell}_{\mu\rho\sigma n}) E^{\ell}_{\mu} E^{\ell}_{\rho} E^{\ell}_{\sigma}$$

$$+ (-\xi^{b}_{n,\mu\rho\sigma} \sin\psi^{\ell r}_{\mu\rho\sigma n} - \eta^{b}_{n,\mu\rho\sigma} \cos\psi^{\ell r}_{\mu\rho\sigma n}) E^{\ell}_{\mu} E^{r}_{\rho} E^{r}_{\sigma}] \ , \tag{3.1-77}$$

and the same with ℓ and r interchanged. Here η and ξ have been defined as

$$\eta^{a}_{n,\mu\rho\sigma} = HN_0 [\mathcal{L}'(\tfrac{1}{2}\nu_\rho - \tfrac{1}{2}\nu_n)\{\mathcal{L}'_1(\nu_\rho - \nu_\sigma) + \mathcal{L}'_2(\nu_\rho - \nu_\sigma)\}$$

$$- \mathcal{L}''(\tfrac{1}{2}\nu_\rho - \tfrac{1}{2}\nu_n)\{\mathcal{L}''_1(\nu_\rho - \nu_\sigma) + \mathcal{L}''_2(\nu_\rho - \nu_\sigma)\}] \ , \tag{3.1-78}$$

$$\xi^{a}_{n,\mu\rho\sigma} = -HN_0 [\mathcal{L}'(\tfrac{1}{2}\nu_\rho - \tfrac{1}{2}\nu_n)\{\mathcal{L}''_1(\nu_\rho - \nu_\sigma) + \mathcal{L}''_2(\nu_\rho - \nu_\sigma)\}$$

$$+ \mathcal{L}''(\tfrac{1}{2}\nu_\rho - \tfrac{1}{2}\nu_n)\{\mathcal{L}'_1(\nu_\rho - \nu_\sigma) + \mathcal{L}'_2(\nu_\rho - \nu_\sigma)\}] \ , \tag{3.1-79}$$

$$\eta^{b}_{n,\mu\rho\sigma} = HN_{2(\mu-n)} [\mathcal{L}'(\omega - \tfrac{1}{2}\nu^{\ell}_{\sigma} - \tfrac{1}{2}\nu^{r}_{n})\{\mathcal{L}'_1(\nu_\rho - \nu_\sigma) + \mathcal{L}'_2(\nu_\rho - \nu_\sigma)\}$$

$$- \mathcal{L}''(\omega - \tfrac{1}{2}\nu^{\ell}_{\sigma} - \tfrac{1}{2}\nu^{r}_{n})\{\mathcal{L}''_1(\nu_\rho - \nu_\sigma) + \mathcal{L}''_2(\nu_\rho - \nu_\sigma)\}], \tag{3.1-80}$$

$$\xi^{b}_{n,\mu\rho\sigma} = -HN_{2(\mu-n)} [\mathcal{L}'(\omega - \tfrac{1}{2}\nu^{\ell}_{\sigma} - \tfrac{1}{2}\nu^{r}_{n})\{\mathcal{L}''_1(\nu_\rho - \nu_\sigma) + \mathcal{L}''_2(\nu_\rho - \nu_\sigma)\}$$

$$+\mathcal{L}''(\omega-\tfrac{1}{2}\nu_\sigma^\ell-\tfrac{1}{2}\nu_n^r)\{\mathcal{L}_1'(\nu_\rho-\nu_\sigma)+\mathcal{L}_2'(\nu_\rho-\nu_\sigma)\}] \ , \qquad (3.1\text{-}81)$$

where

$$\mathcal{L}_k'(\omega) = \gamma_k/(\gamma_k^2+\omega^2) \ , \quad \mathcal{L}_k''(\omega) = \omega/(\gamma_k^2+\omega^2) \ , \quad k = 1, 2,$$

$$\mathcal{L}'(\omega) = \gamma_{12}'/\{(\gamma_{12}')^2+\omega^2\} \ , \quad \mathcal{L}''(\omega) = \omega/\{(\gamma_{12}')^2+\omega^2\} \ , \qquad (3.1\text{-}82)$$

and

$$H = \frac{\sqrt{\pi}}{160}\,\nu\{\mu_{12}^4/(\hbar^3\varepsilon_0 K u)\} \ . \qquad (3.1\text{-}83)$$

Since

$$\Delta, \ \gamma_1, \ \gamma_2, \ \gamma_{12}' \ >> \ \nu_\mu^\alpha - \nu_\rho^\beta + \nu_\sigma^\beta - \nu_n^\alpha \simeq 0 \ , \qquad (3.1\text{-}84)$$

the following approximations have been made in Eqs.(78~81), where Δ is the mode spacing of the resonator.

$$\mathcal{D}(-\tfrac{1}{2}\nu_\mu-\tfrac{1}{2}\nu_\sigma+\nu_\rho) \simeq \mathcal{D}(\tfrac{1}{2}\nu_\rho-\tfrac{1}{2}\nu_n) \ , \qquad (3.1\text{-}85)$$

$$\mathcal{D}(\omega-\tfrac{1}{2}\nu_\mu^\alpha+\tfrac{1}{2}\nu_\rho^\beta-\nu_\sigma^\beta) \simeq \mathcal{D}(\omega-\tfrac{1}{2}\nu_\sigma^\ell-\tfrac{1}{2}\nu_n^r) \ . \qquad (3.1\text{-}86)$$

The combinations of μ, ρ, σ, and n are divided into three groups which satisfy the conditions

$$\text{(i)} \quad \mu = n \ , \quad \sigma = \rho(\equiv m) \ , \qquad (3.1\text{-}87)$$

$$\text{(ii)} \quad \sigma = n \ , \quad \mu = \rho(\equiv m) \ , \qquad (3.1\text{-}88)$$

$$\text{(iii)} \quad \mu + \sigma = \rho + n \ \text{ excluding (i) and (ii)} \ . \qquad (3.1\text{-}89)$$

The first group makes the terms of phase-independent saturation effects on the cw or ccw nth mode from the cw and ccw mth modes. The second group makes those of phase-independent saturation effects between the nth and mth modes both of which are cw or ccw traveling modes, and also makes those of phase-dependent saturation effects between the nth and mth modes which are OT ones. The third group makes so-called combination tone terms which are phase-dependent.

We may calculate the fifth-order polarization, seventh-order polarization and so on. However these higher-order terms are so

complicated that it is practically impossible to solve the equations including those terms. Only in the one-mode operation, exact solutions can be obtained [5] including all the higher-order terms. However it has been shown that the third-order approximation is almost sufficient for not so highly excited gaseous lasers.

Substituting the first-order polarization (49,50) and the third-order polarization (76,77) into the self-consistency equations (9,10), we find the amplitude and phase determining equations to the third-order approximation as follows.

E. Equations for a Ring Laser

$$\dot{E}_n^\alpha = \alpha_n^\alpha E_n^\alpha - \beta^\alpha (E_n^\alpha)^3 - \sum_{m\neq n} \theta_{nm}^a (E_m^\alpha)^2 E_n^\alpha$$

$$- \sum_m \theta_{nm}^b (E_m^\beta)^2 E_n^\alpha - \sum_{m\neq n} (\theta_{nm}^c \cos\psi_{mmnn}^{\alpha\beta} + \tau_{nm}^c \sin\psi_{mmnn}^{\alpha\beta}) E_m^\alpha E_m^\beta E_n^\beta$$

$$- \sum_{\mu,\rho,\sigma}{}'' (\eta_{n,\mu\rho\sigma}^a \cos\psi_{\mu\rho\sigma n}^{\alpha\alpha} + \xi_{n,\mu\rho\sigma}^a \sin\psi_{\mu\rho\sigma n}^{\alpha\alpha}) E_\mu^\alpha E_\rho^\alpha E_\sigma^\alpha$$

$$- \sum_{\mu,\rho,\sigma}{}'' (\eta_{n,\mu\rho\sigma}^b \cos\psi_{\mu\rho\sigma n}^{\alpha\beta} + \xi_{n,\mu\rho\sigma}^b \sin\psi_{\mu\rho\sigma n}^{\alpha\beta}) E_\mu^\alpha E_\rho^\beta E_\sigma^\beta \quad , \qquad (3.1\text{-}90)$$

$$(\nu_n^\alpha + \dot{\phi}_n^\alpha - \Omega_n^\alpha) E_n^\alpha = \sigma_n^\alpha E_n^\alpha + \rho^\alpha (E_n^\alpha)^3 + \sum_{m\neq n} \tau_{nm}^a (E_m^\alpha)^2 E_n^\alpha$$

$$+ \sum_m \tau_{nm}^b (E_m^\beta)^2 E_n^\alpha + \sum_{m\neq n} (\tau_{nm}^c \cos\psi_{mmnn}^{\alpha\beta} - \theta_{nm}^c \sin\psi_{mmnn}^{\alpha\beta}) E_m^\alpha E_m^\beta E_n^\beta$$

$$+ \sum_{\mu,\rho,\sigma}{}'' (\xi_{n,\mu\rho\sigma}^a \cos\psi_{\mu\rho\sigma n}^{\alpha\alpha} - \eta_{n,\mu\rho\sigma}^a \sin\psi_{\mu\rho\sigma n}^{\alpha\alpha}) E_\mu^\alpha E_\rho^\alpha E_\sigma^\alpha$$

$$+ \sum_{\mu,\rho,\sigma}{}'' (\xi_{n,\mu\rho\sigma}^b \cos\psi_{\mu\rho\sigma n}^{\alpha\beta} - \eta_{n,\mu\rho\sigma}^b \sin\psi_{\mu\rho\sigma n}^{\alpha\beta}) E_\mu^\alpha E_\rho^\beta E_\sigma^\beta \quad , \qquad (3.1\text{-}91)$$

where

$$n, \mu, \rho, \sigma = 1, 2, 3, \ldots, \quad \alpha, \beta = r, l \ (\alpha\neq\beta),$$

and $\sum''$ stands for a summation over the combination tone terms given by Eq.(89). The coefficients are given by

$$\alpha_n^\alpha = \frac{1}{2}(\nu/Q^\alpha)\mathcal{N}^\alpha[\ \frac{Z_i(\nu_n^\alpha-\omega)}{\sqrt{\pi}} - \frac{1}{\mathcal{N}^\alpha}]\ ,\quad \sigma_n^\alpha = \frac{1}{2}(\nu/Q^\alpha)\mathcal{N}^\alpha\ \frac{Z_r(\nu_n^\alpha-\omega)}{\sqrt{\pi}}\ ,$$

$$\beta^\alpha = \eta^a_{n,nnn} = \frac{1}{2}(\nu/Q^\alpha)\mathcal{N}^\alpha G > 0\ ,\quad \rho^\alpha = \xi^a_{n,nnn} = 0\ ,$$

$$\theta^a_{nm} = \eta^a_{n,nmm} + \eta^a_{n,mmn}\ ,\ (n\neq m)\ ,\quad \theta^a_{nm} = \theta^a_{mn}\ ,$$

$$\tau^a_{nm} = \xi^a_{n,nmm} + \xi^a_{n,mmn}\ ,\ (n\neq m)\ ,\quad \tau^a_{nm} = -\tau^a_{mn}\ ,$$

$$\tau^a_{nm} \lesseqgtr 0 \text{ according as } n \lesseqgtr m\ ,$$

$$\theta^b_{nm} = \eta^b_{n,nmm}\ ,\ \tau^b_{nm} = \xi^b_{n,nmm}\ ,\ \theta^c_{nm} = \eta^b_{n,mmn}\ ,\ \tau^c_{nm} = \xi^b_{n,mmn}\ . \quad (3.1\text{-}92)$$

here

$$\gamma_{12} = (\gamma_1 + \gamma_2)/2\ ,\qquad G = 3\mu_{12}^2\gamma_{12}/(40\hbar^2\gamma_1\gamma_2\gamma'_{12})\ , \quad (3.1\text{-}93)$$

and relative excitation $\mathcal{N}^\alpha$ is defined as

$$\mathcal{N}^\alpha = N_0/N_T^\alpha \quad (3.1\text{-}94)$$

where N_T^α is the excitation required for threshold oscillations when a cavity frequency Ω_n^α is tuned to the peak ω of the atomic line,

$$(\alpha_n^\alpha)_T = -\frac{1}{2}(\nu/Q^\alpha) + \frac{1}{2}(\nu/\varepsilon_0)(\mu_{12}^2/(3\hbar Ku))Z_i(0)N_T^\alpha = 0\ . \quad (3.1\text{-}95)$$

F. Equations for a Normal Laser

In the case of normal laser $E_n^\ell = E_n^r \equiv E_n$ and so on, then

$$E(z,t) = \sum_n E_n(t)\cos\{\nu_n t + \phi_n(t)\}\sin(K_n z)\ . \quad (3.1\text{-}96)$$

$$\dot{E}_n = \alpha_n E_n - \beta_n (E_n)^3 - \sum_{m\neq n}\theta_{nm}(E_m)^2 E_n$$

$$- \sum_{\mu,\rho,\sigma}{}''(\eta_{n,\mu\rho\sigma}\cos\psi_{\mu\rho\sigma n} + \xi_{n,\mu\rho\sigma}\sin\psi_{\mu\rho\sigma n})E_\mu E_\rho E_\sigma\ , \quad (3.1\text{-}97)$$

$$(\nu_n + \dot{\phi}_n - \Omega_n)E_n = \sigma_n E_n + \rho_n (E_n)^3 + \sum_{m\neq n}\tau_{nm}(E_m)^2 E_n$$

$$+ \sum_{\mu,\rho,\sigma}{}''(\xi_{n,\mu\rho\sigma}\cos\psi_{\mu\rho\sigma n} - \eta_{n,\mu\rho\sigma}\sin\psi_{\mu\rho\sigma n})E_\mu E_\rho E_\sigma\ , \quad (3.1\text{-}98)$$

where

$$n, \mu, \rho, \sigma = 1, 2, 3, \ldots ,$$

$$\alpha_n = \frac{1}{2}(\nu/Q)\mathcal{N}\left[\frac{Z_i(\nu_n-\omega)}{\sqrt{\pi}} - \frac{1}{\mathcal{N}} \right] , \quad \sigma_n = \frac{1}{2}(\nu/Q)\mathcal{N}\frac{Z_r(\nu_n-\omega)}{\sqrt{\pi}} ,$$

$$\beta_n = \eta^a_{n,nnn} + \eta^b_{n,nnn} = \frac{1}{2}(\nu/Q)\mathcal{N}G\left[1 + \frac{(\gamma'_{12})^2}{1+(\omega-\nu_n)^2}\right] ,$$

$$\rho_n = \xi^a_{n,nnn} + \xi^b_{n,nnn} = -\frac{1}{2}(\nu/Q)\mathcal{N}G\frac{(\omega-\nu_n)\gamma'_{12}}{1+(\omega-\nu_n)^2} ,$$

$$\eta_{n,\mu\rho\sigma} = \eta^a_{n,\mu\rho\sigma} + \eta^b_{n,\mu\rho\sigma} , \qquad \xi_{n,\mu\rho\sigma} = \xi^a_{n,\mu\rho\sigma} + \xi^b_{n,\mu\rho\sigma} ,$$

$$\theta_{nm} = \eta_{n,nmm} + \eta_{n,mmn} , \qquad \tau_{nm} = \xi_{n,nmm} + \xi_{n,mmn} . \qquad (3.1\text{-}99)$$

Practically the frequency pulling and pushing effects are very small compared with the mode spacing $\Delta=\Omega_{n+1}-\Omega_n$, thus ν_n^α may be defined, for example, as

$$\nu_n^\alpha = \Omega_p^\alpha + (n-p)\Delta , \quad \alpha = r, l, \qquad (3.1\text{-}100)$$

where Ω_p^α is the empty-cavity resonance frequency nearest to the line center ω.

3.2. Basic Equations -Mixed-Isotope Case-

We consider the case in which the laser medium is composed of two isotopes. The isotope effect is rather significant in some cases, for example, in the competition and self-locking of the oppositely directed traveling-waves in a He-Ne ring laser, even if it is due to a small amount of another isotope. In this case, macroscopic polarization is composed of two parts each of which is produced by one isotope;

$$P(z,t) = P'(z,t) + P''(z,t) . \qquad (3.2\text{-}1)$$

Each macroscopic polarization can be obtained from Sec.3.1. with a change of parameters as shown in Table II, where the mass composition ratio of the two isotopes is $g':g''$.

Table II Change of the notations and parameters from pure isotope case to mixed isotope case.

Pure Isotope	Isotope I	Isotope II
$n(z,t)$	$g'n(z,t)$	$g''n(z,t)$
$\Lambda_n(z,t)$	$g'\Lambda_n(z,t)$	$g''\Lambda_n(z,t)$
$N(z,t)$	$g'N(z,t)$	$g''N(z,t)$
$N_n(t)$	$g'N_n(t)$	$g''N_n(t)$
u	u'	u''
m	m'	m''
ω	ω'	ω''
H	H'	H''
$Z(x)$	$Z'(x)$	$Z''(x)$
N_τ^α	$N_\tau^{\alpha\prime}$	$N_\tau^{\alpha\prime}$
$\mathfrak{N}^\alpha$	$\mathfrak{N}^\alpha$	$\mathfrak{N}^\alpha$

Here other parameters are considered to have same values for the two isotopes. The velocity parameters u' and u'' are related by the effective temperature T by the equation

$$\frac{1}{2}m'(u')^2 = \frac{1}{2}m''(u'')^2 = kT \ . \qquad (3.2\text{-}2)$$

The definition of the relative excitation for the pure isotope case ($g'=1$, $g''=0$) will be used, for simplicity, also in the mixed isotope case. Then the coefficients for Eqs.(3.1-92,99) are given as

$$\alpha = \frac{1}{2}(\nu/Q)\mathfrak{N}\left[g'\frac{Z_\varepsilon'(\nu-\omega')}{\sqrt{\pi}} + \frac{u'}{u''}g''\frac{Z_\varepsilon''(\nu-\omega'')}{\sqrt{\pi}} - \frac{1}{\mathfrak{N}}\right] ,$$

$$\sigma = \frac{1}{2}(\nu/Q)\mathfrak{N}\left[g'\frac{Z_r'(\nu-\omega')}{\sqrt{\pi}} + \frac{u'}{u''}g''\frac{Z_r''(\nu-\omega'')}{\sqrt{\pi}}\right] ,$$

$$\eta = \frac{1}{2}(\nu/Q)\mathfrak{N}G\left[g'\,\bar{\eta}' + \frac{u'}{u''}g''\bar{\eta}''\right] ,$$

$$\xi = \frac{1}{2}(\nu/Q)\mathfrak{N}G[g'\bar{\xi}' + \frac{u'}{u''}g''\bar{\xi}''] \ , \qquad (3.2\text{-}3)$$

where $\bar{\eta}$ and $\bar{\xi}$ will be known from Sec.3.1.

Natural Neon

Mass composition ratio of natural neon is;

Ne^{20} : 90.92 %

Ne^{21} : 0.26 %

Ne^{22} : 8.82 % .

Ignoring Ne^{21}, we may take

$g' = 0.91$ for Ne^{20}, $g'' = 0.09$ for Ne^{22},

then

$$u'/u'' = \sqrt{m''/m'} = \sqrt{21.998/19.999} = 1.049 \ .$$

The measured line shifts are

$\omega'' - \omega' = 875$ MHz for 6328Å line [4.a] ,

and

$\omega'' - \omega' = 261$ MHz for 1.15μ line [4.b] .

Unsaturated line shapes of Ne^{20}, Ne^{22} and natural neon at 6328Å are shown in Fig.3.2-1.

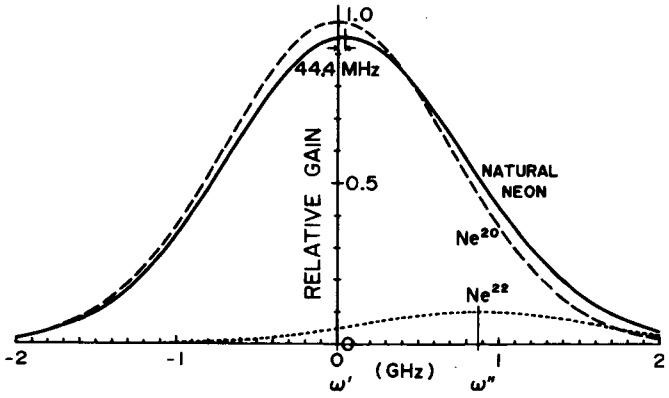

Fig.3.2-1. Unsaturated line shapes of Ne^{20}, Ne^{22} and natural neon at 6328Å. $Ku' = 1$GHz, $\omega'' = \omega' + 875$ MHz.

3.3. Internal Loss-Modulation

An internal loss-modulation may be described by the perturbation of the quadrature component of the electric susceptibility

$$\Delta\chi''(z,t) = \Delta\chi''(z)(1+\cos\nu_m t) \ , \tag{3.3-1}$$

and additional polarization produced by the loss-modulation is given by

$$\Delta P(z,t) = -\frac{1}{2}\sum_n \varepsilon_0\Delta\chi''(z,t)E_n^{\ell}(t)\cos\{\Phi_n^{\ell}(z,t)\}$$
$$+\frac{1}{2}\sum_n \varepsilon_0\Delta\chi''(z,t)E_n^{r}(t)\cos\{\Phi_n^{r}(z,t)\} \ , \tag{3.3-2}$$

where ν_m is the angular frequency of the modulation signal which is approximately equal to k (=1,2,3,..) times the mode spacing Δ of the resonator. The amplitude $\Delta\chi''(z)$ of the perturbation is expanded as follows;

$$\Delta\chi''(z) = \Delta\chi_0 + 2\sum_{n=1}^{\infty}\Delta\chi_n^c\cos\frac{2n\pi}{L}z + 2\sum_{n=1}^{\infty}\Delta\chi_n^s\sin\frac{2n\pi}{L}z \ , \tag{3.3-3}$$

where

$$\Delta\chi_n^c = \frac{1}{L}\int_0^L \Delta\chi''(z)\cos\frac{2n\pi}{L}z\cdot dz \ , \tag{3.3-4}$$

$$\Delta\chi_n^s = \frac{1}{L}\int_0^L \Delta\chi''(z)\sin\frac{2n\pi}{L}z\cdot dz \ . \tag{3.3-5}$$

The periodic expansions of $\Delta\chi''(z)$ for ring and normal lasers are shown in Fig.3.1-1. From the figure, it is obvious that $\Delta\chi_n^s = 0$ for the normal laser. In the usual electro-optic modulator whose length is ℓ, the functional dependence of $\Delta\chi''(z)$ upon z may be simplified as

$$\Delta\chi''(z) = \Delta\chi''(=\text{const.}) \quad \text{for} \quad z_0 - \frac{\ell}{2} \le z \le z_0 + \frac{\ell}{2} \ ,$$
$$= 0 \qquad\qquad \text{elsewhere} \ . \tag{3.3-6}$$

Then, substituting Eq.(3) into (2) and picking up the terms which have the factors $\sin\{\Phi_n^{\alpha}(z,t)\}$ and $\cos\{\Phi_n^{\alpha}(z,t)\}$ ($\alpha=l,r$), we find the additional terms to the self-consistency equations (3.1-9,10) for a ring laser

$$-\frac{1}{2}(\nu/\varepsilon_0)\Delta C_n^{\alpha} = -\frac{\alpha_a c}{2L_R} E_n^{\alpha} - \frac{\alpha_{ck}^{R} c}{2L_R}[E_{n+k}^{\alpha}\cos(\phi_{n+k}^{\alpha} - \phi_n^{\alpha} \pm \frac{2k\pi}{L_R} z_0) + E_{n-k}^{\alpha}\cos(\phi_n^{\alpha} - \phi_{n-k}^{\alpha} \pm \frac{2k\pi}{L_R} z_0)] \quad , \tag{3.3-7}$$

$$-\frac{1}{2}(\nu/\varepsilon_0)\Delta S_n^{\alpha} = -\frac{\alpha_{ck}^{R} c}{2L_R}[E_{n+k}^{\alpha}\sin(\phi_{n+k}^{\alpha} - \phi_n^{\alpha} \pm \frac{2k\pi}{L_R} z_0) - E_{n-k}^{\alpha}\sin(\phi_n^{\alpha} - \phi_{n-k}^{\alpha} \pm \frac{2k\pi}{L_R} z_0)] \quad , \tag{3.3-8}$$

where the upper sign + is for $\alpha=l$ and the lower - for $\alpha=r$, and

$$\alpha_a = \frac{\nu}{c}\, l\cdot\Delta\chi'' \tag{3.3-9}$$

is the amplitude of the fractional power loss of the modulator per pass, and

$$\alpha_{ck}^{R} = \frac{\alpha_a L_R}{2kl\pi}\sin\left(\frac{k\pi l}{L_R}\right) \tag{3.3-10}$$

is the coupling coefficients between the nth mode and $(n\pm k)$th modes. Similarly the additional terms for a normal laser are

$$-\frac{1}{2}(\nu/\varepsilon_0)\Delta C_n = -\frac{\alpha_a c}{2L_N} E_n - \frac{\alpha_{ck}^{N} c}{2L_N}[E_{n+k}\cos(\phi_{n+k} - \phi_n) + E_{n-k}\cos(\phi_n - \phi_{n-k})] \quad , \tag{3.3-11}$$

$$-\frac{1}{2}(\nu/\varepsilon_0)\Delta S_n = -\frac{\alpha_{ck}^{N} c}{2L_N}[E_{n+k}\sin(\phi_{n+k} - \phi_n) - E_{n-k}\sin(\phi_n - \phi_{n-k})] \quad , \tag{3.3-12}$$

where

$$\alpha_{ck}^{r} = \frac{\alpha_a L_r}{lk\pi} \sin\left(\frac{k\pi l}{2L_r} \right) \cos\left(\frac{k\pi z_0}{L_r} \right) . \qquad (3.3\text{-}13)$$

We can see that the degree of the modulation effect for the ring laser is half as much as that for normal laser.

In the investigation of the phase locking phenomena with internal modulation, it is convenient to introduce a detuning parameter $\Delta\nu$ defined by

$$\Delta\nu = \nu_m/k - \Delta , \qquad (3.3\text{-}14)$$

and define ν_n, instead of Eq.(3.1-100), by

$$\nu_n^{\alpha} = \Omega_0^{\alpha} + n(\nu_m/k), \qquad (3.3\text{-}15)$$

$$\Omega_n^{\alpha} = \Omega_0^{\alpha} + n\Delta , \qquad (3.3\text{-}16)$$

then

$$\Omega_n^{\alpha} - \nu_n^{\alpha} = - n\cdot\Delta\nu . \qquad (3.3\text{-}17)$$

Here we are dealing with the case in which mode spacings Δ^{l} and Δ^{r} have no significant difference. For example, usually

$$| \Omega_0^{l} - \Omega_0^{r} | < 2\pi \times 10^8 \text{ radian/sec.} = 100 \text{ MHz},$$

then

$$| \Delta^{l} - \Delta^{r} | < \frac{1}{n_0} \times 2\pi \times 10^8 \simeq 2\pi \times 50 \text{ radian/sec.} = 50 \text{ Hz},$$

because $\Omega_0^{\alpha} = n_0\Delta^{\alpha}$, $\Omega_0^{\alpha} \simeq 2\pi\times5\times10^{14}$, $\Delta^{\alpha} \simeq 2\pi\times10^8$, and $n_0 \simeq 5\times10^6$.

3.4. Normal Standing-Wave Laser

A. Single-Mode Oscillation -Mixed Isotope Effect-

An interesting phenomenon in the single-mode oscillation of the normal laser is appearance of the so-called Lamb dip. Since Lamb's theoretical prediction, it has been investigated not only theoretically but also experimentally [3], and it has been utilized for a frequency-stabilized single-frequency laser. Here mixed-isotope effect to the Lamb dip will be considered.

Intensity of the electric field in the single-mode oscillation is given, from Eq.(3.1-97), by

$$E_1^2 = \alpha_1/\beta_1 \ , \tag{3.4-1}$$

and frequency shift is given from Eq.(3.1-98), by

$$\nu_1 + \dot{\phi}_1 - \Omega_1 = \sigma_1 + \rho_1(\alpha_1/\beta_1) \ . \tag{3.4-2}$$

Oscillation intensity, frequency shift, and the parameters determining them are plotted in Figs.3.4-1~4 versus cavity resonance frequency Ω_1 for 6328Å line of a He-Ne laser. In case of mixed isotopes (Ne^{22}:Ne^{20} = 9 : 91), comparing with a pure isotope (Ne^{20}), the tuning curves of the unsaturated gain α_1 and frequency pulling σ_1 shift a little to the high frequency side, and their symmetrical properties are kept almost completely. However, the curves of the saturation parameters β_1 and ρ_1 deforms slightly, and their center frequencies remain almost at the same point. As a result, asymmetry appears in the intensity curve and the Lamb dip disappears. This isotope effect was observed in experiments [3]. In addition to the asymmetry, some decrease of the mirror mode competition is induced. Especially, mode competition between oppositely traveling waves in a ring laser is seriously diminished as shown in Sec.3.6.

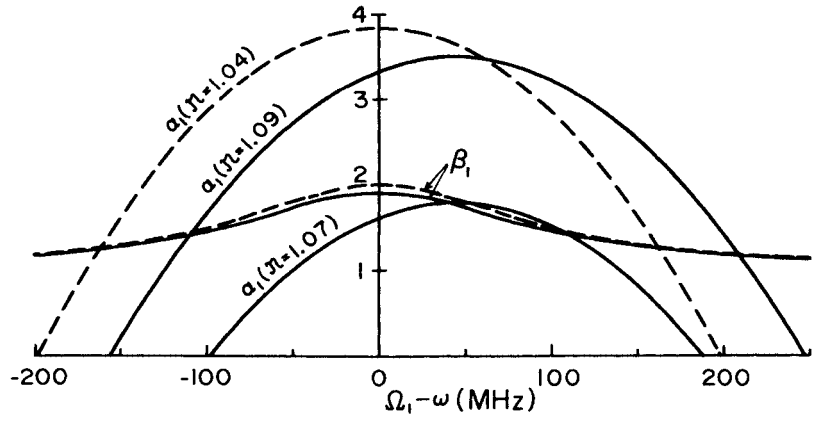

Fig.3.4-1. α_1 and β_1 versus $(\Omega_1-\omega)$. Solid lines are for mixed isotopes (Ne^{20},Ne^{22}) and broken lines are for a pure isotope Ne^{20}. Units of α_1 and β_1 are $\frac{1}{2}(\nu/Q)\mathcal{R}\times 10^{-2}$ and $\frac{1}{2}(\nu/Q)\mathcal{R}G$ respectively.

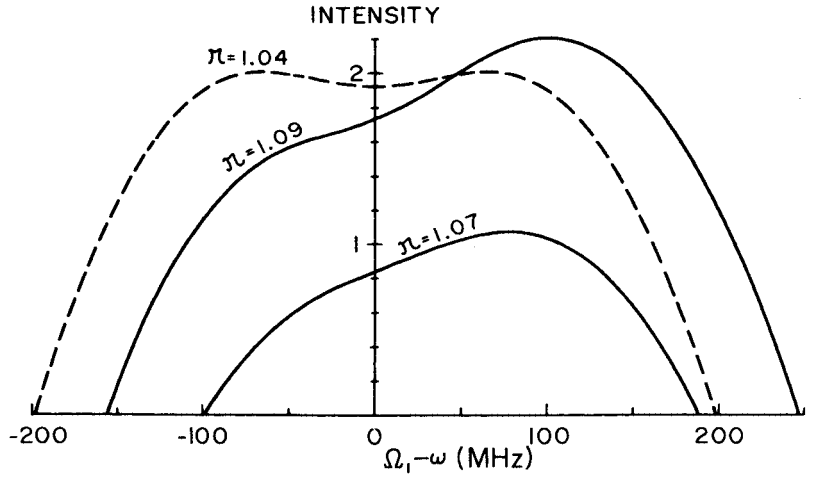

Fig.3.4-2. Single-mode intensity E_1^2 versus $(\Omega_1-\omega)$. Unit is $(1/G)\times 10^{-2}$. Solid lines are for the mixed isotopes and a broken line is for the pure isotope.

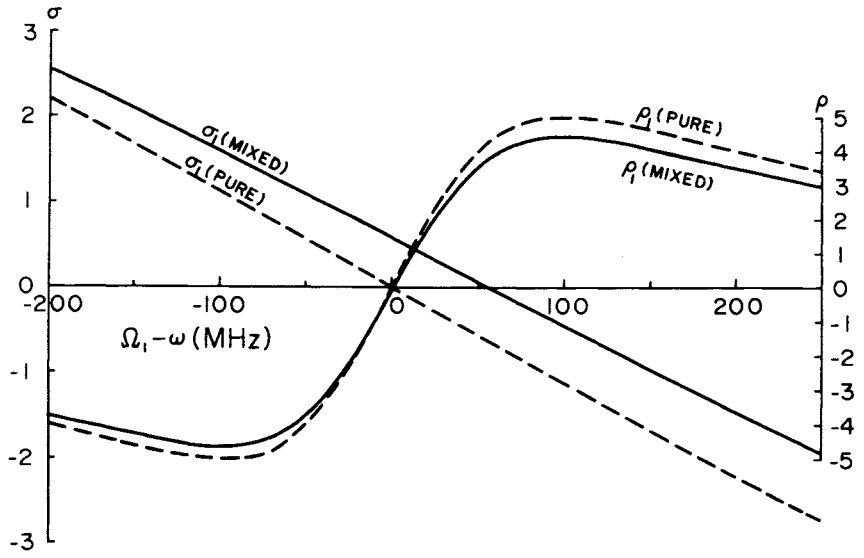

Fig.3.4-3. σ_1 and ρ_1 versus $(\Omega_1-\omega)$. Units of σ_1 and ρ_1 are $\frac{1}{2}(\nu/Q)\mathcal{M}\times 10^{-1}$ and $\frac{1}{2}(\nu/Q)\mathcal{M}\mathcal{G}\times 10^{-1}$, respectively.

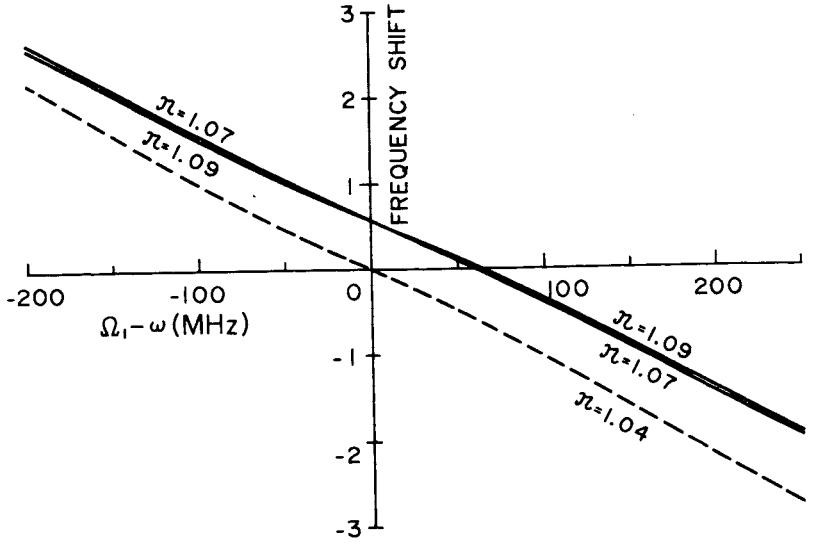

Fig.3.4-4. Frequency shift. Unit is $\frac{1}{2}(\nu/Q)\mathcal{M}\times 10^{-1}$.

B. Mode Competition

In the following two cases, two oscillating modes compete with each other because of significant overlap of their holes burned on the gain curve [8]. In one case, they are neighbouring within the width of the holes. In the other case, they are symmetrically located about the line center. We may call them mirror modes. Because one oscillating mode in a normal laser with a Doppler broadened spectral line makes two holes in the gain curve which are symmetrically located about the line center, the mirror modes compete with each other. A theoretical analysis [12] for three-mode operation and some experimental results for multimode operation will be shown here.

The amplitude determining equations in the M-mode operation* are, ignoring the terms of combination tones, given from Eq.(3.1-97).

$$\dot{E}_i = E_i(\alpha_i - \beta_i E_i^2 - \sum_{j \neq i}^{M} \theta_{ij} E_j^2) , \qquad i = 1, 2, \ldots, M. \tag{3.4-3}$$

It is natural to consider the quantity defined by

$$\alpha_i' = \alpha_i - \beta_i E_i^2 - \sum_{j \neq i}^{M} \theta_{ij} E_j^2 \tag{3.4-4}$$

as effective or saturated gain of the ith mode. Introducing the squared amplitude

$$X_i = E_i^2 , \qquad i = 1, 2, \ldots, M, \tag{3.4-5}$$

Eq.(3) become

$$\dot{X}_i = 2X_i(\alpha_i - \beta_i X_i - \sum_{j \neq i}^{M} \theta_{ij} X_j) , \qquad i = 1, 2, \ldots, M. \tag{3.4-6}$$

The characteristic equation for an equilibrium state**

---

* When the number of modes whose unsaturated gains α_i are positive is M, it is said to be in the M-mode operation.

** No states described by limit cycles are considered.

$X_0 = (X_{10}, X_{20}, \ldots, X_{M0})$ is given by

$$\begin{vmatrix} f_1 - \lambda & -\theta_{12}X_{10} & \cdots\cdots & -\theta_{1M}X_{10} \\ -\theta_{21}X_{20} & f_2 - \lambda & \cdots\cdots & -\theta_{2M}X_{20} \\ \cdots\cdots & \cdots\cdots & \cdots\cdots & \cdots\cdots \\ -\theta_{M1}X_{M0} & -\theta_{M2}X_{M0} & \cdots\cdots & f_M - \lambda \end{vmatrix} = 0 , \quad (3.4\text{-}7)$$

where

$$f_i = \alpha_i - 2\beta_i X_{i0} - \sum_{j \neq i}^{M} \theta_{ij} X_{j0} , \quad i = 1, 2, \ldots, M. \quad (3.4\text{-}8)$$

The stability condition for this state is that the real part of every root of the characteristic equation is negative and $X_{i0} \geq 0$ for all i. The equilibrium states and their stability conditions for three-mode operation are shown in Appendix A. The effective gain of the quenched mode can be proved to be negative from the stability condition.

Numerical examples for a pure isotope He-$\dot{N}e^{20}$ laser are shown in Fig.3.4-5. Outside the one-mode region, monostable (three- or two-mode), bistable, or tri-stable oscillation arises in turn along the limit line of three-mode operation according as the cavity length becomes longer. That is, adjacent modes can not oscillate simultaneously when the fundamental mode spacing $\Delta = \pi c/L$ becomes narrower than the holes burned in the gain curve.

We can make two mode-groups from every two modes, three mode-groups from every three modes, and so on in multimode operation. The competition phenomena between those mode-groups will correspond to the mode competition in the three-mode operation shown in Fig.3.4-5. Monostable, bistable, and tristable regions of the three-mode operation will be connected to the corresponding regions of multimode operation with high excitation or short cavity length.

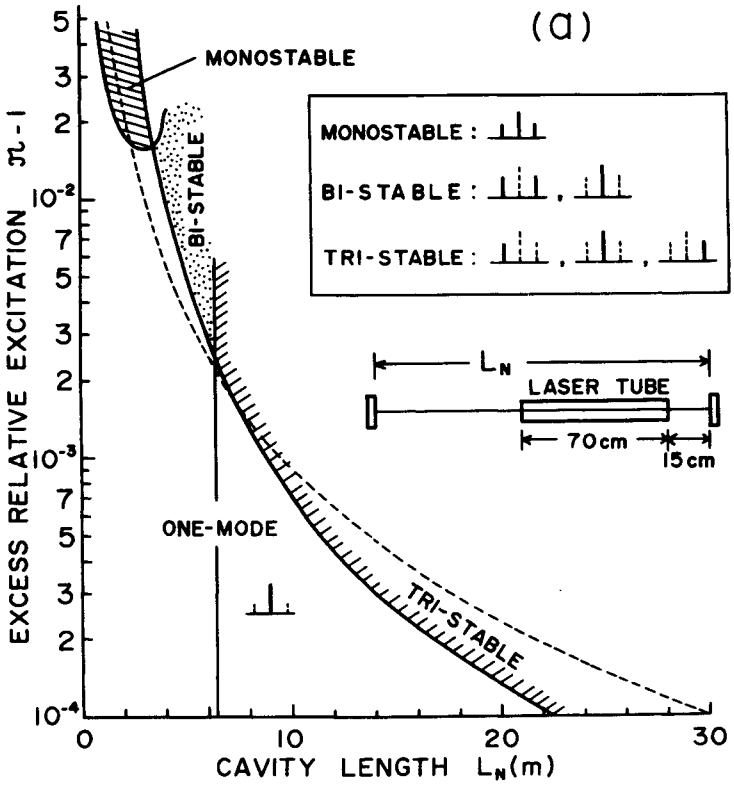

Fig.3.4-5.(a) Numerical examples of the mode competition in the three-mode operation of a He-Ne laser. $\underline{\Omega_2 = \omega}$, $\gamma_{12}'/2\pi$ = 62 MHz, $\gamma_1/2\pi$ = 25 MHz, $\gamma_2/2\pi$ = 12 MHz, $Ku/2\pi$ = 1000MHz. The dotted lines indicate the upper limit of the relative excitation or the longer limit of the cavity length for three-mode operation.

An experimental result is shown in Fig.3.4-6 for a He-Ne laser (natural neon). To achieve three-mode operation, cavity length should be made extraordinarily long or laser medium should be excited very slightly above threshold. The experimental setup was not stable enough for this requirement, although the experiment was made at midnight. Therefore the experiments were made in multimode operation with sufficient excitation and ordinary cavity length. In the regions shown by solid lines, the oscillating modes were self-phase locked. In the unlocked regions shown by dotted lines, the mode spectra were

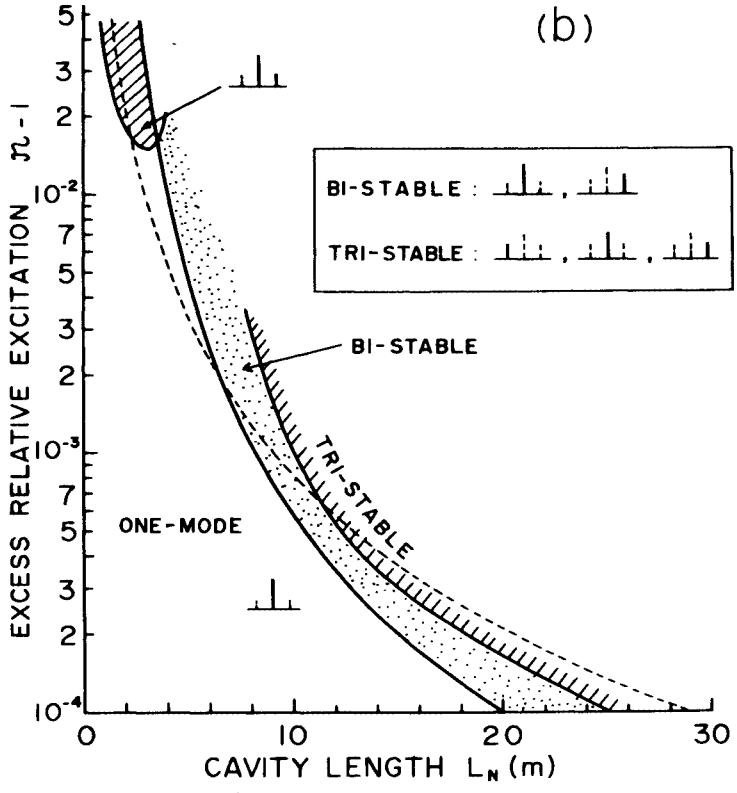

Fig.3.4-5.(b) $\Omega_2 = \omega - 0.1\Delta$. Other parameters are identical with those of Fig.3.4-5.(a).

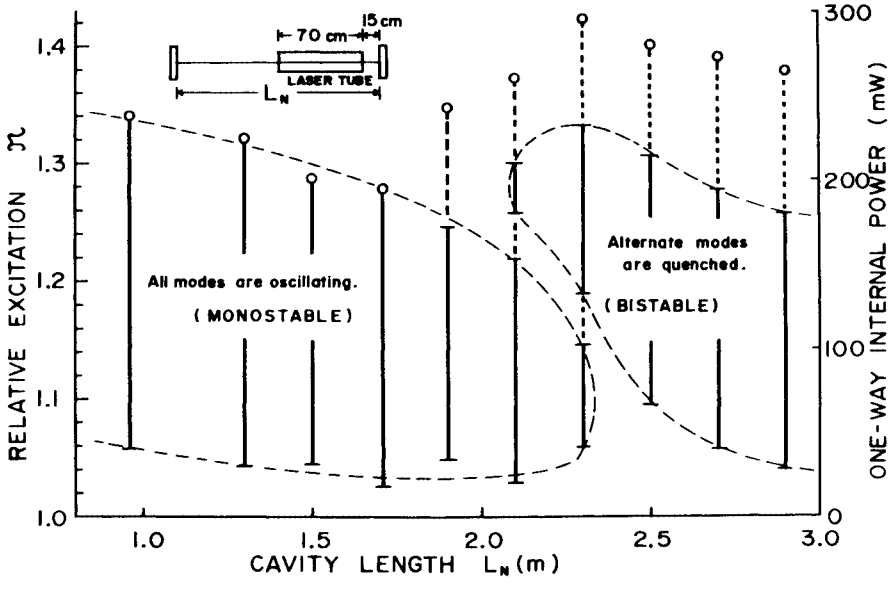

Fig.3.4-6. An experimental result of the mode competition and self-phase locking in a He-Ne laser (6328Å). Dotted lines denote unlocked oscillation.

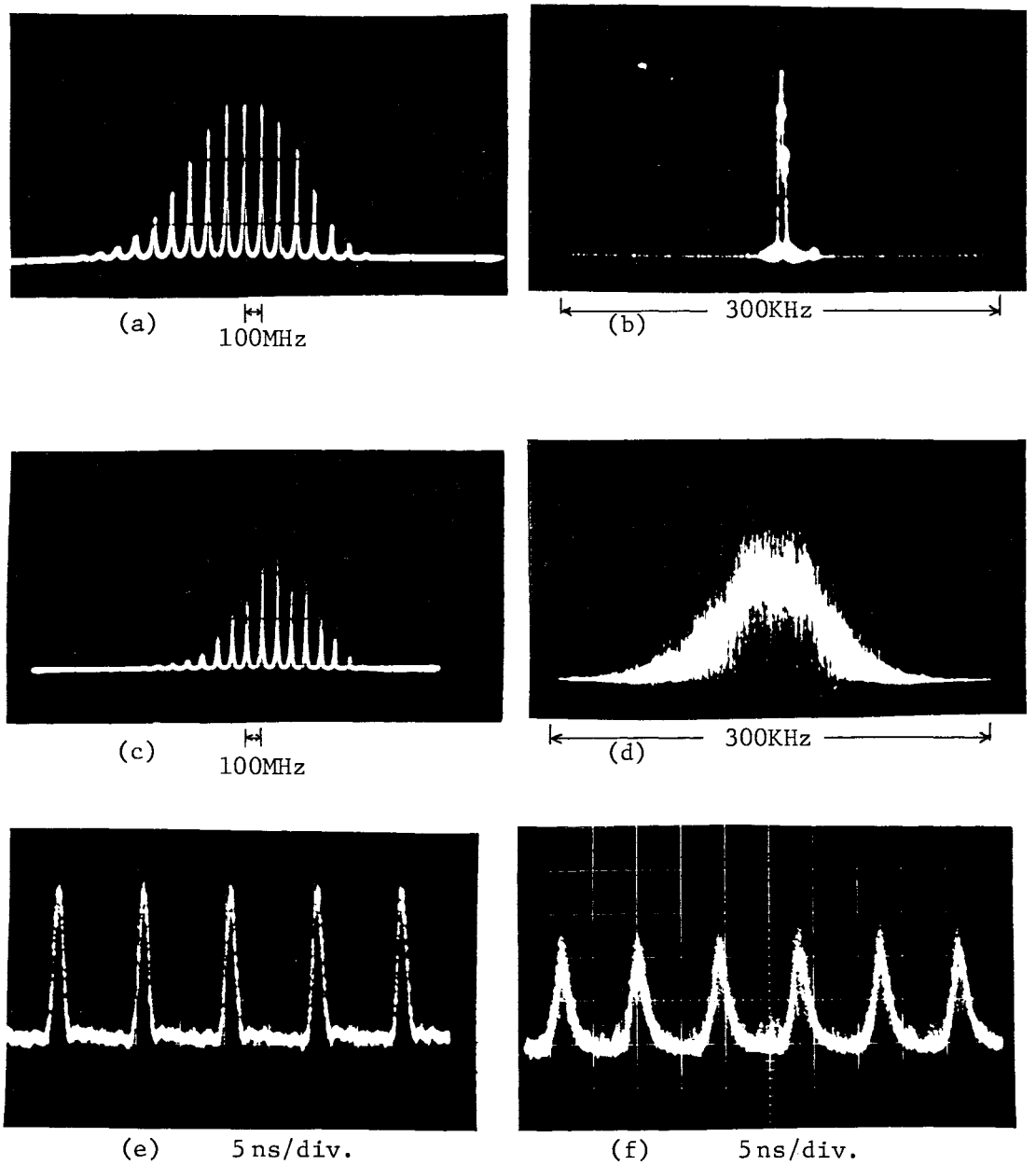

Fig.3.4-7. Mode spectra (a),(c), first beat spectra (b),(d) of the output beams; and output pulse trains (e),(f):
(a) and (b) in a locked state,
(c) and (d) in an unlocked state,
(e) in a monostable state ($L_M \simeq 150$ cm), and
(f) in a bistable state ($L_M \simeq 270$ cm).

varying fast with time. In the low excitation region (for instance, $\mathfrak{N} < 1.06$), the cavity length-dependence of the monostable and bistable oscillations is seen to agree well with the theoretical ones for three-mode operation. When $2.1\,\mathrm{m} < L_M < 2.3\,\mathrm{m}$, monostable oscillation arises with low excitation and bistable one with high excitation. This is because the width of a hole burned on the gain curve becomes wider according to the oscillation intensity of the mode [8]. Such a phenomenon does not appear in the theoretical investigation in the three-mode operation, since the number of the oscillating modes is too small. Figs.3.4-7 shows mode spectra and first beat spectra of the laser outputs in the locked and unlocked states as well as wave forms of the output pulse trains. The mode spectra were obtained by a scanning Fabry-Perot interferometer; the beat spectra by a radio-frequency spectrum analyzer; and the pulse trains were detected by a high-speed PIN photodiode.

C. Self-Phase Locking

High repetition rate optical pulse trains obtained from phase-locked multimode lasers have great utility to application. There is an interesting phenomenon. The repetition rate of the pulse train may be equal to a multiple of the fundamental mode spacing, even if mode quenching does not occur. This problem was investigated experimentally in He-Ne lasers by Crowell [16], Nash [14], and Uchida [13].

Here it will be considered theoretically in the most simple case *i.e.* in the three-mode operation. Then, the repetition rate of the mode-locked pulse is Δ (0-type) or 2Δ (π-type). It has been studied theoretically by several investigators which type of self-locking will occur in normal lasers. Sargent III [21] and Bambini *et al.* [22] investigated this problem in case of a short laser tube using Lamb's equations. They found that if the active medium is placed near one mirror, "0-type" locking will occur; on the contrary, if the active medium is placed at the center of the cavity, "π-type" locking will

occur*. Statz *et al.* [67] have obtained the reverse of this result on the basis of the maximum emission principle. This discrepancy arises perhaps from the fact that the inhomogeneous broadening of the spectral line in the papers of Statz *et al.* is of the first type mentioned in the first part of this chapter. Therefore it is questionable whether their results are applicable to gas lasers.

The amplitude and phase determining equations given in Sec.3.1 have been solved numerically by Runge-Kutta-Gill method for three-mode operation ($n = 1,2,3$) of a pure isotope He-Ne^{20} laser. Parameters are identical with those used in Fig.3.4-5. From the results, stable steady state values of ψ_{2123} ($\equiv \psi$) are plotted versus asymmetry in Fig.3.4-8,9. Here the aymmetry δ is defined by

$$\delta = (\Omega_2 - \omega)/\Delta \ , \qquad (-0.5 < \delta < 0.5) \ . \tag{3.4-9}$$

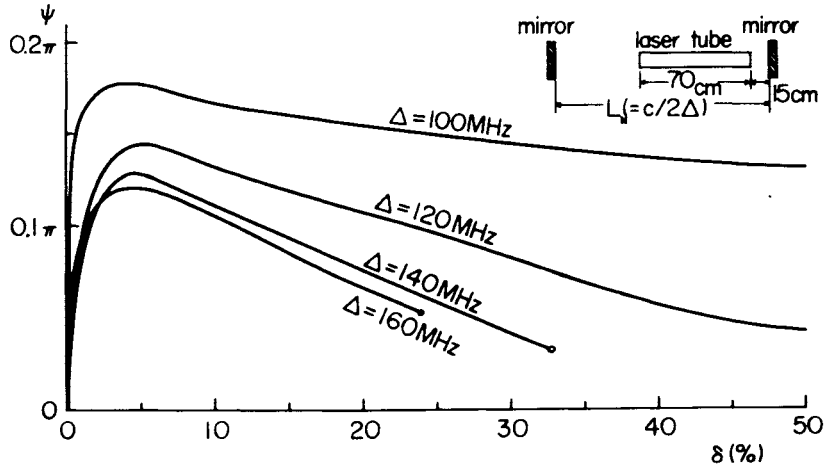

Fig.3.4-8. Phase ψ versus asymmetry δ for a normal laser (pure isotope case). $\mathcal{R} = 1.04$. "0-type locking" The small circles indicate the ends of the three-mode operation.

---

* Bambini *et al.* used the uncorrected Lamb's equations, so they obtained the reversed results. It has been assured by the author that the corrected Lamb's equations lead to the above result in their investigation.

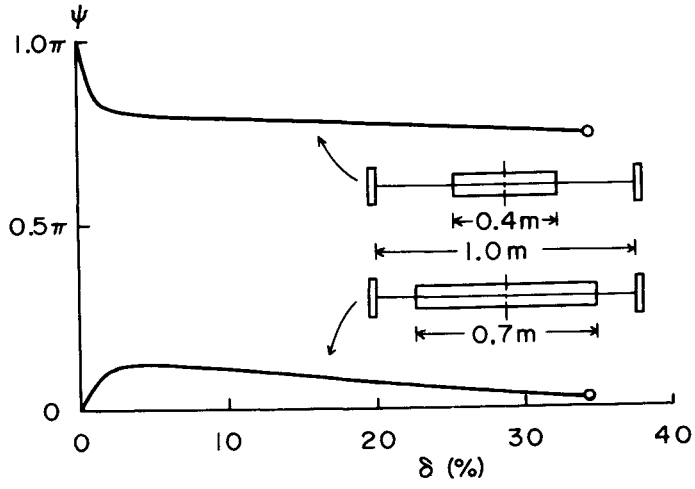

Fig.3.4-9. Phase ψ versus asymmetry δ for a normal laser (pure isotope case). $\mathcal{N} = 1.04$. $\Delta = 150$ MHz. The laser medium is at the center of the cavity.

The phase ψ is plotted only versus positive δ, since ψ is an anti-symmetric function of δ. When $\psi \simeq 0$, the locked state is called "0-type" and the repetition rate of the output pulse train is equal to the fundamental mode spacing Δ. When $\psi \simeq \pi$, it is called "π-type" and the repetition rate of the output pulse train is 2Δ and optical phase of the pulse train is varying with a repetition rate equal to Δ.

As shown in Fig.3.4-8, "0-type" locking occurs when the mode spacing $\Delta$is between 100 MHz and 160 MHz, *i.e.* the active medium occupies almost half the cavity. When Δ is smaller than 100 MHz, *i.e.* the active medium is near the end of the cavity, self-locking cannot occur stably. Also in the multimode operation, "0-type" locking occurs usually. In the experimental result shown in Fig.3.4-6, "0-type" locking occured usually and "π-type" locking occured only in a short time duration on some critical conditions, which has been also assured by Jones [23] in the three-mode operation. In the bistable region, although repetition rate of the output pulse train is double the mode spacing, it is not "π-type" locking state but alternate modes are quenched and surviving modes are in the "0-type" locking state. However it is deduced theoretically as shown in Fig.3.4-9 that

"π-type" locking will occur if a rather short laser tube is placed in the center of the cavity, which has been already assured by Sargent III. Any experimental demonstration of it has not yet been made.

In conclusion, "0-type" locking occurs usually in the normal gas laser and "π-type" locking might occur only when a rather short laser tube is placed at the center of a long cavity.

D. Phase Locking by Internal Loss-Modulation with Double the Mode Spacing

Various types of phase locking occur depending on the configuration of laser oscillator, modulation power, modulation frequency, etc., when laser oscillator is internally loss- or phase-modulated with a frequency approximately equal to a multiple of the mode spacing. In the usual phase-locked state, the total laser intensity makes a pulse train of a repetition rate equal to the mode spacing. However, when mode quenching happens or a certain phase relationship is established between the oscillating modes, a pulse train of a multiple repetition rate is generated. Hirano and Kimura [34] have made experiments on the dependence of the type of phase locking on the fine tuning and on the multiplicity of the modulation frequency, in the case of phase-modulation with frequencies approximately equal to three, four, and five times the mode spacing. Theoretical analysis of these types of phase locking has hardly been made.

D1. Theoretical Investigation

Harris and McDuff [33] have analyzed the phase locking with intracavity loss- or phase-modulation at a frequency approximately equal to the fundamental mode spacing. A theoretical analysis of the phase locking caused by the loss-modulation with double the mode spacing and experiments on a He-Ne laser oscillator will be shown in this section. The equations are given in Sec.3.1~3. In this case,

phase relationships between oscillating modes are determined predominantly by the loss-perturbation, therefore we can ignor the combination tone terms as well as the mixed isotope effect. The equations for a pure isotope case have been solved numerically using Runge-Kutta-Gill method,with $k = 2$, $\mathcal{N} = 1.07$, $L_{\mathcal{N}} = 1.5$ m ($\Delta/2\pi = 100$MHz),

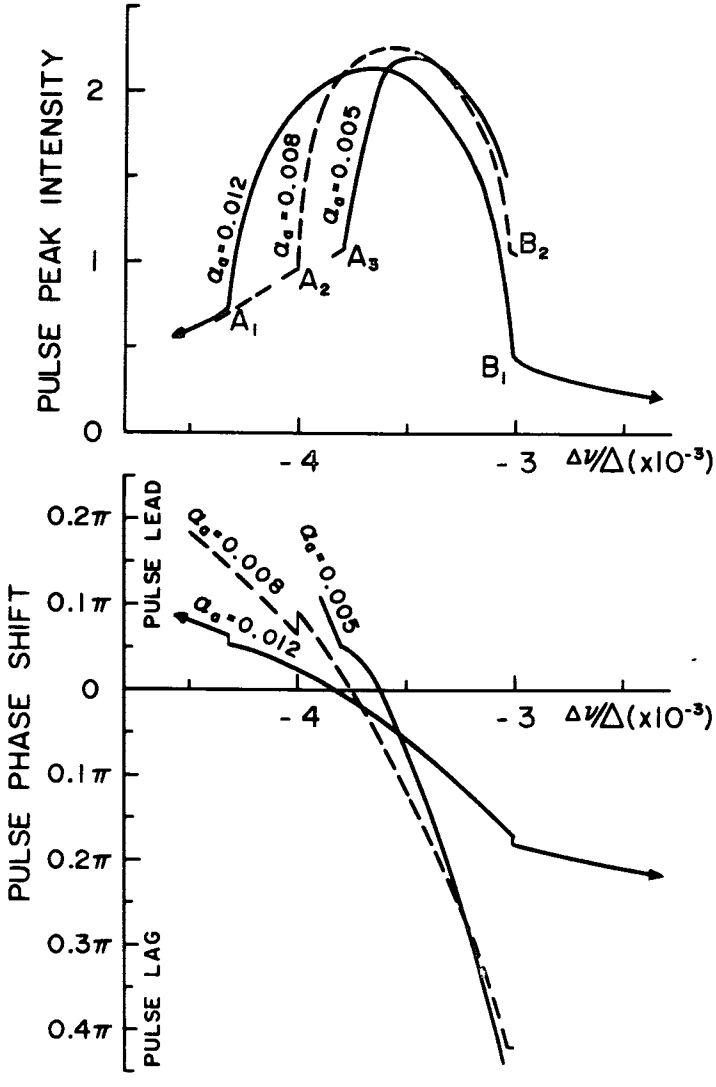

Fig.3.4-10. Peak intensity and phase shift of the forward traveling pulse versus detuning. $\nu_m \simeq 2\Delta$.

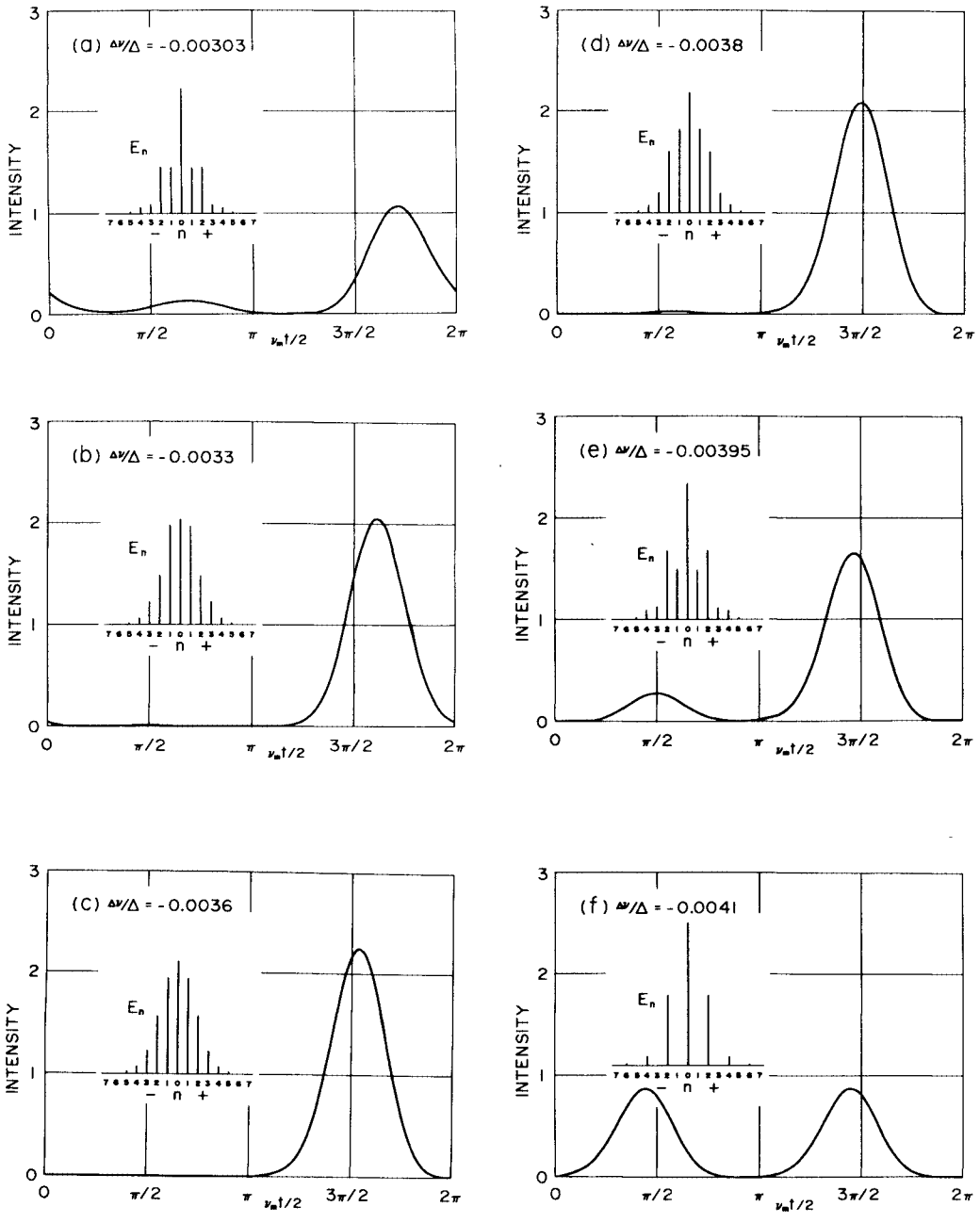

Fig.3.4-11. Output wave forms and their mode spectra of a He-Ne laser internally loss-modulated with double the mode spacing.
$k = 2$, $\alpha_a = 0.08$, $L_N = 1.5$ m .

$l = 0.02$ m , $z_0 = 0.06$ m , $Ku/2\pi = 1000$ MHz, $\gamma_1/2\pi = 25$ MHz, $\gamma_2/2\pi = 12$ MHz, $\gamma'_{12}/2\pi = 62$ MHz, $\nu/2\pi Q = 7$ MHz, and number of modes $M = 15$. In the case of steady states, the total laser intensity makes a pulse train, whose peak value is plotted versus detuning in Fig.3.4-10. Here detuning parameter $\Delta\nu$ is defined by

$$\Delta\nu = \nu_m/2 - \Delta \ . \qquad (3.4\text{-}10)$$

Phase shift of the optical pulse traveling forward (see Fig.3.1-1) from the modulation signal is also plotted versus detuning in Fig.3.4-10. Since $z_0 \neq 0$, the optical pulse lags usually at the optimum detuning which gives the maximum peak intensity. In the regions between points A_i and B_i on each curve, normal phase locking occurs and a pulse train of a repetition rate of $\nu_m/2$ is generated. In the regions outside of points A_i and B_i, alternate modes are quenched, and surviving modes are phase-locked, and a pulse train of a repetition rate of ν_m is generated. The maximum peak intensity for $\alpha_a = 0.012$ is smaller than that for $\alpha_a = 0.008$ and 0.005 because of larger average transmission loss of the modulator. The pulsive wave forms of the output beams and their mode spectra are shown in Fig.3.4-11.

The equations have been solved also for modulation with the fundamental mode spacing. The locking width is approximately equal to that of the above case, but the peak value of the pulse train with the optimum detuning is smaller about 10 % than that of the above one.

D2. Experimental Results

Experiments were also carried out on a He-Ne laser. The results are shown in Fig.3.4-12. It can be said that these results are in good qualitative agreement with the theoretical ones.

The ratio of the maximum peak intensity of the mode-quenched region to that of the normally mode-locked region is about 1/2 for $\alpha_a = 0.005$ in the theoretical results but it is $1/4 \sim 1/4.5$ in the

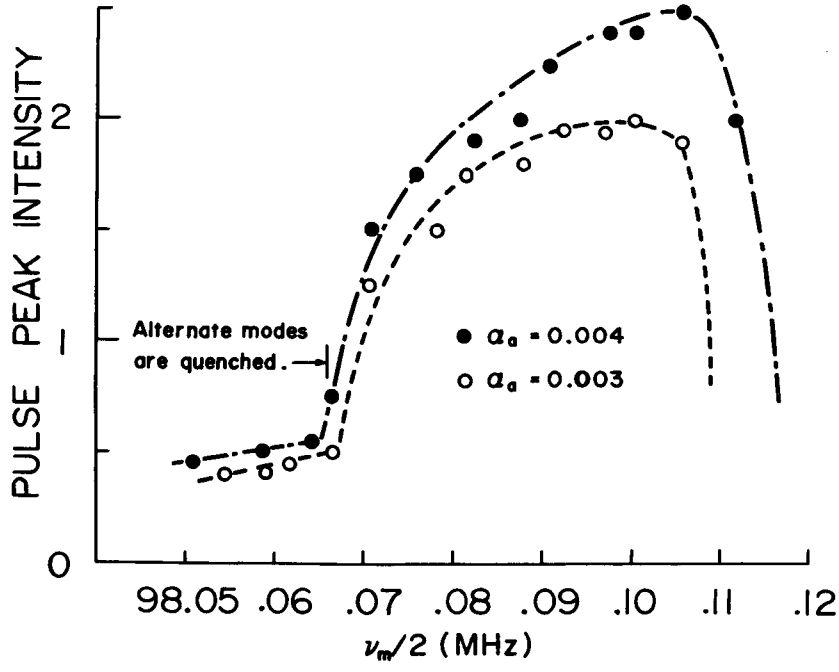

Fig. 3.4-12. Experimental results of phase locking by internal loss-modulation with double the mode spacing in a He-Ne laser.

experiments. This will be partially due to the instability of the mode-quenched region. This region is bistable. Either of the two mode groups each of which is composed of alternate cavity modes oscillates predominantely and the other mode group is completely or usually partially quenched depending upon the position of their mode spectra with respect to the gain curve which varies sufficiently with a microscopic cavity-length variation in a fraction of 1 μm. Since there were various kinds of acoustic vibrations which arrived to the experimental table, averaged wave forms of the two varying mode groups were observed on a sampling oscilloscope. The width of the mode-locked region is about 65 KHz, *i.e.* 6.5×10^{-4} in $\Delta\nu/\Delta$ for α_a = 0.004 in the experiment and 8×10^{-4} in $\Delta\nu/\Delta$ for $\alpha_a = 0.005$ in the theoretical results. This shows a good agreement.

The mode spectra and wave forms of the output pulses in the

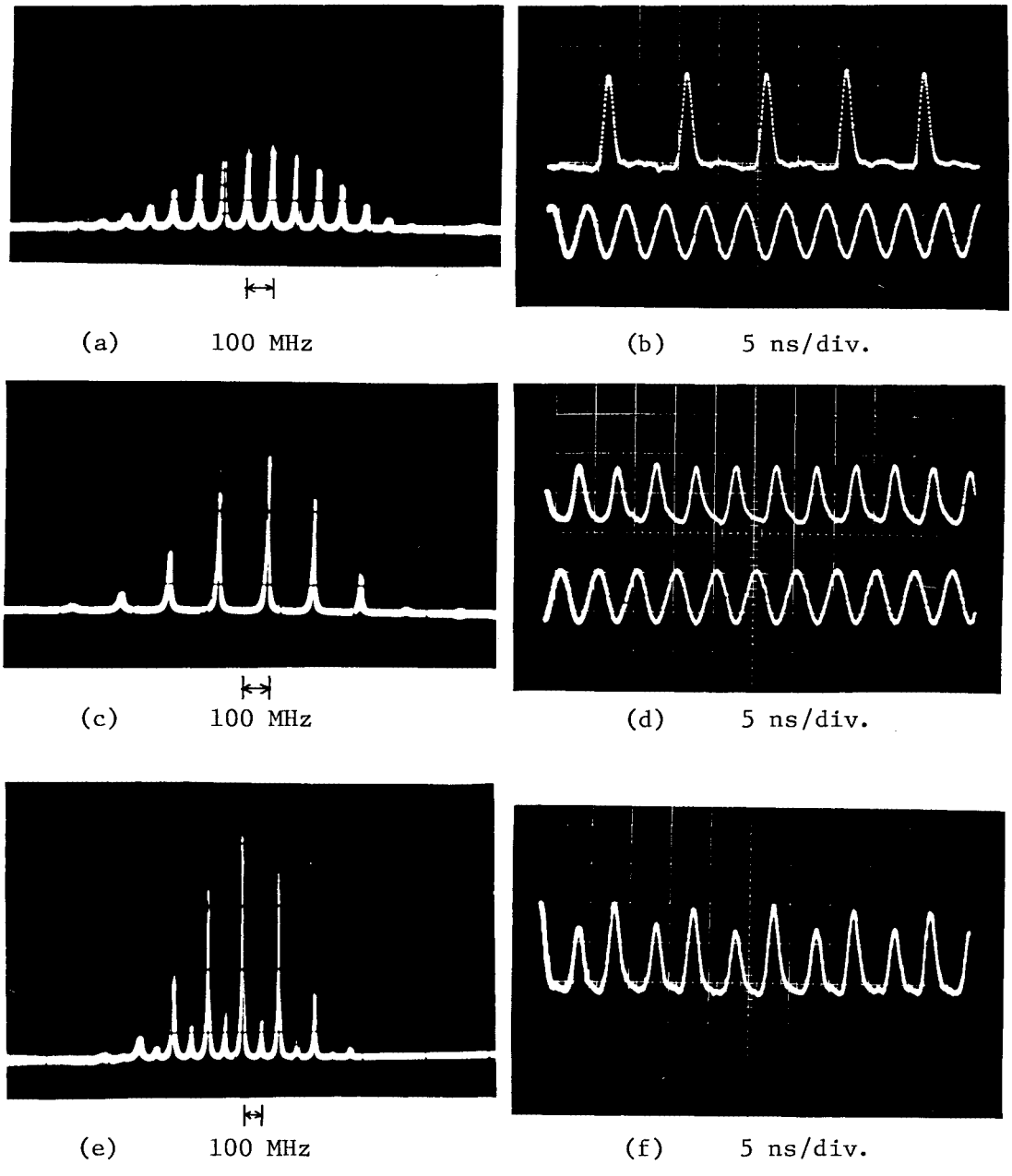

Fig. 3.4-13. Mode spectra and wave forms.
(a) Mode spectrum of normal mode locking and (b) its wave form (the lower trace is the modulation signal);
(c) and (d) for mode-quenched regions;
(e) and (f) for partially mode-quenched states.

mode quenched region as well as those in the normal mode-locked region are shown in Fig.3.4-13. Stationary mode spectra such as (c) and (e) for the mode quenched regions were obtained only temporarily. The wave forms (d) and (f) were somewhat smoothed on a sampling-oscilloscope.

D3. Experimental Technique

Block diagram of the experimental apparatus is shown in Fig.3.4-14. The cavity length L_N was approximately 1.5 m, so the fundamental

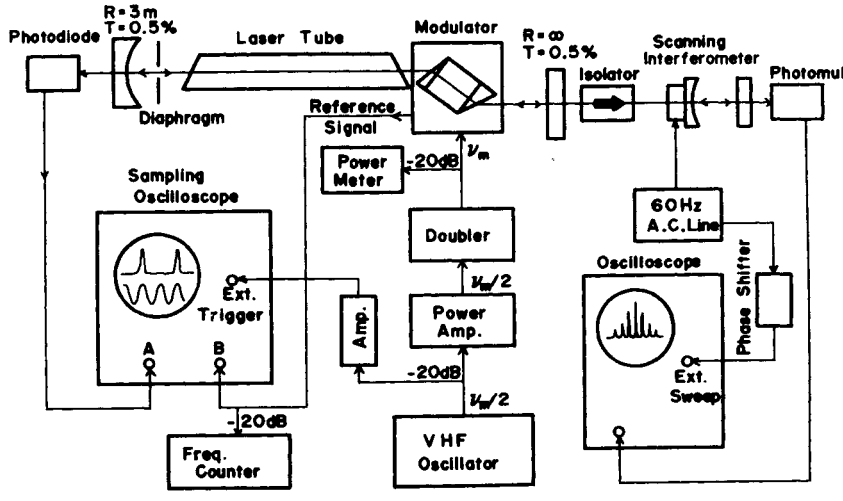

Fig.3.4-14. Block diagram of the experimental apparatus.

mode spacing $\Delta/2\pi \simeq 100$ MHz. The excitation level $\mathcal{N}$ was approximately 1.07 which corresponds to five or six mode free-running. The effective length of the He-Ne laser tube is 70 cm. The parameters are almost identical with those used in the theoretical investigation. With the aid of a doubler, although the modulation frequency was ν_m, the sampling oscilloscope was triggered at a frequency $\nu_m/2$. Otherwise the output wave forms in the normal locking region can not be traced correctly on the sampling oscilloscope.

The loss-modulator is composed of 0°z-cut KDP crystal ($7 \times 7 \times 15$

mm), BK_7 glass prism and calcite prism (Fig.3.4-15) similar to that used by Uchida [83], which is an application of the linear electro-optic (Pockel) effect.

The fractional power loss of the modulator per pass is given by

$$\alpha = \sin^2\left(\frac{\pi}{2}\cdot\frac{V}{V_\pi}\right) , \qquad (3.4\text{-}11)$$

where V is the applied voltage and V_π is the half-wave voltage of the KDP crystal given by

$$V_\pi = \lambda/(2n_0{}^3\gamma_{63}) \qquad (3.4\text{-}12)$$

with the ordinary refractive index n_0 and an electro-optic coefficient γ_{63}. Applying a small modulation signal

$$v = V_0\cos\nu_m t \qquad (3.4\text{-}13)$$

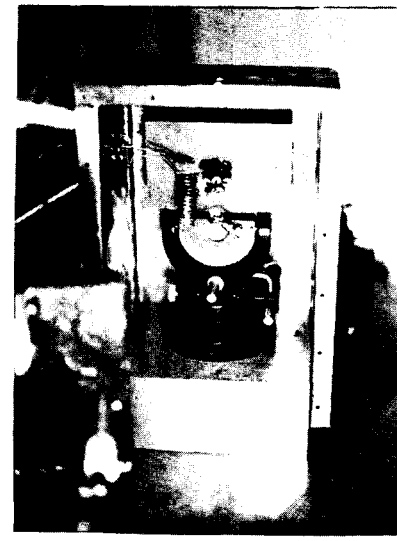

(a)

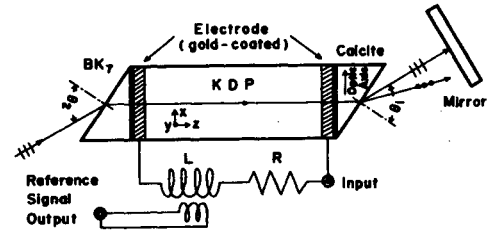

(b)

Fig.3.4-15. Loss-Modulator. In the figure (b), θ_1 and θ_2 are Brewster angles for calcite and BK_7 respectively.

to the modulator with a bias voltage V_B as shown in Fig.3.4-16, we obtain the time-varying fractional power loss per pass

$$\alpha \simeq \sin^2\left(\frac{\pi}{2}\cdot\frac{V_B}{V_\pi}\right) + \frac{\pi}{2}\cdot\frac{V_0}{V_\pi}\sin\left(\pi\frac{V_B}{V_\pi}\right)\cos\nu_m t \ . \qquad (3.4\text{-}14)$$

Then the amplitude of the fractional power loss per pass α_a defined in Sec.3.3 is given by

$$\alpha_a = \frac{\pi}{2} \cdot \frac{V_0}{V_\pi} \sin\left(\pi \frac{V_B}{V_\pi}\right) . \qquad (3.4\text{-}15)$$

The modulator can be also optically biased by nodding slightly itself and the bias point V_B can be determined by applying the commercial A.C. line and watching the intensity of the transmitted light beam as shown in Fig. 3.4-17. The capacitance of the KDP crystal and an induction coil are designed to make a series resonance circuit (Fig. 3.4-15), and impeadance of the circuit at resonance frequency

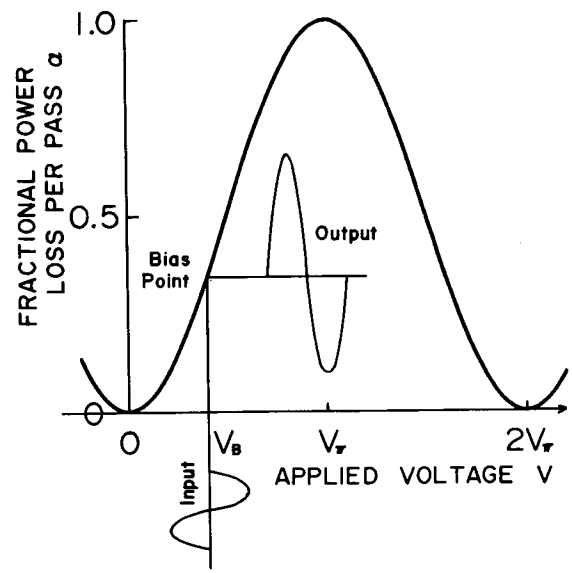

Fig.3.4-16. Fractional power loss of the loss-modulator per pass versus applied voltage.

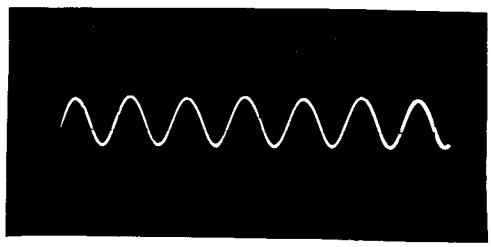

(a) $V_0 < V_B$

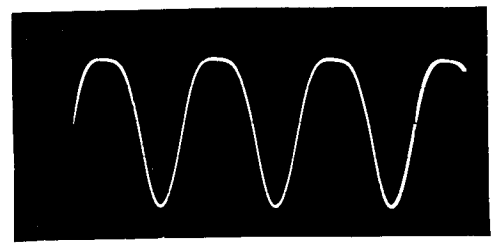

(b) $V_0 = V_B$

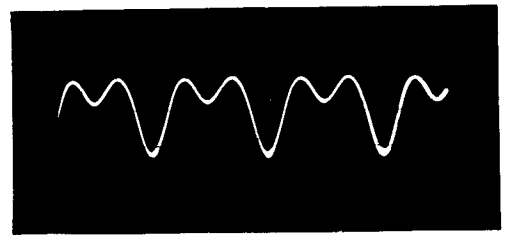

(c) $V_0 > V_B$

Fig.3.4-17. Measurement of the optical bias point V_B of the slightly nodded modulator. V_0 is the amplitude of the applied test signal (60 Hz).

is made 50Ω within a 1% error. The voltage v applied to KDP crystal is Q times as large as the voltage applied to the circuit and the Q value is determined from the resonance curve of the circuit. In the experiments, V_{π} = 9.1kv, $V_{\beta} = \sqrt{2} \times 300$ v, $V_0 = \sqrt{2} \times 2 \sim \sqrt{2} \times 18$ v, $Q \simeq 7.0$. The optical isolator is composed of a Rochon prism and a Fresnel rhomb. It prevents the externally reflected light beam from re-entering into the resonator so that the laser oscillator is not disturbed. Mode spectra were observed by the scanning Fabry-Perot interferometer [84] whose spacing was scanned at 60 Hz by an electro-strictive vibrator of $BaTiO_3$ (Fig. 3.4-18) and a photomultiplier RCA 7102. Instantaneous intensity of the output laser beam was detected by a high-speed response (rise time < 1 ns) PIN photodiode *hp*4204.

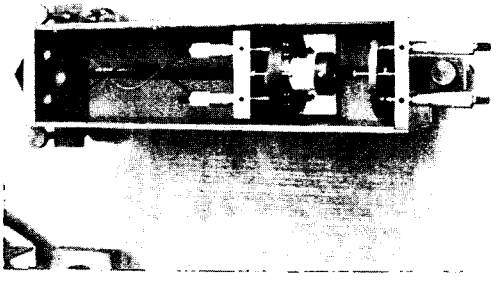

Fig.3.4-18. Scanning Fabry-Perot interferometer

3.5. Unidirectional Traveling-Wave Ring Laser

We can obtain unidirectional traveling-wave oscillation in a ring laser by i) inserting a nonreciprocal optical element such as a Faraday isolator [45], ii) using such a nonreciprocal ring resonator [43] as shown in Fig.3.5-1, iii) internal loss-modulation (Sec.3.6), or iv) using an unstable ring resonator [44].

Mode competition or saturation effects are weaker in the unidirectional ring laser than in the normal laser, since there is no mirror mode competition or saturation mentioned in Sec.3.4, in other words, no mode competition between the oppositely traveling-waves, which is shown in the fact that Lamb dip does not appear in the unidirectional ring laser, and that the mode spectrum is fairly symmetrical in the multimode operation [46]. Thus the output beam from the unidirectional ring laser will have larger peak intensity than the normal laser.

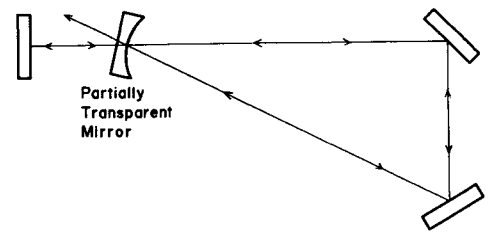

Fig.3.5-1. A nonreciprocal ring resonator.

In this section we will investigate the unidirectional ring laser with a nonreciprocal optical element. The results may be also applied to the dynamically obtained unidirectional oscillation by internal loss-modulation (Sec.3.6).

A. Self-Phase Locking

Some differences will appear in the self-phase locking between a normal standing-wave laser and a unidirectional traveling-wave laser.

A1. Theoretical Investigation

The amplitude and phase determining equations for the unidirectional three-mode operation are obtained from Secs.3.1 and 3.2, including the mixed isotope case, as follows:

$$\dot{E}_1 = \alpha_1 E_1 - \beta^{a} E_1{}^3 - \theta^{a}_{12} E_1 E_2{}^2 - \theta^{a}_{13} E_1 E_3{}^2 - (\eta^{a}_{21}\cos\psi - \xi^{a}_{21}\sin\psi) E_2{}^2 E_3 \ ,$$

$$\dot{E}_2 = \alpha_2 E_2 - \beta^{a} E_2{}^3 - \theta^{a}_{12} E_2 E_1{}^2 - \theta^{a}_{12} E_2 E_3{}^2 - \eta^{a}_{13}\cos\psi \cdot E_1 E_2 E_3 \ ,$$

$$\dot{E}_3 = \alpha_3 E_3 - \beta^{a} E_3{}^3 - \theta^{a}_{13} E_3 E_1{}^2 - \theta^{a}_{12} E_3 E_2{}^2 - (\eta^{a}_{21}\cos\psi + \xi^{a}_{21}\sin\psi) E_2{}^2 E_1 \ , \tag{3.5-1}$$

$$\dot{\phi}_1 = \sigma_1 + \tau^{a}_{12} E_2{}^2 + \tau^{a}_{13} E_3{}^2 - (\eta^{a}_{21}\sin\psi + \xi^{a}_{21}\cos\psi) E_2{}^2 E_3 / E_1 \ ,$$

$$\dot{\phi}_2 = \sigma_2 - \tau^{a}_{12} E_1{}^2 + \tau^{a}_{12} E_3{}^2 + \eta^{a}_{13}\sin\psi \cdot E_1 E_3 \ ,$$

$$\dot{\phi}_3 = \sigma_3 - \tau^{a}_{13} E_1{}^2 - \tau^{a}_{12} E_2{}^2 - (\eta^{a}_{21}\sin\psi - \xi^{a}_{21}\cos\psi) E_2{}^2 E_1 / E_3 \ , \tag{3.5-2}$$

where

$$\psi \equiv \psi_{2123} = 2\phi_2 - \phi_1 - \phi_3 \ , \tag{3.5-3}$$

$$\eta^{a}_{21} \equiv \eta^{a}_{3,212} = \eta^{a}_{1,232} \ , \quad \eta^{a}_{13} \equiv \eta^{a}_{2,123} + \eta^{a}_{2,321}$$

$$\xi^{a}_{21} \equiv \xi^{a}_{3,212} = -\xi^{a}_{1,232} \ . \tag{3.5-4}$$

From the phase determining equations, we find

$$\dot{\psi} = A + B\sin\psi + C\cos\psi \ , \tag{3.5-5}$$

where

$$A = 2\sigma_2 - \sigma_1 - \sigma_3 - (2\tau^{a}_{12} - \tau^{a}_{13})(E_1{}^2 - E_3{}^2) \ ,$$

$$B = 2\eta^{a}_{13} E_1 E_3 + \eta^{a}_{21}(E_3/E_1 + E_1/E_3) E_2{}^2 \ ,$$

$$C = \xi^{a}_{21}(E_3/E_1 - E_1/E_3)E_2{}^2 \ . \qquad (3.5\text{-}6)$$

To obtain a simple criterion, we now consider a special case that the three oscillating modes are almost symmetric against the gain curve, then $E_1 \simeq E_3$, and

$$A \simeq C \simeq 0 \ . \qquad (3.5\text{-}7)$$

The stable steady-state solution is given by

$$\psi = 0 \quad \text{when } B < 0, \qquad (3.5\text{-}8)$$

and

$$\psi = \pi \quad \text{when } B > 0, \qquad (3.5\text{-}9)$$

Now, η^{a}_{13} is always positive, but η^{a}_{21} is positive or negative according as the mode spacing Δ is smaller or larger than a certain value which is approximately equal to $\sqrt{\gamma'_{12}(\gamma_1+\gamma_2)/2}$. Thus B is positive or negative *i.e.* self-locking is "π-type" or "0-type", according as the mode spacing is smaller or larger than a certain value.

Admixture of an isotope will make no qualitative effects in the unidirectional ring laser, since all the coupling coefficients are independent of the transient frequencies ω' and ω'' of the two isotopes and only the unsaturated gain α curve and its dispersion σ curve become slightly asymmetric as shown in Secs.3.2 and 3.4.

To obtain exact solutions Eqs.(1) and (5) have been solved numerically for a pure isotope He-Ne laser. Steady state solutions are shown in Fig.3.5-2 and 3. As in the normal laser, ψ is an antisymmetric function of δ.The length of the active medium and the decay rates are identical with those used for the normal laser in Sec.3.4. In this case, "0-type" or "π-type" locking occurs according as the mode spacing is larger or smaller than 120 MHz. At transient

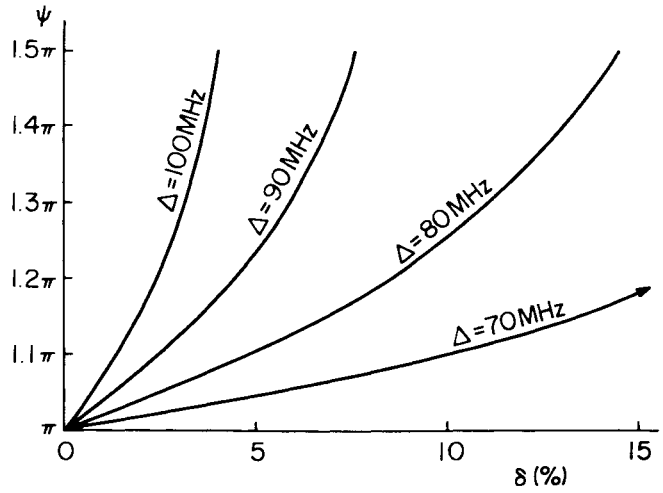

Fig. 3.5-2. Phase ψ versus asymmetry δ. $\mathfrak{N}$ = 1.04. "π-type locking"

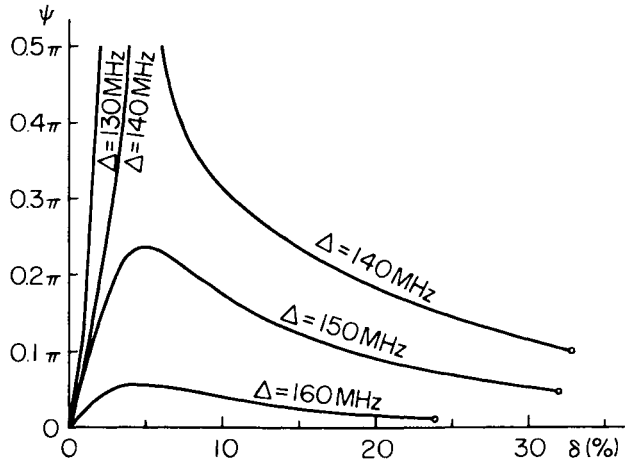

Fig. 3.5-3. Phase ψ versus asymmetry δ. $\mathfrak{N}$= 1.04. "0-type" The small circles indicate the ends of the three-mode operation.

mode spacings, permissible asymmetry δ for self-locking is very narrow. At Δ = 140 MHz, an interruption of self-locking occurs in a region of δ. These phenomena are characteristic of the ring laser (cf. Figs. 3.4-8 and 9).

A2. Experimental Results

A unidirectional traveling-wave ring laser has been constructed with a He-Ne laser tube (70 cm long), three mirrors, and a Faraday isolator as shown in Fig.3.5-4~5. The Faraday isolator is composed of the lead glass (one end face Brewster-cutted, 2 cm long,

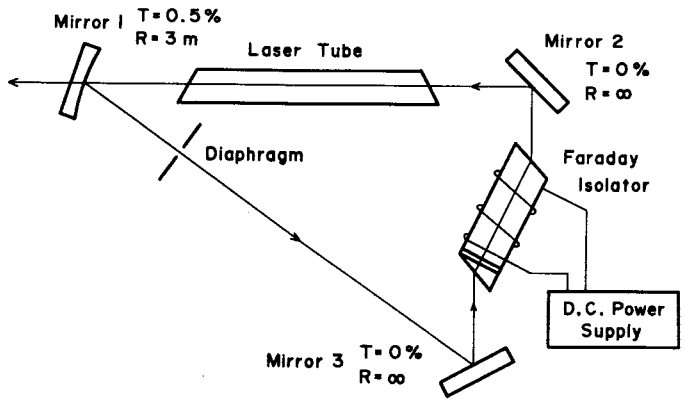

Fig.3.5-4. Constitution of the unidirectional traveling-wave ring laser. The mirrors 2 and 3 are designed for a incident angle 45°.

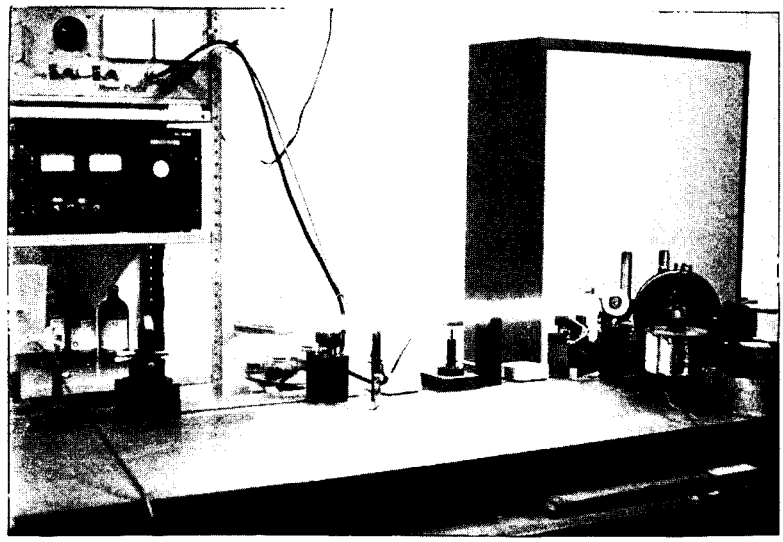

Fig.3.5-5(a). The unidirectional traveling-wave ring laser.

refractive index $n = 2.0$, absorption coefficient $\alpha = 0.01$/cm, Verdet constant $V = 0.08'$/cm-gauss at 6328 Å), a quartz half-wave plate, and a BK_7 prism. The principal axis of the quartz half-wave plate is rotated by 3° from the direction of the dominant electric polarization of the resonator which is determined by Brewster windows, so that the additional 5 % transmission loss is imposed on one direction. The required magnetic flux density for unidirectional oscillation was about 2000 gauss.

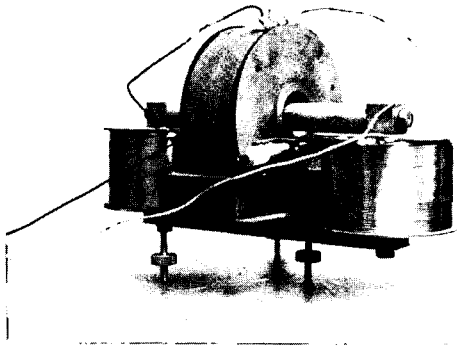

Fig.3.5-5(b) The Faraday isolator.

The observed self-locking regions are shown in Fig.3.5-6. It is shown in the figure that 0-type or π-type locking occurs according as the mode spacing $\Delta/2\pi$ is larger or smaller than about 65 MHz. This transient frequency of 65 MHz is largely different from the theoretically evaluated value 120 MHz for the three-mode operation. This discrepancy will be partially due to a difference of the number

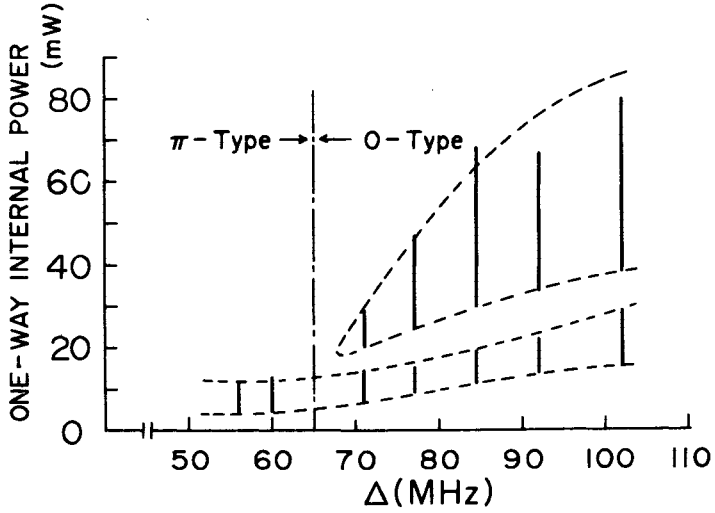

Fig.3.5-6. Self-phase locking of a He-Ne unidirectional traveling-wave ring laser. Solid lines show phase-locked region.

of the oscillating modes between the experiment and the theory, and to the mechanical instability of the laser oscillator. Due to random mechanical variation of the cavity length, the oscillating modes were not always fixed symmetrically to the gain curve, *i.e.* $\delta \neq 0$, but drifted back and forth at random. Even in a π-type locking state, the phase ψ is equal to π only when $\delta = 0$ as shown in Figs.3.5-2 and 3. Therefore the first beat note does not neccessarily vanish nor neccessarily become smaller than the second one. However, since there have been no other criteria to be applied, a locked state is considered to be "π-type" in Fig.3.5-6 if the first beat note is smaller than the second one as shown in Fig.3.5-7. Hence the π-type locking region will be underestimated.

It should be noticed that these self-phase locking characteristics of the unidirectional traveling-wave ring laser differ very markedly from that of the normal standing-wave laser discussed in Sec.3.4 (see Fig.3.4-6). For small mode spacing Δ, mode quenching occurs in the normal laser; on the other hand, π-type locking occurs in the unidirectional traveling-wave laser. However, the repetition rate of the output pulse train is equal to 2Δ in both cases. One of

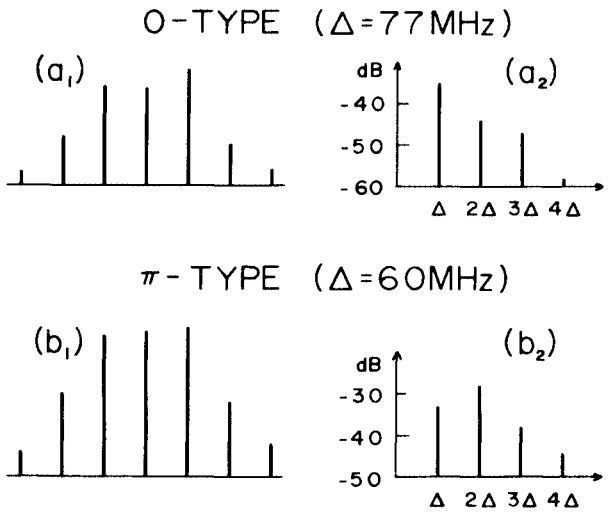

Fig.3.5-7. Examples of mode spectra (left) and beat spectra (right) for 0-type and π-type lockings.

the reasons for this difference will be that there is no mirror-mode competition in the unidirectional ring laser.

Since insertion loss of the Faraday isolator was rather large, the oscillation intensity was so small that the intensity of the electric signal obtained by detection of the output laser beam with a photodiode was insufficient for a sampling oscilloscope, although it was enough for a spectrum analyzer. Hence wave forms of the output beams could not be observed.

B. Phase-Locking by Internal Loss-Modulation

Phase-locking phenomena in the unidirectional traveling-wave ring laser with internal loss-modulation were investigated theoretically as in the normal laser in Sec.3.4. The numerical results are shown in Fig.3.5-8. Numerical results for the normal laser on the same condition are also plotted for a comparison. In the regions with

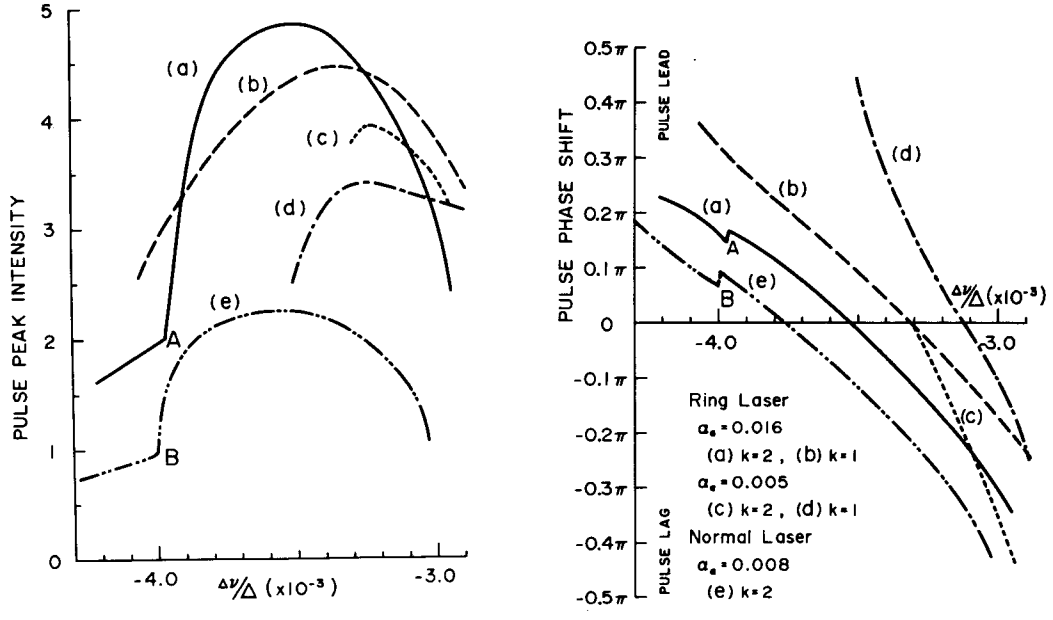

Fig.3.5-8. Pulse peak intensity and phase shift versus detuning. $L = L_R = 2L_N = 1.5$ m ($\Delta/2\pi = 100$ MHz). Parameters are identical with those for the normal laser in Sec.3.4.

smaller $\Delta\nu$ than the points A or B on the two curves, alternate modes are quenched and the surviving modes are phase-locked. In the other locked regions, normal phase locking occurs. In qualitative behavior, the ring and normal lasers are identical, but there are some distinct differences in quantity. Since L_R corresponds to $2L_N$, modulation effect in the ring laser is half as large as that in the normal laser, which will be understood from Eqs.(3.3-7),(3.3-8),(3.3-11), and (3.3-12). Therefore the locking width is narrower in the ring laser than in the normal laser. However the pulse peak intensity of the ring laser at optimum detuning is about twice as large as that of the normal laser on the same condition as expected at the beginning of this section. At optimum detuning, the pulse peak intensity with $k = 2$ ($\nu_m \simeq 2\Delta$) is larger about 10 % than that with $k = 1$ ($\nu_m \simeq \Delta$).

3.6. Bidirectional Traveling-Wave Ring Laser

The greatest interest of this section is in phase locking and competition between the oppositely directed traveling-waves in a ring laser. To begin with, a qualitative investigation will be made for the simplest two-mode operation and an insight into the general behavior in the multimode operation will be obtained. Next numerically obtained exact solutions will be shown for two- and five-mode operations. Detailed experimental results [52,53] on a He-Ne ring laser will be shown compared with the theoretical results.

A. Self-Phase Locking

In a bidirectional ring laser, there exist two kinds of self-phase locking. One is the usual one, as in a normal laser, in the clockwise (cw) traveling modes or in the counter-clockwise (ccw) traveling modes. The other is the one between the oppositely traveling (OT) waves. The former makes OT waves pulse trains of a repetition rate $n\Delta$ ($n = 1,2,...$) and the latter locks the phases of the OT pulse

trains. The bidirectional two-mode operation is the simplest one in which the second kind of self-phase locking occurs. The phase determining equations in this operation are given, including mixed isotope case, as

$$\dot{\phi}_1^{\ell} = \Sigma_1^{\ell} + (\tau_{12}^{c}\cos\phi^{-} - \theta_{12}^{c}\sin\phi^{-})E_2^{\ell}E_2^{r}E_1^{r}/E_1^{\ell} , \qquad (3.6\text{-}1)$$

$$\dot{\phi}_2^{\ell} = \Sigma_2^{\ell} + (\tau_{21}^{c}\cos\phi^{-} + \theta_{21}^{c}\sin\phi^{-})E_1^{\ell}E_1^{r}E_2^{r}/E_2^{\ell} , \qquad (3.6\text{-}2)$$

$$\dot{\phi}_1^{r} = \Sigma_1^{r} + (\tau_{12}^{c}\cos\phi^{-} + \theta_{12}^{c}\sin\phi^{-})E_2^{r}E_2^{\ell}E_1^{\ell}/E_1^{r} , \qquad (3.6\text{-}3)$$

$$\dot{\phi}_2^{r} = \Sigma_2^{r} + (\tau_{21}^{c}\cos\phi^{-} - \theta_{21}^{c}\sin\phi^{-})E_1^{r}E_1^{\ell}E_2^{\ell}/E_2^{r} , \qquad (3.6\text{-}4)$$

where

$$\Sigma_n^{\alpha} = \sigma_n^{\alpha} + \tau_{nm}^{a}(E_m^{\alpha})^2 + \tau_{nn}^{b}(E_n^{\beta})^2 + \tau_{nm}^{b}(E_m^{\beta})^2 ,$$

$$n, m = 1, 2; \qquad \alpha, \beta = r, \ell, \qquad (3.6\text{-}5)$$

and

$$\phi^{-} = (\phi_2^{\ell} - \phi_1^{\ell}) - (\phi_2^{r} - \phi_1^{r}) . \qquad (3.6\text{-}6)$$

It is impossible to obtain exact analytical solutions of the above equations, thus the exact solutions should be numerical ones. However, approximate solutions give an insight into the general behavior of the exact solutions.

Usually

$$\Omega_n^{\ell} = \Omega_n^{r} , \quad E_n^{\ell} \simeq E_n^{r} \ (\equiv E_n) , \quad n = 1, 2 . \qquad (3.6\text{-}7)$$

Then, from Eqs.(1)-(4),

$$\dot{\phi}^{-} = 2(\theta_{12}^{c}E_2^{\,2} + \theta_{21}^{c}E_1^{\,2})\sin\phi^{-} . \qquad (3.6\text{-}8)$$

Stable steady state solution of this equation is

$$\text{(i)} \quad \phi^- = \pi \quad \text{when} \quad S > 0 \ , \tag{3.6-9}$$

$$\text{(ii)} \quad \phi^- = 0 \quad \text{when} \quad S < 0 \ , \tag{3.6-10}$$

where

$$S = \theta^{c}_{12} E_2^{\,2} + \theta^{c}_{21} E_1^{\,2} \ . \tag{3.6-11}$$

Crossing points z_c of the cw and ccw traveling-wave packets are related with the phase difference ϕ^- by

$$z_c = -\frac{\phi^-}{4\pi} L_R + \frac{L_R}{4} \pm \frac{L_R}{4} \ . \tag{3.6-12}$$

Evaluating θ^{c}_{12} and θ^{c}_{21}*, we find that they are positive or negative approximately according as $\Delta \lesseqgtr \sqrt{\gamma'_{12}(\gamma_1 + \gamma_2)}$ in the pure isotope (Ne^{20}) case, on the contrary, S is always positive for ordinary mode spacing Δ in the mixed isotope (Ne^{20}, Ne^{22}) case. In other words, the OT wave packets encounter at $z = 0$ (center of the laser medium) and $L_R/2$, or at $z = \pm L_R/4$ according as $\Delta \gtreqless \sqrt{\gamma'_{12}(\gamma_1 + \gamma_2)}$ in the pure isotope case, however, in the mixed isotope case, they encounter always at $z = \pm L_R/4$.

Exact numerical solutions of the amplitude and phase determining equations show that the above investigation is correct (see Fig.3.6-1). In the pure isotope case, the crossing points are at $z = \pm L_R/4$ when $\Delta/2\pi < 70$ MHz which is equal to $\sqrt{\gamma'_{12}(\gamma_1 + \gamma_2)}/2\pi$, however, when $\Delta/2\pi >$ 70 MHz, the laser makes bistable unidirectional two-mode oscillation due to mirror mode competition between OT waves since the modes deviate far from the line center and get only small gain. In the mixed isotope case, the crossing points are also at $z = \pm L_R/4$ when

---

* Here we assume that $N_2 > 0$, *i.e.* the length of the active medium is less than one half of the perimeter of the ring resonator. This assumption is usually fulfilled.

$\Delta/2\pi > 60$ MHz, however, when $\Delta/2\pi < 60$ MHz, the laser makes bidirectional one-mode oscillation since the holes burned by the two modes overlap largely with each other and they have unequal gain. In this case mirror mode competition is very weak since the gain curve is a superposition of two lines with different center frequencies, therefore unidirectional oscillation does not occur. This has been

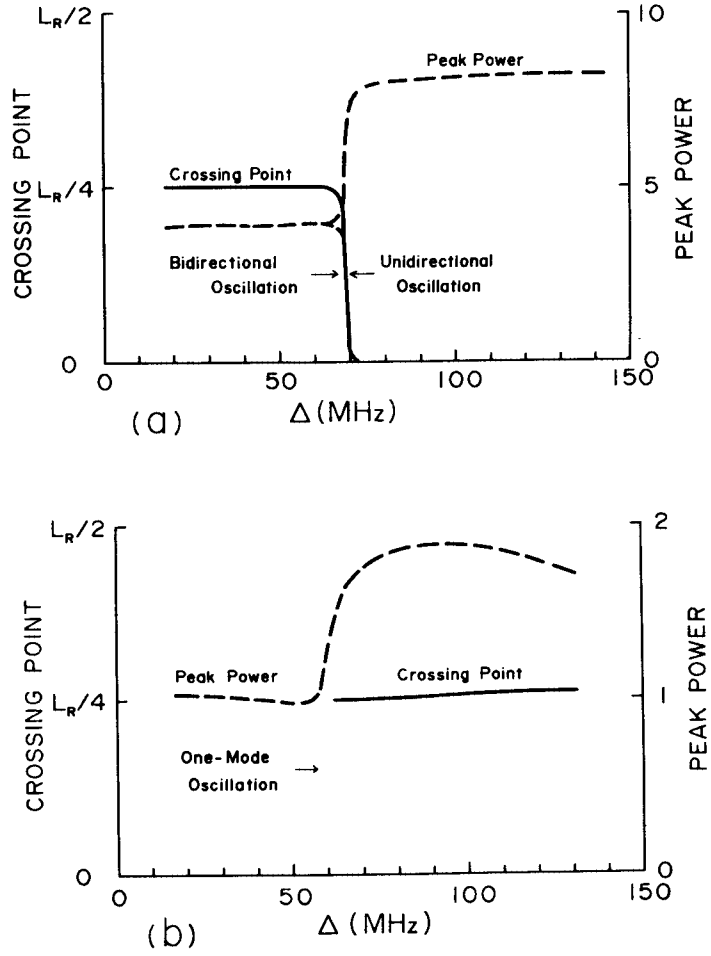

Fig. 3.6-1. Crossing point and peak power versus mode spacing in a bidirectional two-mode ring laser. $Ku/2\pi = 1000$MHz, $\gamma_1/2\pi = 34$MHz, $\gamma_2/2\pi = 15$MHz, $\gamma'_{12}/2\pi = 100$MHz, $\sqrt{\gamma'_{12}(\gamma_1+\gamma_2)}/2\pi \simeq 70$MHz. (a) pure isotope ($Ne^{20}$) case. $\mathcal{N}^{\ell} = \mathcal{N}^{r} = 1.04$, $\omega = (\Omega_1+\Omega_2)/2$. (b) mixed isotope case. $Ne^{20} : Ne^{22} = 0.91 : 0.09$, $(\Omega_1+\Omega_2)/2 - \omega' = 2\pi \times 60.0$MHz, $\mathcal{N}^{\ell} = 1.07$, $\mathcal{N}^{r} = 1.07007$.

derived theoretically in the single-mode operation by Aronowitz [38] and also verified experimentally by Hutchings *et al.* [39].

Experiments were made on a He-Ne laser of natural neon (mixed isotopes). Crossing points were measured from the visibility curve of the interference pattern of the OT pulses and also by observing directly the instantaneous intensities of the OT pulses on a sampling oscilloscope using high speed PIN photodiodes. The crossing points were verified to be at $z = \pm L_R/4$ independent of number of oscillating modes with realizable mode spacing (50 MHz $< \Delta/2\pi <$ 150 MHz), which is completely in good agreement with the theoretical results in the mixed isotope case. These points are called natural crossing points

B. Phase-Locking and Competition between the Oppositely Directed Traveling-Waves by Internal Loss-Modulation

Locking region of the bidirectional traveling-wave oscillation (BTWO) by internal modulation does not coincide with that of the unidirectional traveling-wave oscillation (UTWO) in modulation frequency. Therefore, there are such frequency regions where only the UTWO can be phase-locked or it has larger total average power than the BTWO. It may be expected that, in those regions, the UTWO becomes stable. In other words, mode competition between the OT waves is intensified by the internal modulation depending upon its frequency. In the other regions, the ring laser oscillates bidirectionally.

B1. Approximate Analytical Investigation

An internally loss-modulated ring laser of the most simple symmetrical two-mode operation will be investigated analytically in the pure isotope case. In this operation,

$$\Omega_n^{\ell} = \Omega_n^{r} \equiv \Omega_n \quad (n = 1, 2),$$

$$\omega = (\Omega_1 + \Omega_2)/2 \ ,$$

then it may be assumed that

$$E_1^{\alpha} = E_2^{\alpha} \equiv E^{\alpha} \qquad (\alpha = r,\ l) \ . \tag{3.6-13}$$

Let us introduce new variables

$$\phi^+ = \phi_l + \phi_r \ , \qquad \phi^- = \phi_l - \phi_r \ ,$$

$$I^+ = I_l + I_r \ , \qquad I^- = I_l - I_r \ , \tag{3.6-14}$$

where

$$\phi_l = \phi_2^l - \phi_1^l \ , \quad \phi_r = \phi_2^r - \phi_1^r \ , \quad I_l = (E^l)^2 \ , \quad I_r = (E^r)^2 \ ,$$

then we find that the equations of the ring laser given in Sec.3.1 become

$$\frac{1}{2}\dot{\phi}^+ = -\Delta\nu - 2\sigma_1 + (\tau_{21}^a + \tau_{22}^b)I^+ + \tau_{21}^c I^+ \cos\phi^- - \theta_{12}^c I^- \sin\phi^-$$

$$+ 2\alpha \sin\frac{\phi^+}{2}\cos\left(\frac{\phi^-}{2} + \frac{2\pi z_0}{L_R}\right),$$

$$\frac{1}{2}\dot{\phi}^- = (\tau_{21}^a - \tau_{22}^b)I^- + \theta_{12}^c I^+ \sin\phi^- - \tau_{21}^c I^- \cos\phi^-$$

$$+ 2\alpha\cos\frac{\phi^+}{2}\sin\left(\frac{\phi^-}{2} + \frac{2\pi z_0}{L_R}\right) \ , \tag{3.6-15}$$

$$\dot{I}^l/2I^l = \alpha_1 - (\beta^a + \theta_{12}^a)I^l - (\beta^a + \theta_{11}^b)I^r - (\theta_{12}^c \cos\phi^- - \tau_{21}^c \sin\phi^-)I^r$$

$$- \alpha_m - \alpha\cos\left(\phi_l + \frac{2\pi z_0}{L_R}\right),$$

$$\dot{I}^r/2I^r = \alpha_1 - (\beta^a + \theta_{12}^a)I^r - (\beta^a + \theta_{11}^b)I^l - (\theta_{12}^c \cos\phi^- + \tau_{21}^c \sin\phi^-)I^l$$

$$- \alpha_m - \alpha\cos\left(\phi_r - \frac{2\pi z_0}{L_R}\right) \ , \tag{3.6-16}$$

where

$$\alpha = \alpha_{c1}^R c/(2L_R) \ , \qquad \alpha_m = \alpha_a c/(2L_R) \ .$$

Here, symmetrical or antisymmetrical properties of the coefficients have been used.

From the above equations, the UTWO solution, for example ccw one, is given as

$$\phi_{\ell}^{0} + \frac{2\pi z_0}{L_R} = \pi + \theta_u \ ,$$

$$I_u \equiv I_{\ell}^{0} = (\alpha_1 - \alpha_m - \alpha\cos\theta_u)/(\beta^a + \theta_{12}^a) \ , \qquad (3.6\text{-}17)$$

where

$$\sin\theta_u = -\{\Delta\nu - (\Delta\nu_0)_u\}/(2\alpha) \qquad (-\frac{\pi}{2} \le \theta_u < \frac{\pi}{2}) \ ,$$

$$(\Delta\nu_0)_u = -2\sigma_1 + 2\tau_{21}^a I_u \ , \quad \tau_{21}^a > 0 \ .$$

Pulse phase shift from the minimum-transmission-loss phase of the modulator is given by

$$(\phi_{\ell}^{0} + \frac{2\pi z_0}{L_R}) - \pi = \theta_u \ . \qquad (3.6\text{-}18)$$

When the optical pulse leads, the pulse phase shift θ_u is positive. Let $(\Delta\nu_0)_u'$ be the value of $(\Delta\nu_0)_u$ at $\theta_u = 0$ when the oscillation intensity I_u reaches a maximum. As $\Delta\nu$ departs from $(\Delta\nu_0)_u'$, $(\Delta\nu_0)_u$ decreases. Therefore the locking region for $\Delta\nu \ge (\Delta\nu_0)_u'$ is shrunk and that for $\Delta\nu \le (\Delta\nu_0)_u'$ is expanded. Such deformation appears generally in the locking curves as shown later.

The BTWO solution with $z_0 = L_R/4$ is given as

$$\phi_0^{+} = 2\theta_B \ , \qquad \phi_0^{-} = \pi \ ,$$

$$I_B/2 \equiv I_{\ell}^{0} = I_{\gamma}^{0} = (\alpha_1 - \alpha_m + \alpha\cos\theta_B)/(2\beta^a + \theta_{12}^a + \theta_{11}^b - \theta_{12}^c) \qquad (3.6\text{-}19)$$

where

$$\sin\theta_B = -\{\Delta\nu - (\Delta\nu_0)_B\}/(2\alpha) \qquad (-\frac{\pi}{2} \le \theta_B < \frac{\pi}{2}) \ ,$$

$$(\Delta\nu_0)_B = -2\sigma_1 + (\tau_{21}^a + \tau_{22}^b - \tau_{21}^c) I_B \ .$$

In this solution, the OT waves encounter at $z = \pm L_R/4$. There is also another equilibrium solution in which the OT waves encounter at $z = 0$ and $L_R/2$. However it can not be stable* since they suffer a large loss from the modulator, which will be shown below in the exact numerical solution. The OT waves encounter at $z = z_0 = \pm L_R/4$ even if $\theta_{12}^{c} < 0$, which is not true in the self-phase locking. The pulse phase shift is given by θ_B.

The difference between the optimum detunings $(\Delta\nu_0)_U$ and $(\Delta\nu_0)_B$ for UTWO and BTWO, respectively, is given by

$$(\Delta\nu_0)_U - (\Delta\nu_0)_B = \tau_{21}^{a}(2I_U - I_B) + (\tau_{21}^{c} - \tau_{22}^{b})I_B \ .$$

Since $\tau_{21}^{a} > 0$, $I_U \simeq I_B$, and $\tau_{21}^{c} \gtrsim \tau_{22}^{b} > 0$, this difference is positive, *i.e.* the locking region of the UTWO exists on the larger side of the detuning than that of the BTWO. Therefore the UTWO will become stable in the larger $\Delta\nu$ part of the locking region in which $I_U > I_B$.

Numerically calculated values of I_U, I_B, θ_U, and θ_B are plotted versus $\Delta\nu$ in Fig.3.6-2. Parameters are $\Delta/2\pi = 100$ MHz, $\gamma_1/2\pi = 25$ MHz, $\gamma_2/2\pi = 12$ MHz, $\alpha_a = 0.01$, $\mathfrak{N} = 1.04$, and $\nu/2\pi Q = 7$ MHz. Indeed, in this figure, $I_B \gtrless I_U$ according as $\Delta\nu/\Delta \lesseqgtr -3.83 \times 10^{-3}$.

Exact analytical solutions for $z_0 \neq \pm L_R/4$ can not be given. The first order approximate solution for $z_0 = L_R/4 + l$ ($|l| << L_R$) is obtained as follows. It is the unperturbed solution for $z_0 = L_R/4$ plus small deviation from it:

$$\phi^{+} = \phi_0^{+} + \bar{\phi}^{+} \ , \qquad \phi^{-} = \phi_0^{-} + \bar{\phi}^{-} \ ,$$
$$I^{l} = I_0 + i^{l} \ , \qquad I^{r} = I_0 + i^{r} \ , \qquad (3.6\text{-}20)$$

where

$$|\bar{\phi}^{+}| \ , \ |\bar{\phi}^{-}| \ , \ |i^{l}/I_0| \ , \ |i^{r}/I_0| << 1 \ .$$

---

* The stability condition can be obtained exactly. However it is too complicated to obtain analytically its parameter dependence.

Substituting Eqs.(20) into Eqs. (15) and (16), we find the first order term:

$$\bar{\phi}^{+} = 0 , \quad i^{\ell} + i^{r} = 0 ,$$

$$\bar{\phi}^{-} = -\frac{1}{A} \times \{(\theta_{12}^{a} - \theta_{11}^{b} + \theta_{12}^{c})\cos\theta_{B} + (\tau_{21}^{a} - \tau_{22}^{b} + \tau_{21}^{c})\sin\theta_{B}\} \frac{4\pi\alpha l}{L_R} ,$$

$$i^{\ell} - i^{r} = \frac{2}{A} (-\theta_{12}^{c}\sin\theta_{B} + \tau_{21}^{c}\cos\theta_{B}) \times I_0 \frac{4\pi\alpha l}{L_R} , \qquad (3.6\text{-}21)$$

where

$$A = \begin{vmatrix} 2\theta_{12}^{c} I_0 + \alpha\cos\theta_{B} & -(\tau_{21}^{a} - \tau_{22}^{b} + \tau_{21}^{c}) \\ 2\tau_{21}^{c} I_0 + \alpha\sin\theta_{B} & \theta_{12}^{a} - \theta_{11}^{b} + \theta_{12}^{c} \end{vmatrix} .$$

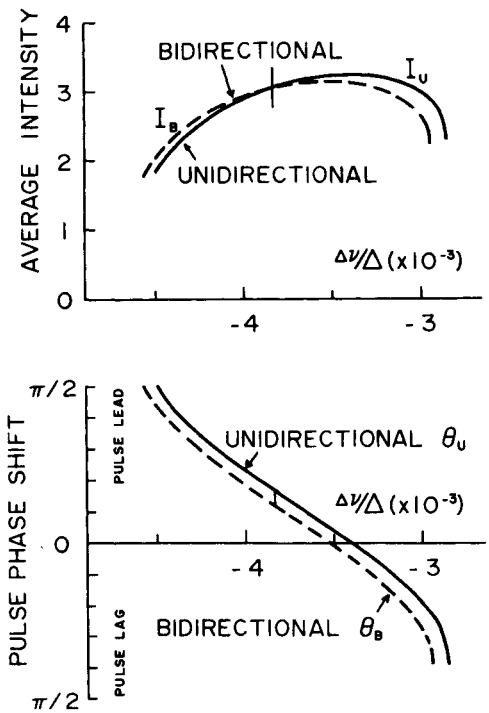

Fig.3.6-2. Comparison of locking characteristics of UTWO and BTWO. $z_0 = L_R/4$.

It is shown in this solution that the total average intensity $I^{\ell} + I^{r}$ is kept constant in the first order approximation and that the cw and ccw traveling intensities I^{ℓ} and I^{r} depart from each other in proportion to l. Numerical examples of this solution are shown in Fig.3.6-3 for $l = \pm 0.05 L_R$. Parameters are identical with those for Fig.3.6-2. Pulse phase shifts of cw and ccw traveling-wave pulses are, respectively,

$$(\phi_r - \frac{2\pi z_0}{L_R}) + \pi = \theta_B - \frac{\bar{\phi}^{-}}{2} - \frac{2\pi l}{L_R} ,$$

$$(\phi_{\ell} + \frac{2\pi z_0}{L_R}) - \pi = \theta_B + \frac{\bar{\phi}^{-}}{2} + \frac{2\pi l}{L_R} .$$

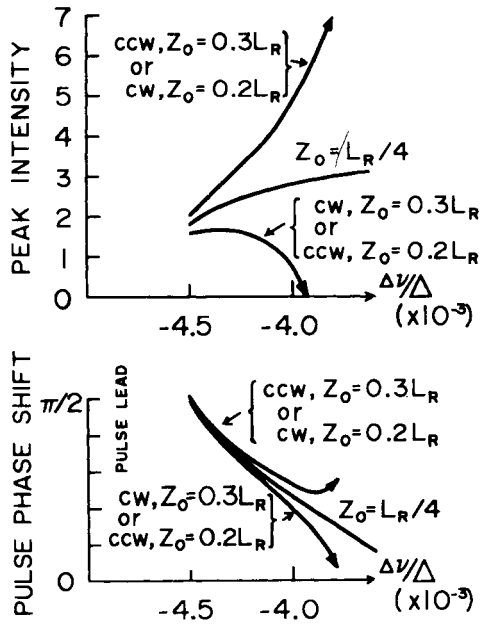

Fig.3.6-3. First order approximate solution for $l = \pm 0.05 L_R$ *i.e.* $z_0 = 0.3L_R$ and $0.2L_R$.

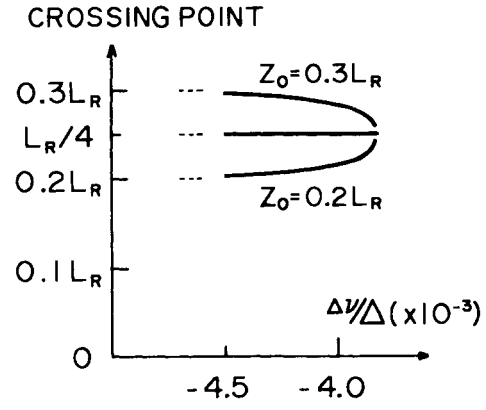

Fig.3.6-4. Crossing point z_c versus detuning for the first order approximate solution.

In this figure it is shown that the cw or ccw traveling-wave oscillation is more intense than the other according as $l \lesseqgtr 0$ even in the bidirectional oscillation. The crossing points are from Eq.(12)

$$z_c = \pm L_R/4 - \frac{\bar{\phi}}{4\pi} L_R = \pm \frac{L_R}{4} + \frac{\alpha A_2}{A_1 + \alpha A_2} l \ , \qquad (3.6\text{-}22)$$

where

$$A_1 = 2\{\theta^c_{12}(\theta^a_{12} - \theta^b_{11} + \theta^c_{12}) + \tau^c_{21}(\tau^a_{21} - \tau^b_{22} + \tau^c_{21})\}I_0 \ ,$$

$$A_2 = (\theta^a_{12} - \theta^b_{11} + \theta^c_{12})\cos\theta_B + (\tau^a_{21} - \tau^b_{22} + \tau^c_{21})\sin\theta_B \ .$$

Therefore, as modulation depth α becomes deeper, the crossing point z_c is pulled more to the modulator, which is also shown in Fig.3.6-4.

B2. Exact Numerical Solutions

To begin with, let us consider the internally loss-modulated two-

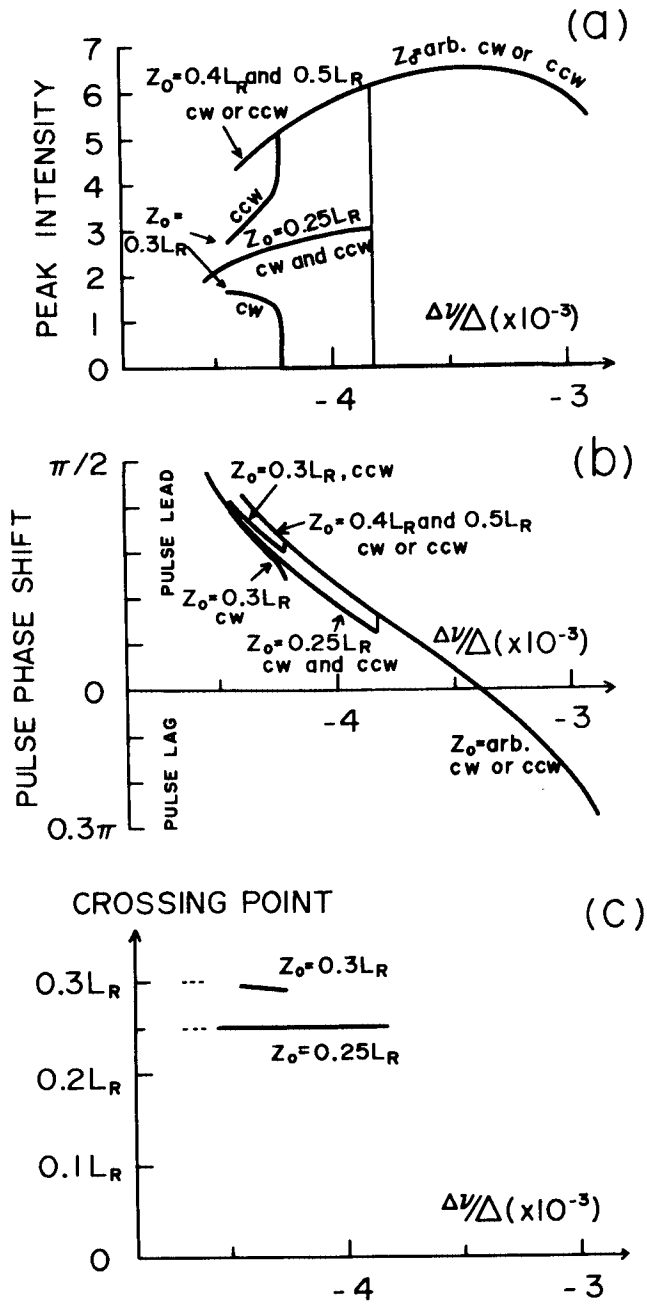

Fig.3.6-5. (a)Pulse peak intensity, (b)pulse phase shift, and (c) crossing point versus detuning for an internally loss-modulated two-mode He-Ne ring laser (pure isotope case). $\Delta = 100$ MHz, $\gamma_1/2\pi = 25$ MHz, $\gamma_2/2\pi = 12$ MHz, $\gamma'_{12} = 62$ MHz, $\alpha_a = 0.01$, $\nu/2\pi Q = 7$ MHz, $(\Omega_1 + \Omega_2)/2 = \omega$, $\mathcal{R} = 1.04$.

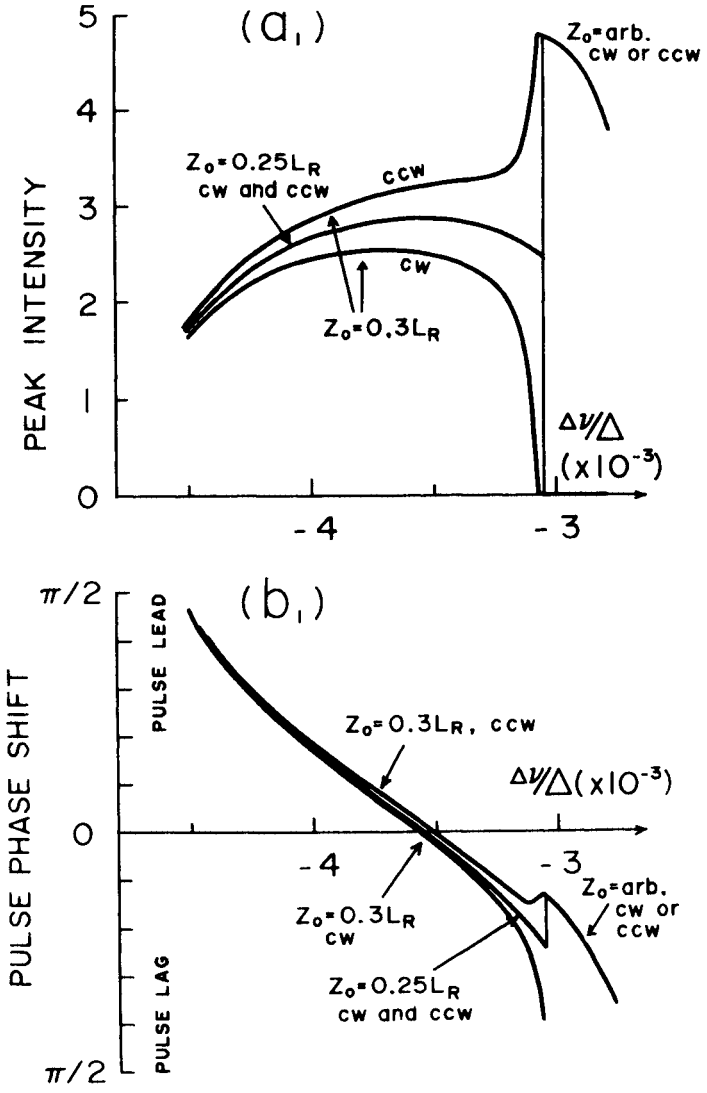

Fig. 3.6-6. (a_1)Pulse peak intensity and (b_1)pulse phase shift. (see page 89)

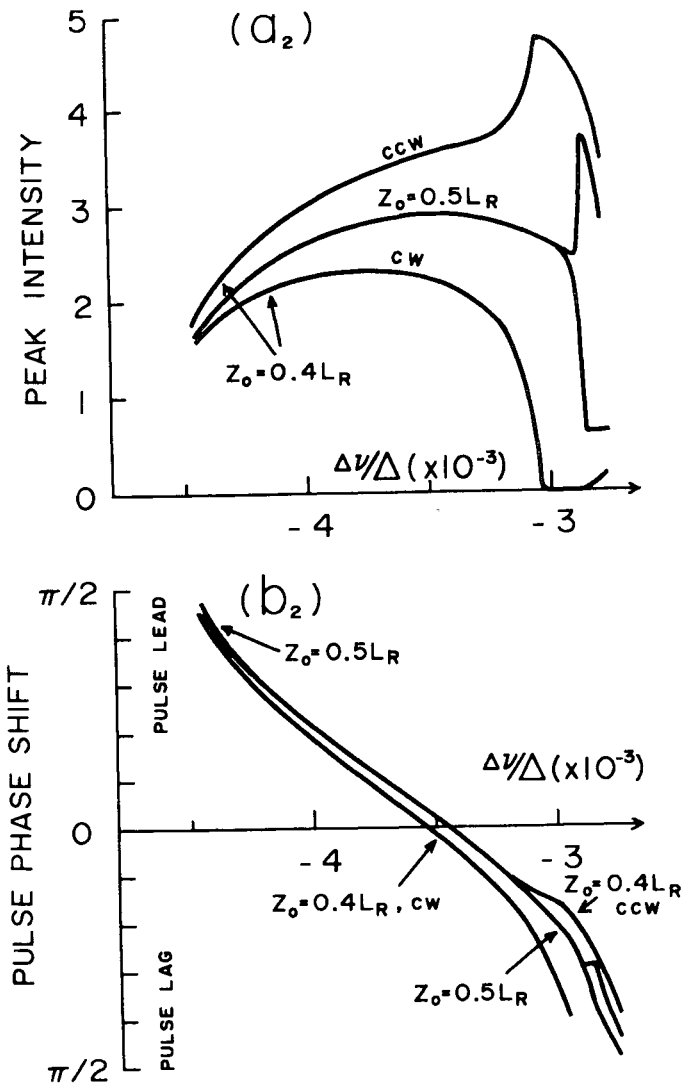

Fig.3.6-6. (a_2)Pulse peak intensity and (b_2)pulse phase shift. (see page 89)

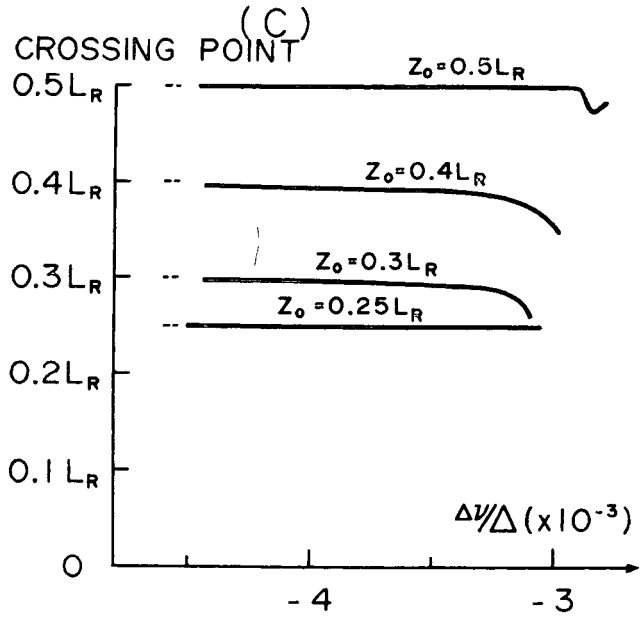

Fig.3.6-6.(a)Pulse peak intensity, (b)pulse phase shift, and (c)crossing point versus detuning for an internally loss-modulated two-mode He-Ne ring laser (mixed isotope case). $\Delta = 100$ MHz, $\alpha_a = 0.01$, $\nu/2\pi Q = 7$ MHz. The parameters are identical with those of Fig.3.6-1(b).

mode ring laser for which an approximate analytical investigation has been made. The differential equations given in Secs.3.1~3.3 were solved numerically for this ring laser.From the steady state solutions locking curves are plotted in Fig.3.6-5. These are in good agreement with the approximate analytical investigation. Indeed the boundary between the UTWO and BTWO regions for $z_0 = L_R/4$ is at $\Delta\nu/\Delta = -3.83 \times 10^{-3}$, which has been expected from the analytical investigation. As the modulator position z_0 varies from $z = L_R/4$ to $z = L_R/2$, the UTWO region becomes larger, and the UTWO is stable in all the locking region when $0.4L_R \lesssim z_0 \leq L_R/2$. In the UTWO regions, either of the two OT waves oscillates depending upon the initial condition. However the ccw traveling-wave oscillates more probably when $L_R/4 < z_0 < L_R/2$ or $-L_R/4 < z_0 < 0$, and so does the cw one when $0 < z_0 < L_R/4$ or

$-L_R/2 < z_0 < -L_R/4$.

Numerical solutions for the mixed isotope case, which are applicable to the usual He-Ne ring laser, are shown in Fig.3.6-6. Also in the forced locking, the mixed isotope case differs much from the pure isotope case in the following points (compare Fig.3.6-6 with Fig.3.6-5). The UTWO width is relatively narrow and hardly varies with z_0. The BTWO is stable in almost all the locking region even when $z_0 \simeq L_R/2$. In other words, the OT waves interact or compete with each other very weakly in the mixed isotope case. This is because equi-intensity two-mode spectrum is symmetrical about neither of the line centers of the two isotopes, then the mirror-mode competition, which is the only competition between the OT waves, is very weak.

However, as the number of the oscillating modes increases, the differences between the pure and mixed isotope cases decreases. Hence the theoretical results for the five-mode operation of the pure isotope case can be compared with experiments without more complex calculations for the mixed isotope case.

Next, as a more general example, numerical solutions for five-mode operation are shown in Figs.3.6-7~10 for pure isotope case. There are forty combination tone terms in the equations. In the bidirectional traveling-wave ring laser, the combination tones generate phase-dependent interactions between the OT waves as well as those between modes of cw or ccw one. The internal modulation does not make the OT waves interact directly with each other. Therefore those combination tone terms, as well as the phase-independent and phase-dependent saturation terms, play an important role in the phase locking and competition phenomena between the OT waves of the internally modulated ring laser, although they can be ignored in the normal standing-wave laser.

The behaviors of the pulse peak intensity, pulse phase shift and crossing point versus detuning are similar to those for the two-

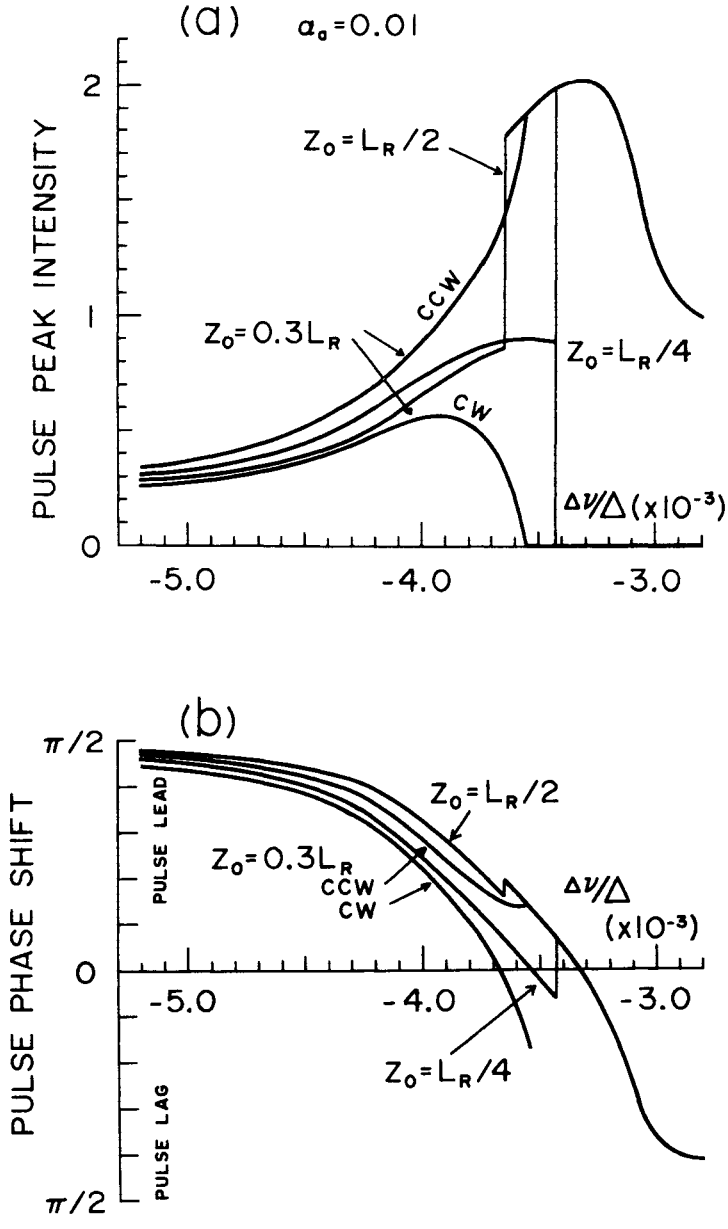

Fig.3.6-7.(a)Pulse peak intensity and (b)pulse phase shift. (see next page)

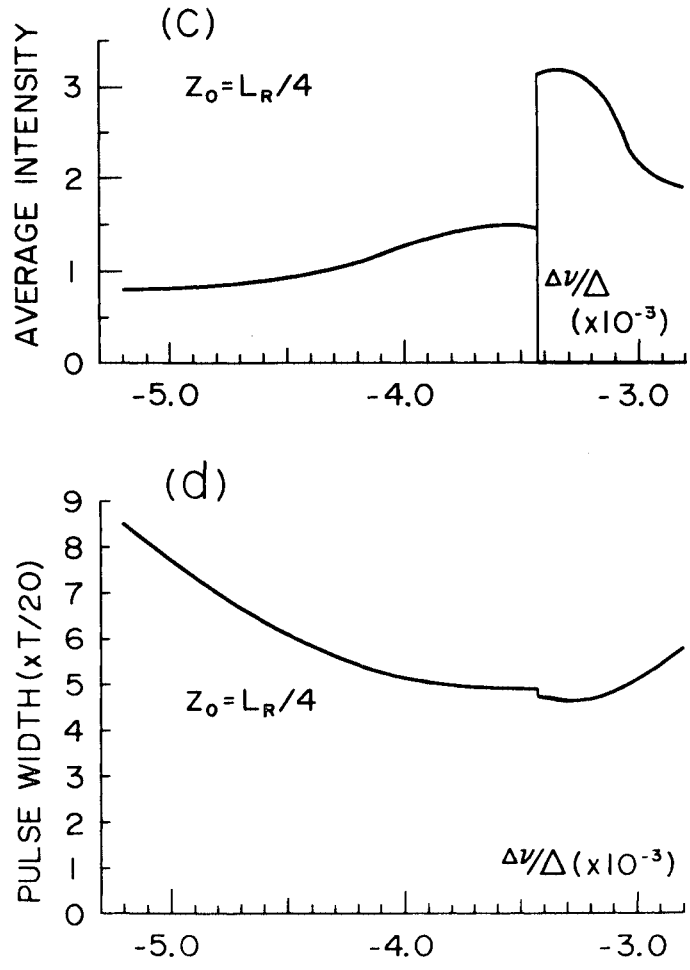

Fig. 3.6-7. Numerical results for a five-mode ring laser (pure isotope case) (a)Pulse peak intensity, (b)pulse phase shift, (c)average power ($z_0 = L_R/4$), and (d)pulse width ($z_0 = L_R/4$)(full width at half intensity) versus detuning. $\Delta/2\pi = 100$ MHz, $\mathcal{R} = 1.05$, $\gamma_1/2\pi = 34$ MHz, $\gamma_2/2\pi = 15$ MHz, $\gamma'_{12}/2\pi = 100$ MHz, $\nu/2\pi Q = 7$ MHz, $\alpha_a = 0.01$, $\Omega_3 = \omega$. In the figure (d), T is a period of the modulator.

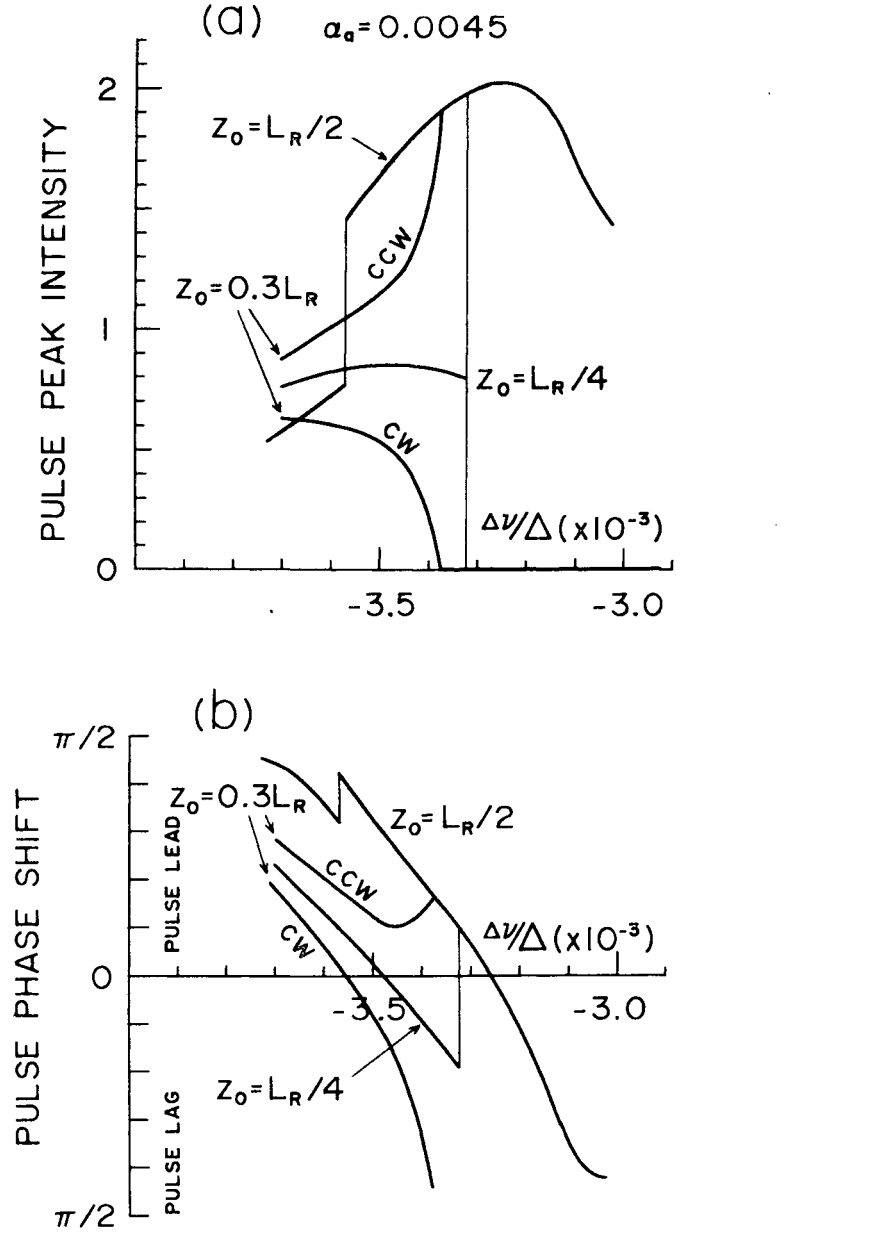

Fig. 3.6-8. (a)Pulse peak intensity and (b)pulse phase shift. $\alpha_a = 0.0045$. (see next page)

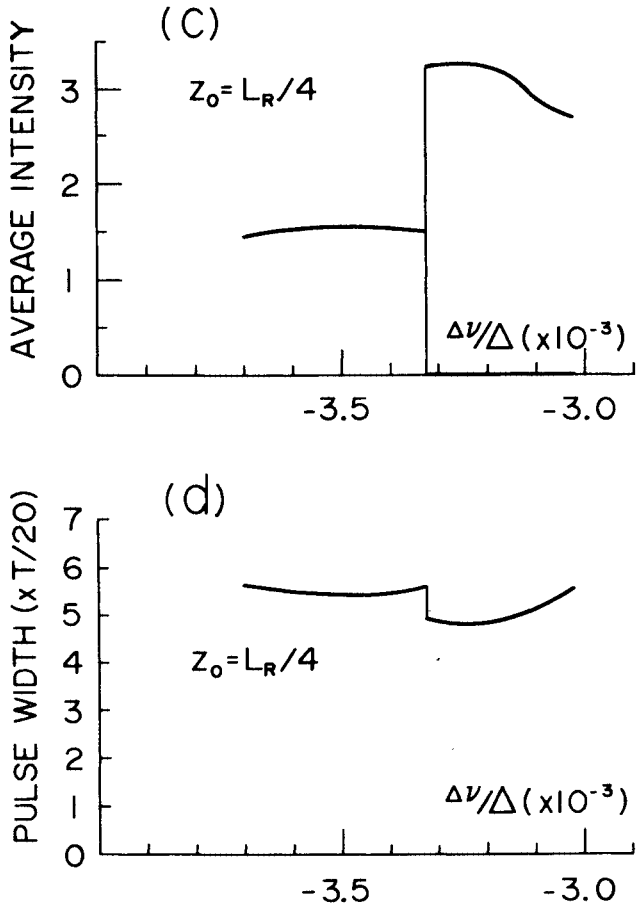

Fig.3.6-8. Numerical results for a five-mode ring laser (pure isotope case) (a)pulse peak intensity, (b)pulse phase shift, (c)average power ($z_0 = L_R/4$), and (d)pulse width (full width at half intensity) ($z_0 = L_R/4$) versus detuning. $\alpha_a = 0.0045$. The other parameters are identical with those for Fig.3.6-7.

mode operation. However there is a distinct difference between them. The UTWO region is relatively wide and, further, it covers all the locking region when $z_0 \simeq L_R/2$ in the two-mode operation. On the contrary, in the five-mode operation, the UTWO region is relatively narrow and the BTWO occurs also even when $z_0 \simeq L_R/2$. The reason for this difference is that the interaction between the OT waves is, compared with that between the oscillating modes of cw or ccw

traveling-waves, strong in the two-mode operation (see Fig.3.6-1(a)) and comparable in the five-mode or multimode operation. This is explained from the hole burning effect as follows. In the two-mode operation, the holes are shalow and narrow since the mode intensities are weak, therefore the overlaps of adjacent modes are very small. However the mirror-modes *i.e.* OT modes compete fully with each other. On the contrary, in the multimode operation, the holes are deep and wide, therefore the adjacent-mode interaction is not negligible compared with the mirror-mode competition.

The mode locked UTWO region becomes wider monotonously as z_0 moves from $L_R/4$ to $L_R/2$, and there exists a mode locked BTWO region even when $z_0 \simeq L_R/2$. The total mode locking width in detuning is almost independent of z_0. The optimum detuning will be defined as the detuning at which the pulse peak intensity takes a maximum value. The pulse phase shift becomes zero at the optimum detuning in the UTWO region. The pulse width is narrowest at the optimum detuning in the

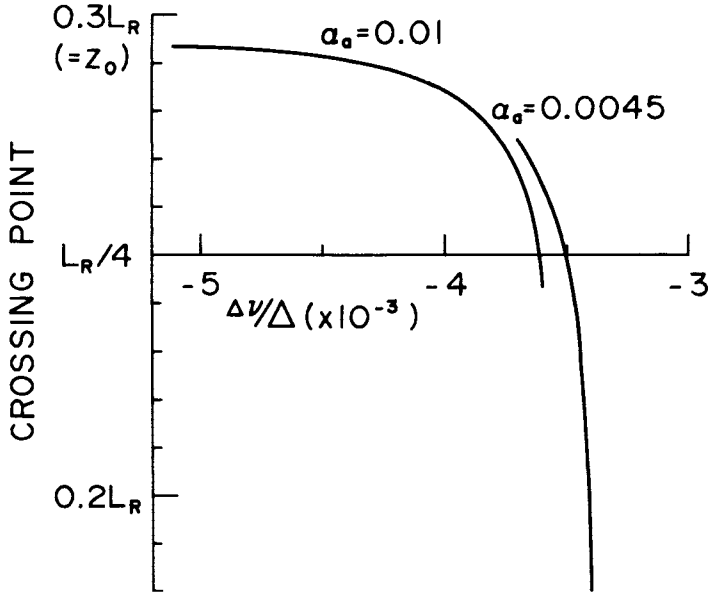

Fig.3.6-9. Crossing point versus detuning.
$z_0 = 0.3L_R$.

UTWO locking region indeed, but it hardly varies between the UTWO and BTWO regions. Therefore the average power varies with detuning with almost the same manner as the peak power. The maximum pulse peak intensity in the UTWO region is 2.2～2.4 times as large as that in the BTWO region when $z_0 = L_R/4$. This is because the OT waves couple only weakly with each other and the nonlinear property of the medium is relatively weak. This is not the case for a ring laser with a homogeneously broadened spectral line, which will be shown in Sec.4.4.

When $z_0 = L_R/4$, the crossing point is also at $z = L_R/4$ independently of the modulation frequency. When $z_0 = 0.3L_R$, as shown in Fig.3.6-9, it is pulled more to z_0 as α_a increases. At the lowest modulation frequency of the locking region, it is nearest to z_0. As modulation frequency increases it returns to the natural crossing

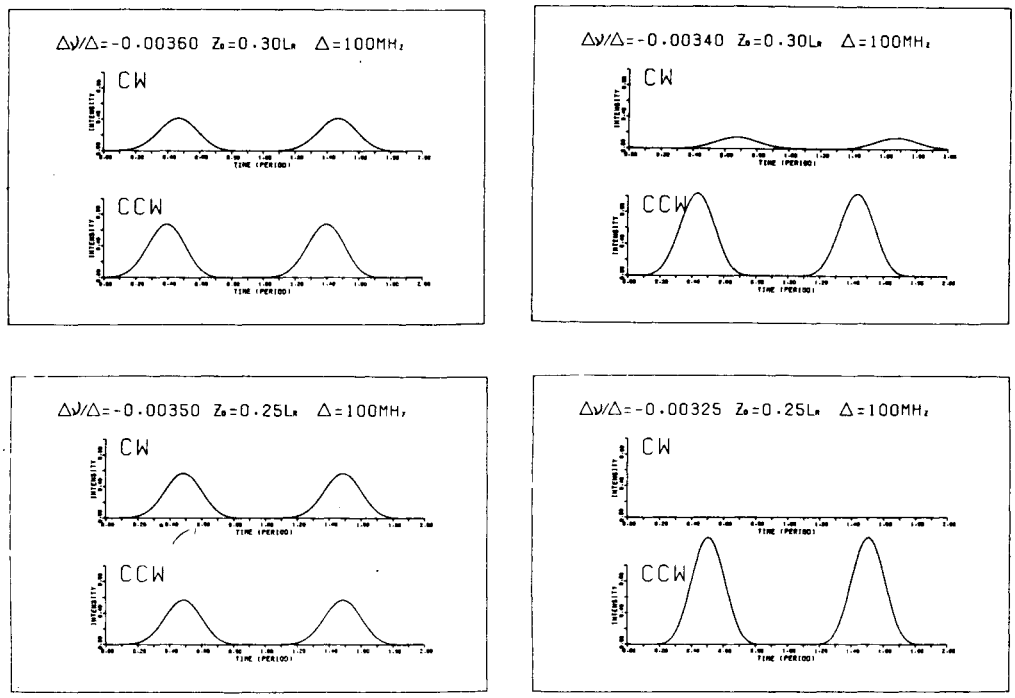

Fig.3.6-10. Examples of the output wave forms of the internally loss-modulated five-mode He-Ne ring laser. $\alpha_a = 0.0045$.

point $z = L_R/4$. It will be anomalous that the crossing point moves far from $z = L_R/4$ in the opposite direction to z_0 when $\alpha_a = 0.0045$.

Some examples of the output wave forms from which Figs.3.6-7~9 are plotted are shown in Fig.3.6-10 using a XY plotter.

B3. Experimental Results

Block diagram of the experimental setup is shown in Fig.3.6-11. The laser medium was a He-Ne discharge tube filled with mixed isotopes of neon, *i.e.*, natural neon (Ne^{20}: Ne^{21}: Ne^{22} = 90.92 : 0.26 : 8.82). The modulator is the one shown in Fig.3.4-15. The instantaneous intensities of the output optical pulses were detected by two PIN photodiodes (*hp* 4204). The average output power was measured by a solar cell. The pulse phase shift was known from the phase difference, which was measured by a vector voltmeter, between the electric signal detected

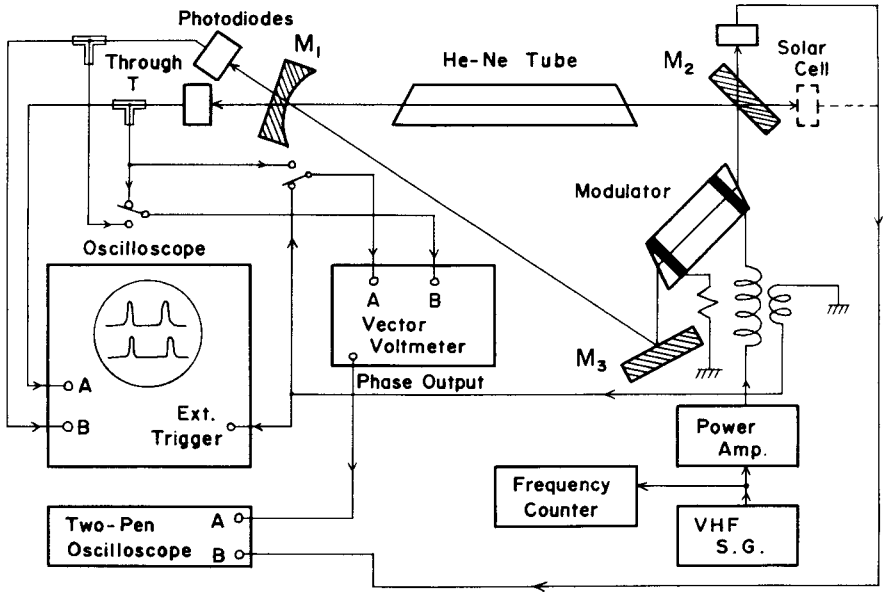

Fig.3.6-11. Block diagram of the experimental setup.
M_1 : R(radius of curvature) = 3 m, T(transparency) ≃ 0.5 %;
M_2 and M_3 : $R = \infty$, $T \lesssim 0.1$ % (at an incident angle of 45°).

from the output optical pulse train and the modulation signal coupled out from the modulator circuit. The origin of the pulse phase shift was known from a theoretically derived fact that the pulse peak intensity in the UTWO locking region reaches maximum when the pulse phase shift is zero. The phase difference ϕ^- between the OT pulses was measured also by the vector voltmeter and the crossing point was calculated from Eq.(12). In this case, the origin of ϕ^- was determined by an experimental fact that the OT pulses encounter at $z = \pm L_R/4$ in the self-phase locked state (see page 80). Although the vector voltmeter was sensible of only the fundamental frequency component of the input pulse, it would have accurately the phase of the input pulse since the pulse was almost symmetric. Those measured values were recorded on a pen-oscilloscope versus modulation frequency. The modulator was placed at $z = L_R/4$ or $z = 0.3L_R$ ($L_R = 3$ m). The experimental results shown below are usually restricted within locking regions. Whether it was locked or not was decided according as the output pulse train appeared on a sampling oscilloscope was synchronous with the modulation signal or not. Since the laser oscillation near threshold is easily disturbed by small mechanical vibrations, the experiment in few-mode operation is not easy. Hence the experiment was made in a usual state, *i.e.*, in about ten-mode operation. Since only two quantities could be recorded simultaneously, three groups of quantities, *i.e.*, 1) average intensity and pulse phase shift of the cw traveling-wave, 2) those of the ccw one, and 3) average intensity of the cw one and crossing point of the OT pulses were recorded successively. Hence those recorded curves versus detuning do not completely correspond with each other due to some thermal and mechanical drifts. The crossing point curves lack their beginnings and ends,since the vector voltmeter could not follow the input signal at those parts. The phase accuracy of the vector voltmeter is $\pm 3° \sim \pm 4.5°$ depending upon the voltage difference between the two input signals, which corresponds to the crossing-point

accuracy of $\pm 0.004L_R \sim \pm 0.006L_R$.

$z_0 = L_R/4$: As expected from the previous theoretical investigation, BTWO occured in the low frequency part of the locking range and UTWO in the high frequency part (see Fig3.6-12). Average intensities as well as pulse phase shifts of the OT waves were almost identical with each other. Then the crossing point was always in the

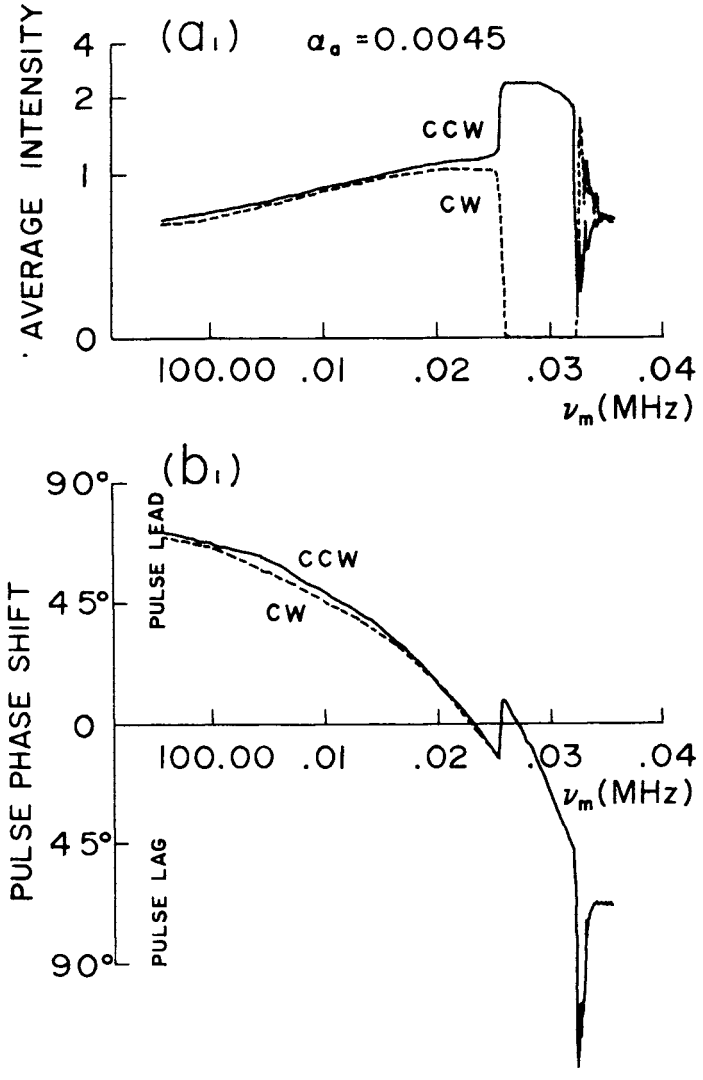

Fig.3.6-12 (a_1) and (b_1).Experimental results for $z_0 = L_R/4$ ($L_R \simeq 3$ m). (a_1)average intensity (b_1) pulse phase shift versus modulation frequency.

immediate neighborhood of $z = z_0 (= L_R/4)$ almost independently of modulation frequency ν_m and depth α_a. The average intensity of the UTWO was about twice as large as that of the BTWO*. The pulse peak

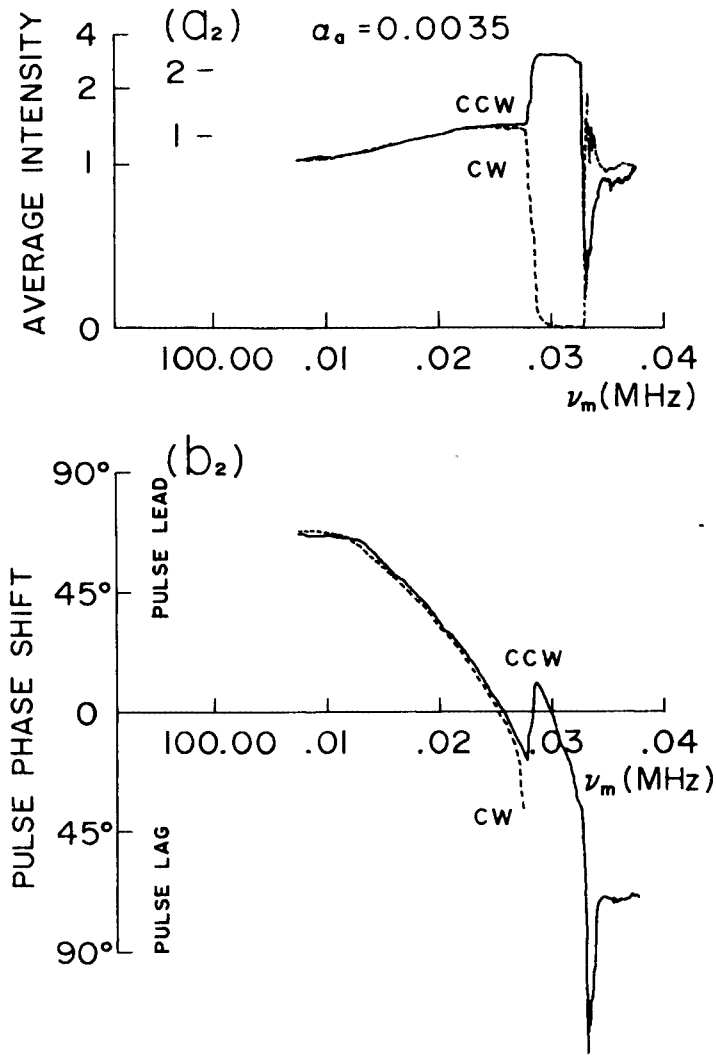

Fig.3.6-12(a_2) and (b_2).

---

* It should be noticed that the ordinates are on a nonlinear scale in Figs.3.6-12(a_1) and (a_2), and also in Figs.3.6-14(a_1) and (a_2). In the figures (a_2), two scales of different units are shown conveniently.

intensity of the UTWO was also twice as large as that of the BTWO (see Fig.3.6-13). In the UTWO region, either cw UTWO or ccw one occured in equal probability depending upon initial conditions. Hence a small injection signal to cw or ccw direction through the output mirror made the cw or ccw UTWO monostable respectively. The injection signal might be an externally reflected beam (see Fig.3.5-1) or an output beam from another laser oscillator. As modulation depth α_a increased, the locking range became wider but the average power decreased since average transmission loss of the modulator increased. Hence the highest peak power of the UTWO was obtained with a rather small α_a. Dependence of the mode-locking range upon α_a is shown in Fig.3.6-15(a). The locking widths of the BTWO and UTWO increased monotonously with α_a. When α_a was too small, *i.e.*, $0.0003 < \alpha_a < 0.0015$, only mode-locked BTWO occured. When $\alpha_a = 0.0045$, the locking width of the BTWO was 30 kHz, *i.e.*, 3×10^{-4} in $\Delta\nu/\Delta$, which agrees with the theoretically evaluated width 3.8×10^{-4} in $\Delta\nu/\Delta$ (see Fig.3.6-8). However, the width of the UTWO was 7 kHz, *i.e.*, 0.7×10^{-4} in $\Delta\nu/\Delta$, which differs too much from the theoretical width 3×10^{-4}. The reasons for this difference will be as follows: 1) In the actual

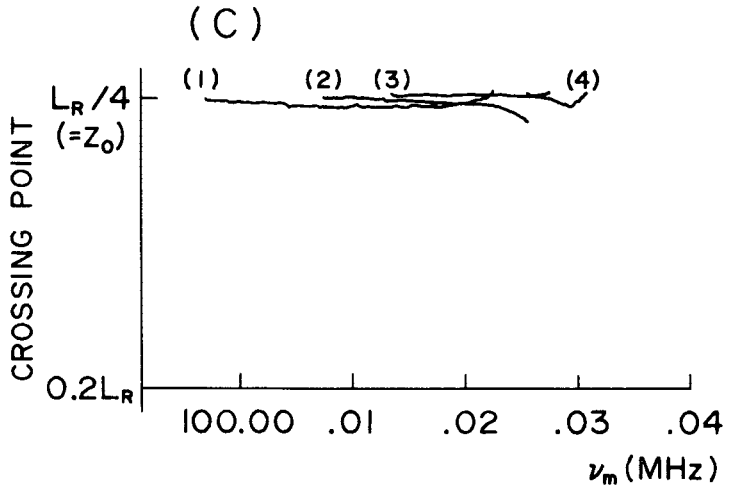

Fig.3.6-12(c). Crossing point versus modulation frequency. (1) $\alpha_a = 0.0045$, (2) $\alpha_a = 0.0035$, (3) $\alpha_a = 0.0025$, (4) $\alpha_a = 0.0005$.

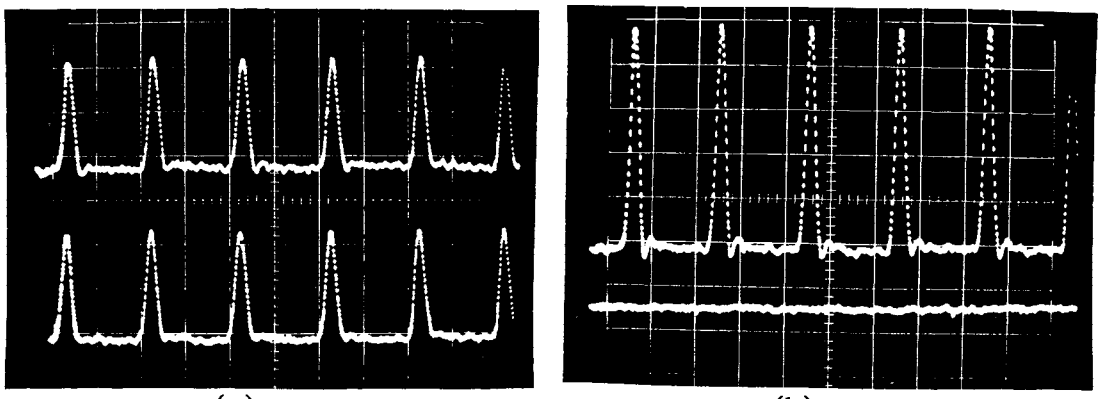

(a) (b)

Fig.3.6-13. Output pulse trains on a sampling oscilloscope. (a)mode-locked BTWO, and (b)mode-locked UTWO. (5 ns/div.)

He-Ne ring laser, competition between the OT waves was weaker, *i.e.*, the laser medium was more inhomogeneous than theoretically considered. Maybe also the isotope effect was responsible for it. 2) As number of the oscillating modes increases, the locking range will generally become narrower, since the dispersion of the frequency differences between the oscillating modes becomes larger. The number of the oscillating modes was about ten in the experiment and five in the theoretical calculation. 3) Modulation signal might not fully applied to the KDP crystal, then the modulation depth α_a was overestimated in the experiment.

$z_0 = 0.3L_R$: As expected from the theoretical investigation, the ccw traveling-wave oscillated usually in the mode-locked UTWO region, and, even in the BTWO region, the ccw one oscillated more intensely than the cw one (see Fig.3.6-14). However, the cw one was more intense at the beginning of the locking region and just above it. The ccw pulse phase shift was more leading than the cw one, *i.e.*, the ccw traveling pulse passed the modulator leading the cw one. Hence the crossing point was located between $z = z_0 (= 0.3L_R)$ and $z = 0$. It was pulled more to the modulator (at $z = z_0$) as the modulation depth α_a increased or the modulation frequency ν_m decreased in the

BTWO locking range. In the theoretical calculation with $\alpha_A = 0.0045$ (see Fig.3.6-9), the crossing point moves far beyond $z = L_R/4$ to $z = 0.2L_R$ in transition from BTWO to UTWO. However it stopped near $z = L_R/4$ in the experiment (Fig.3.6-14(c)). This is because the vector voltmeter could not follow the too small cw pulse. From the experimental curves of the pulse phase shift, the crossing point is known to have moved far beyond $z = L_R/4$ to $z = 0.2L_R$. The α_A-dependence of the locking range is shown in Fig.3.6-15(b). Compared with the

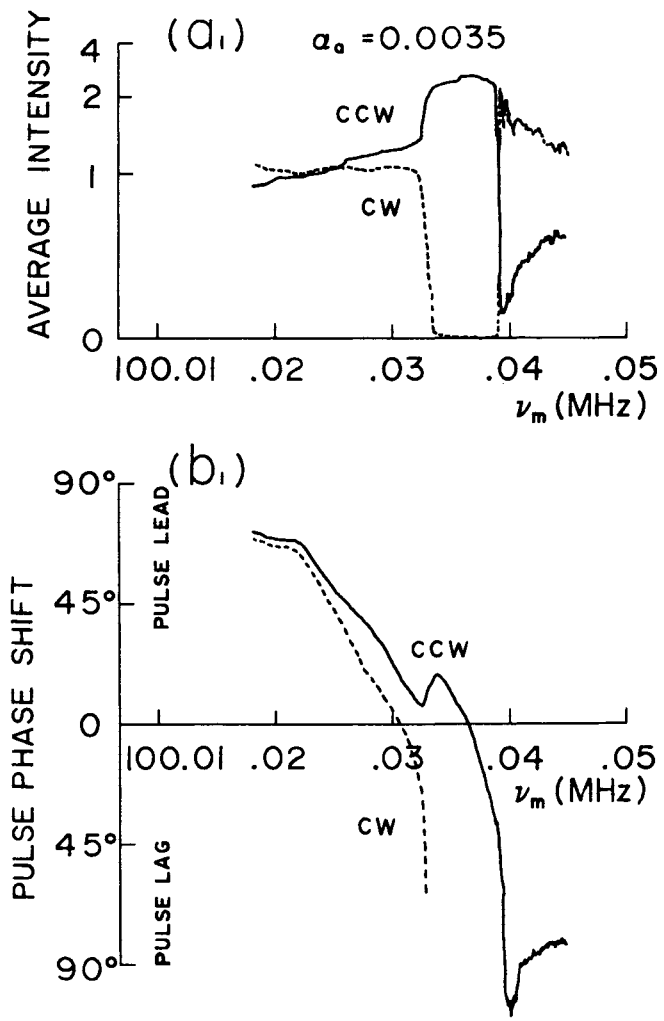

Fig.3.6-14(a_1) and (b_1). Experimental results for $z_0 = 0.3L_R$ ($L_R \simeq 3$ m). (a_1)average intensity (b_1) pulse phase shift versus modulation frequency.

results for $z_0 = L_R/4$, the mode-locked UTWO took place with small α_a and its width was wide when $\alpha_a \lesssim 0.0045$. As α_a increased, the UTWO and BTWO locking widths increased at first but decreased after reaching a maximum at $\alpha_a = 0.0035$. When $\alpha_a = 0.0045$, the BTWO locking width was 17 kHz, *i.e.*, 1.7×10^{-4} in $\Delta\nu/\Delta$, which is about half as large as the theoretical width 3.2×10^{-4}. The UTWO width was 7 kHz, *i.e.*, 0.7×10^{-4} in $\Delta\nu/\Delta$, which is a fifth part of the theoretical one 3.5×10^{-4}.

In the mode-locked UTWO region, the ccw traveling-wave oscillated usually; however, small cw traveling-wave oscillations

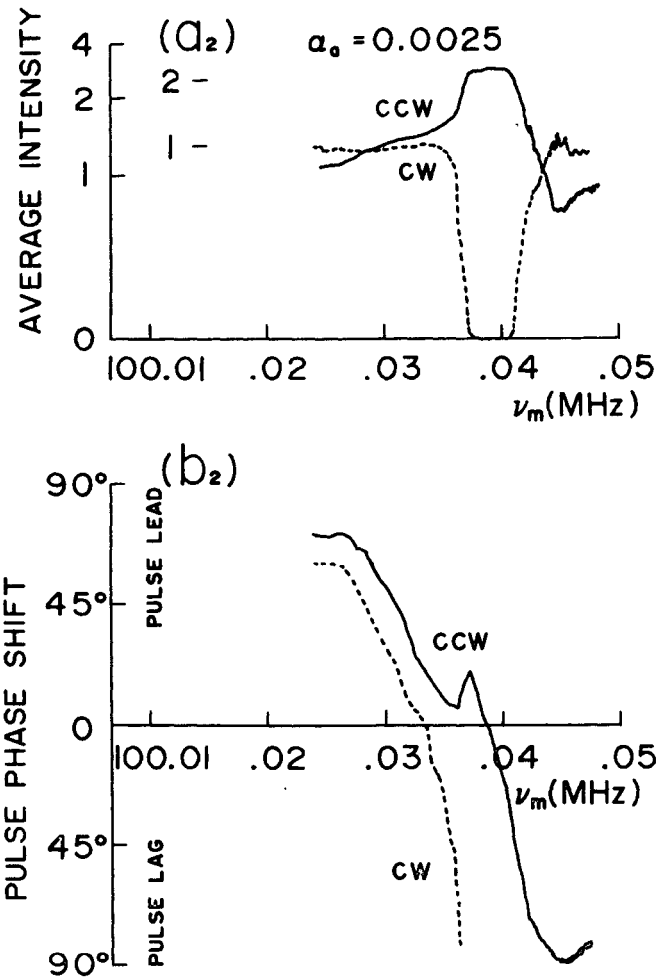

Fig.3.6-14(a_2) and (b_2).

were induced temporarily by some turbulences and sometimes the cw UTWO occured depending upon initial condition, which was, however, followed by the ccw UTWO soon. When a mirror was placed outside the ring resonator so that the output of the cw traveling-wave was injected into the ccw one, the ccw UTWO became very stable and almost completely independent of usual turbulences. On the contrary, when a mirror was placed so that the ccw traveling-wave was injected into the cw one, the cw UTWO was obtained. In other words, the direction of the UTWO couled be reversed by an externally placed mirror.

B4. Discussion

It has been derived theoretically and verified experimentally that the mode-locked UTWO is obtainable by internally loss-modulating a He-Ne ring laser. The pulse peak intensity of the UTWO was only about twice as high as that of the BTWO in the experiment and also in the theory. This shows that the OT waves couple with each other only weakly in the gas laser due to inhomogeneous Doppler line broadening. In a laser with a homogeneously broadened line, which will be investigated in the next chapter, the ratio of the pulse peak

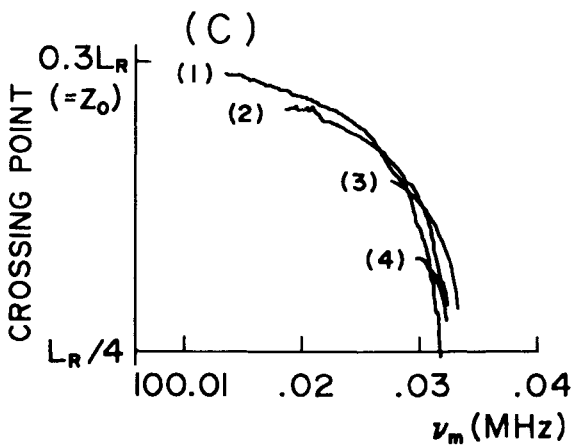

Fig.3.6-14(c). Crossing point versus modulation frequency. (1) $\alpha_a = 0.0045$, (2) $\alpha_a = 0.0035$, (3) $\alpha_a = 0.0015$, (4) $\alpha_a = 0.0005$.

intensities of the UTWO and BTWO becomes as large as five to one.

The mode-locked UTWO will be obtained also in the AM locking region (or phase locking region [33.a]) by an internal phase-

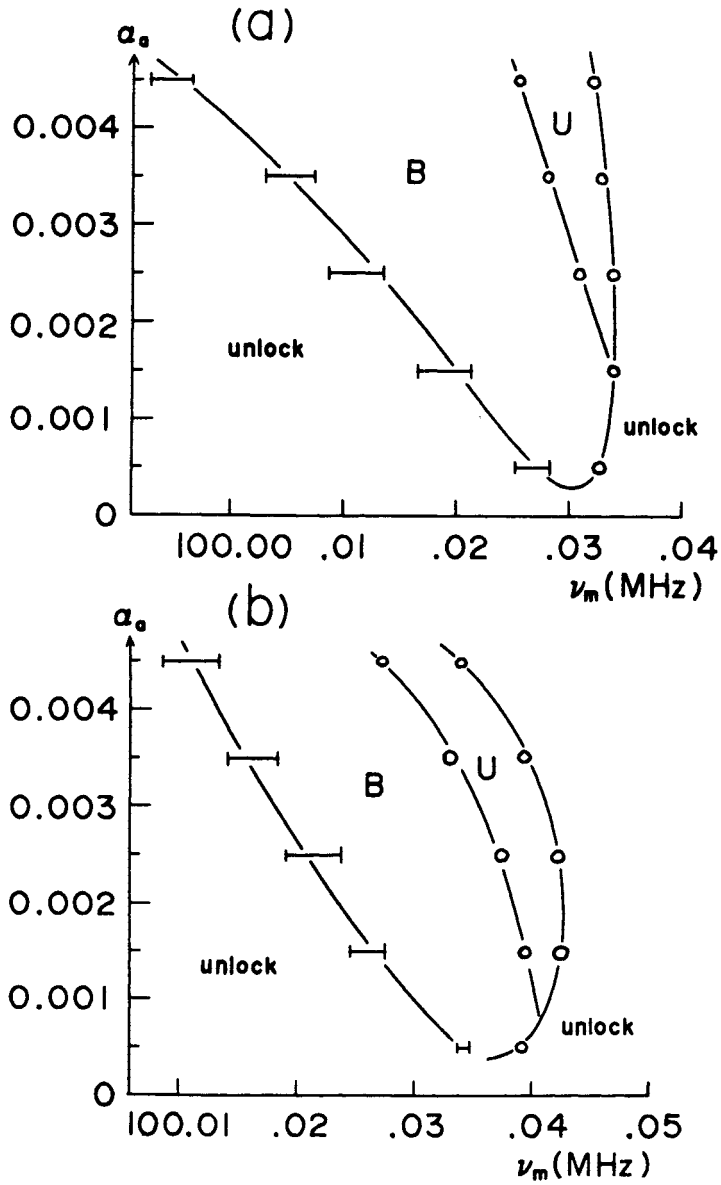

Fig.3.6-15. Locking regions of UTWO and BTWO denoted by U and B respectively.
(a) $z_0 = L_R/4$, (b) $z_0 = 0.3L_R$.

modulation. This may be considered to be advantageous because the insertion loss of the phase-modulator can be very small unlike that of the loss-modulator. However the locking characteristics are very complicated. There are "π-jump" of the pulse phase to the modulation signal even in the AM locking region, and also quenched and FM regions in addition.

CHAPTER 4

MODE LOCKING OF A LASER WITH A HOMOGENEOUSLY BROADENED LINE

(Time Domain Theory)

Mode locking phenomena in a homogeneous laser will be investigated in the time domain from a point of view that a CW oscillation, *i.e.*, single-mode oscillation at a cavity resonance frequency nearest to the line center occurs naturally but, when mode-locked, this CW oscillation becomes unstable and a regular pulse oscillation arises. Multimode oscillation of the normal standing-wave laser is explained from the fact that this CW oscillation is always unstable in the normal laser due to spatial hole burning, *i.e.*, spatial pulsation of the population inversion with a period of a half of an optical wave length. The multimode oscillation due to spatial hole burning is by no means a necessary condition for mode locking. On the contrary, the inhomogeneous laser makes naturally multimode oscillation and the oscillating modes may be phase-locked by some means.

In the homogeneous laser, since every active particle interacts equally with electric field, saturation or competition between oscillating modes is very strong. Consequently, single-mode oscillation occurs usually, and, even when multimode oscillation occurs, its mode spectrum gathers about the line center. Therefore, if mode-locked unidirectional traveling-wave oscillation is obtained, its mode spectrum spreads much more widely than that of the standing-wave one since the saturation between the OT waves vanishes, and its mode-locked pulses have a high peak power and a short length. In this respect, the homogeneous laser differs sharply from the inhomogeneous one.

The relaxation rates used in the calculations are not necessarily for some homogeneous laser. Although the ratio of the longitudinal relaxation rate to the transverse one may be adequate to a dye laser or to a Nd laser with a saturable absorber, the ratio of the transverse rate to the cavity-mode spacing is too small for them. These ratios are rather for an inhomogeneous He-Ne laser. With the exception of the effects of the strong mode competition of the homogeneous laser, the results of this chapter will explain well the mode locking characteristics of the He-Ne laser. This chapter will be, however, devoted only to making clear the features of the various types of mode locking viewed in the time domain.

4.1. Basic Equation

In this section, the basic equation for a bidirectional traveling-wave ring laser and a normal standing-wave laser with homogeneous line broadening is given.

A. Matter Equation and Field Equation

Let us start from the equation of motion, *i.e.*, Eqs.(2-16)~(2-18), described in terms of density matrix. Now

$$\mathrm{Tr}\,\rho = \sum_n \langle n|\rho|n\rangle = \sum_n \rho_{nn} = 1 \ . \tag{4.1-1}$$

For an idealized two level system

$$\rho_{11} + \rho_{22} = 1 \ . \tag{4.1-2}$$

Using this condition, we find, from Eqs.(2-16)~(2-18),

$$\frac{\partial}{\partial t}\boldsymbol{d} = -\gamma_{\perp}(d - d^{e}) - \frac{2}{\hbar} qE \ , \tag{4.1-3}$$

$$\frac{\partial}{\partial t} q = \omega p - \gamma_{\perp} q + \frac{2}{\hbar} dE\mu_{12}^2 \cos^2\theta \ , \tag{4.1-4}$$

$$\frac{\partial}{\partial t} p = -\omega q - \gamma_{\perp} p \ , \tag{4.1-5}$$

where

$$d = \rho_{22} - \rho_{11} \ , \ d^{e} = \rho_{22}^{e} - \rho_{11}^{e} \ , \ p = \mu_{12}(\rho_{21} + \rho_{12})\cos\theta \ ,$$

$$q = i\mu_{12}(\rho_{21} - \rho_{12})\cos\theta \ , \ \gamma_{\parallel} = 2\gamma_1\gamma_2/(\gamma_1 + \gamma_2) \ , \ \gamma_{\perp} = \gamma_{12}' \ . \tag{4.1-6}$$

Substituting q from Eq.(5) into Eqs.(3) and (4), we find the matter equations for one particle;

$$\frac{\partial}{\partial t} d = \gamma_{\parallel}(d^{e} - d) + \frac{2}{\hbar\omega} E \frac{\partial}{\partial t} p \ , \tag{4.1-7}$$

$$\frac{\partial^2}{\partial t^2} p + 2\gamma_{\perp} \cdot \frac{\partial}{\partial t} p + \omega^2 p = -\frac{2\omega}{\hbar} \mu_{12}^2 E d \cos^2\theta \ . \tag{4.1-8}$$

Here it has been assumed that $\frac{\partial p}{\partial t} \Big/ p \simeq \omega >> \gamma_{\perp}$. Since the θ-dependence can not be included rigidly in this treatment and, further, it will have no importance in this case, the factor $\cos^2\theta$ in the equation may be replaced, as usually done, by

$$\langle \cos^2\theta \rangle \equiv \int_0^{\pi} \cos^2\theta \cdot \Theta(\theta) d\theta = \frac{1}{3} \ . \tag{4.1-9}$$

Then the macroscopic polarization $P(z,t)$, population inversion $D(z,t)$, and its thermal equilibrium state $D^{e}(z,t)$ are given, as in Sec.3.1, by

$$P(z,t) = n(z,t) \langle p(\lambda,z,t) \rangle_{\lambda} \ , \tag{4.1-10}$$

$$D(z,t) = n(z,t) \langle d(\lambda,z,t) \rangle_{\lambda} \ , \tag{4.1-11}$$

$$D^{e}(z,t) = n(z,t) \langle d^{e}(\lambda,z,t) \rangle_{\lambda} \ . \tag{4.1-12}$$

The number of the particles in the unit volume $n(z,t)$ may be assumed to be $\overset{a}{\wedge}$slowly varying function of t. Then, the macroscopic matter

equations are given, from Eqs.(7) and (8), by

$$\frac{\partial}{\partial t} D = \gamma_{\parallel}(D^{e} - D) + \frac{2}{\hbar\omega} E \frac{\partial P}{\partial t} , \tag{4.1-13}$$

$$\frac{\partial^2}{\partial t^2} P + 2\gamma_{\perp} \cdot \frac{\partial}{\partial t} P + \omega^2 P = - \frac{2\omega}{3\hbar} \mu_{12}^2 DE . \tag{4.1-14}$$

The field equation in the laser medium is given by Eq.(3.1-1), *i.e.*,

$$\frac{\partial^2}{\partial t^2} E + \frac{\sigma}{\varepsilon} \frac{\partial}{\partial t} E - c^2 \frac{\partial^2}{\partial z^2} E = \frac{\nu^2}{\varepsilon} P , \tag{4.1-15}$$

where c is the phase velocity of light in the host material, and σ is the fictional conductivity including transmission loss of the host material, reflection loss at optical surfaces, and insertion loss of the modulator if it is inserted.

We represent $E(z,t)$ by two OT waves;

$$E(z,t) = \tilde{E}^{+}(z,t)\exp[i\omega(t + \frac{z}{c})] - \tilde{E}^{-}(z,t)\exp[i\omega(t - \frac{z}{c})] + \text{c.c.} \tag{4.1-16}$$

Similarly

$$P(z,t) = \tilde{P}^{+}(z,t)\exp[i\omega(t + \frac{z}{c})] - \tilde{P}^{-}(z,t)\exp[i\omega(t - \frac{z}{c})] + \text{c.c.}, \tag{4.1-17}$$

$$D(z,t) = \tilde{D}_0(z,t) + [\tilde{D}_2(z,t)\exp(i2\frac{\omega}{c} z) + \text{c.c.}]. \tag{4.1-18}$$

The optical frequency ω is much larger than the inverse of any other time constant involved in the matter equation, therefore the rotating wave approximation can be used. Complex amplitudes $\tilde{E}^{+}$, $\tilde{E}^{-}$, $\tilde{P}^{+}$, $\tilde{P}^{-}$, $\tilde{D}_0$, and $\tilde{D}_2$ may be assumed to be slowly varying function of z and t, that is, they are treated as constants in a wavelength and during an optical period. The spatial Fourier components of $D(z,t)$ higher than the first order are ignored because they make the spatially burned

holes only slightly sharp and will have no practical effects in this case. The laser medium are further assumed to make no spatial cross-relaxation since its time constant is usually very long compared with any time constant involved in the equation and also with the build-up time of the spike oscillation.

B. Normalization

Substituting Eqs.(16)~(18) into Eqs.(13)~(15) and making the rotating wave approximation, we find

$$\frac{\partial}{\partial t}\tilde{P}^{+} + \gamma_{\perp}\tilde{P}^{+} = i\,\frac{\mu_{12}^{2}}{3\hbar}\,(\tilde{E}^{+}\tilde{D}_{0} - \tilde{E}^{-}\tilde{D}_{2}) \ ,$$

$$\frac{\partial}{\partial t}\tilde{P}^{-} + \gamma_{\perp}\tilde{P}^{-} = i\,\frac{\mu_{12}^{2}}{3\hbar}\,(\tilde{E}^{-}\tilde{D}_{0} - \tilde{E}^{+}\tilde{D}_{2}^{*}) \ , \qquad (4.1\text{-}19)$$

$$\frac{\partial}{\partial t}\tilde{D}_{0} = \gamma_{\parallel}(D^{e} - \tilde{D}_{0}) - \frac{2i}{\hbar}\,\{\tilde{E}^{+}(\tilde{P}^{+})^{*} + \tilde{E}^{-}(\tilde{P}^{-})^{*} - \text{c.c.}\} \ , \qquad (4.1\text{-}20)$$

$$\frac{\partial}{\partial t}\tilde{D}_{2} = -\gamma_{\parallel}\tilde{D}_{2} + \frac{2i}{\hbar}\,\{\tilde{E}^{+}(\tilde{P}^{-})^{*} - (\tilde{E}^{-})^{*}\tilde{P}^{+}\} \ , \qquad (4.1\text{-}21)$$

$$\frac{\partial}{\partial t}\tilde{E}^{\pm} \mp c\,\frac{\partial}{\partial z}\tilde{E}^{\pm} + \frac{\sigma}{2\varepsilon}\,\tilde{E}^{\pm} = -\frac{i\omega}{2\varepsilon}\,\tilde{P}^{\pm} \ . \qquad (4.1\text{-}22)$$

Here the energy flow $E\,\frac{\partial P}{\partial t}$ from the electric field into the laser medium was averaged over one period in time.

For further consideration, it is convenient to normalize the polarization, electric field and population inversions to the stationary (CW) z and t independent solution of Eqs.(19)~(22) with $\tilde{D}_{2} = 0$ and equal cw and ccw oscillations;

$$\tilde{P}_{cw} = i\,\frac{\sigma}{\omega}\,\tilde{E}_{cw} \ , \qquad (4.1\text{-}23)$$

$$\tilde{D}_{0\,cw} = \frac{3\hbar\sigma\gamma_{\perp}}{\omega\mu_{12}^{2}} \ , \qquad (4.1\text{-}24)$$

$$(\tilde{E}_{cw})^{2} = \frac{\gamma_{\parallel}\hbar\omega}{8\sigma}\,(D^{e} - \tilde{D}_{0\,cw}) \ , \qquad (4.1\text{-}25)$$

i.e., we introduce the reduced quantities

$$P^{\pm} = \tilde{P}^{\pm}/\tilde{P}_{cw} \ , \quad E^{\pm} = \tilde{E}^{\pm}/\tilde{E}_{cw} \ , \quad D_0 = \tilde{D}_0/\tilde{D}_{0cw} \ , \quad D_2 = \tilde{D}_2/\tilde{D}_{0cw} . \tag{4.1-26}$$

For more convenience, we introduce the normalized pump parameter λ, time τ, and position x_m as follows;

$$\lambda = (D^e - \tilde{D}_{0cw})/\tilde{D}_{0cw} \ , \tag{4.1-27}$$

$$\tau = \gamma_\perp t \ , \qquad x_m = \frac{\gamma_\perp}{c} z \ . \tag{4.1-28}$$

In the steady state, $\tilde{D}_0 = D^e$ without the electric field, and $\tilde{D}_0 = \tilde{D}_{0cw}$ for the unidirectional CW oscillation. In the latter case, there is no available excessive gain. Hence $\tilde{D}_{0cw}$ is the threshold value of D^e for the laser oscillation (see Eq.(4.1-25) and Sec.4.4.). Consequently the pumping parameter λ means how many times above the threshold the laser medium is pumped. The relative excitation $\mathfrak{N}$ defined in Sec.3.1 is equal to $D^e/\tilde{D}_{0cw}$, *i.e.*,

$$\mathfrak{N} = \lambda + 1 \ . \tag{4.1-29}$$

It should be noticed that the units $\tilde{P}_{cw}$ and $\tilde{E}_{cw}$ of the normalized quantities $P^{\pm}$ and $E^{\pm}$ vary with λ proportionally. The normalized equations are obtained as

$$\frac{\partial}{\partial\tau} P^+ + P^+ = E^+ D_0 - E^- D_2 \ , \tag{4.1-30}$$

$$\frac{\partial}{\partial\tau} P^- + P^- = E^- D_0 - E^+ D_2^* \ ,$$

$$\frac{\partial}{\partial\tau} D_0 + \gamma D_0 = \gamma(\lambda + 1) - \frac{\gamma\lambda}{4} \{E^+(P^+)^* + E^-(P^-)^* + \text{c.c.}\} \ , \tag{4.1-31}$$

$$\frac{\partial}{\partial\tau} D_2 + \gamma D_2 = \frac{\gamma\lambda}{4} \{E^+(P^-)^* + (E^-)^* P^+\} \ , \tag{4.1-32}$$

$$\frac{\partial}{\partial\tau} E^{\pm} \mp \frac{\partial}{\partial x_m} E^{\pm} = k(P^{\pm} - E^{\pm}) \ , \tag{4.1-33}$$

where

$$\gamma = \gamma_\parallel/\gamma_\perp \ , \quad k = \frac{\sigma}{2\varepsilon} /\gamma_\perp \ . \tag{4.1-34}$$

The above equations are the basic equations to be solved. For later

purposes, it is useful to introduce polar coordinates

$$P^{\pm} = |P^{\pm}|\exp(i\psi^{\pm}), \quad E^{\pm} = |E^{\pm}|\exp(i\phi^{\pm}), \quad D_2 = |D_2|\exp(i\theta) \ .$$

The basic equations are thus transformed into

$$\frac{\partial}{\partial\tau}|P^{\pm}| + |P^{\pm}| = |E^{\pm}|D_0\cos(\phi^{\pm} - \psi^{\pm}) - |E^{\mp}||D_2|\cos(\phi^{\mp} - \psi^{\pm} \pm \theta) \ , \tag{4.1-35}$$

$$\frac{\partial}{\partial\tau} D_0 + \gamma D_0 = \gamma(\lambda + 1) - \frac{\gamma\lambda}{2}\{|E^{+}||P^{+}|\cos(\phi^{+} - \psi^{+}) + |E^{-}||P^{-}|\cos(\phi^{-} - \psi^{-})\} \ , \tag{4.1-36}$$

$$\frac{\partial}{\partial\tau}|D_2| + \gamma|D_2| = \frac{\gamma\lambda}{4}\{|E^{+}||P^{-}|\cos(\phi^{+} - \psi^{-} - \theta) + |E^{-}||P^{+}|\cos(\phi^{-} - \psi^{+} + \theta)\}, \tag{4.1-37}$$

$$\frac{\partial}{\partial\tau}|E^{\pm}| \mp \frac{\partial}{\partial x_m}|E^{\pm}| + k|E^{\pm}| = k|P^{\pm}|\cos(\psi^{\pm} - \phi^{\pm}) \ , \tag{4.1-38}$$

$$\frac{\partial}{\partial\tau}\psi^{\pm} = (|E^{\pm}|D_0/|P^{\pm}|)\sin(\phi^{\pm} - \psi^{\pm}) - (|E^{\mp}||D_2|/|P^{\pm}|)\sin(\phi^{\mp} - \psi^{\pm} + \theta), \tag{4.1-39}$$

$$\frac{\partial}{\partial\tau}\theta = \frac{\gamma\lambda}{4}[(|E^{+}||P^{-}|/|D_2|)\sin(\phi^{+} - \psi^{-} - \theta) - (|E^{-}||P^{+}|/|D_2|)\sin(\phi^{-} - \psi^{+} + \theta)] \ , \tag{4.1-40}$$

$$\frac{\partial}{\partial\tau}\phi^{\pm} \mp \frac{\partial}{\partial x_m}\phi^{\pm} = k(|P^{\pm}|/|E^{\pm}|)\sin(\psi^{\pm} - \phi^{\pm}) \ . \tag{4.1-41}$$

In the free space, the phase velocity c in Eq.(16) is replaced by the velocity c_a for the free space. The normalized equations are given by

$$\frac{\partial}{\partial\tau} E^{\pm} \mp \frac{\partial}{\partial x_a} E^{\pm} = 0 \ , \tag{4.1-42}$$

where

$$x_a = \frac{\gamma_{\perp}}{c_a} z \ . \tag{4.1-43}$$

C. Periodic Boundary Conditions

The periodicity of the resonators (see Fig.4.1-1) requires the boundary conditions

$$\tilde{E}^{\pm}(0,t)\exp[i\omega t] = \tilde{E}^{\pm}(L_R,t)\exp[i\omega(t \pm \frac{L_R}{c'})] \tag{4.1-44}$$

for the ring laser, and

$$\tilde{E}^{+}(0,t)\exp[i\omega t] = \tilde{E}^{-}(0,t)\exp[i\omega t] ,$$
$$\tilde{E}^{-}(L_N,t)\exp[i\omega(t-\frac{L_N}{c'})] = \tilde{E}^{+}(L_N,t)\exp[i\omega(t+\frac{L_N}{c'})] \qquad (4.1\text{-}45)$$

for the normal laser in the z-t coordinate system. Here c' is the effective phase velocity over a round of the resonator, *i.e.*,

$$\frac{L}{c'} = \frac{L'}{c} + \frac{L-L'}{c_a} \text{ , where } L' = L_1$$

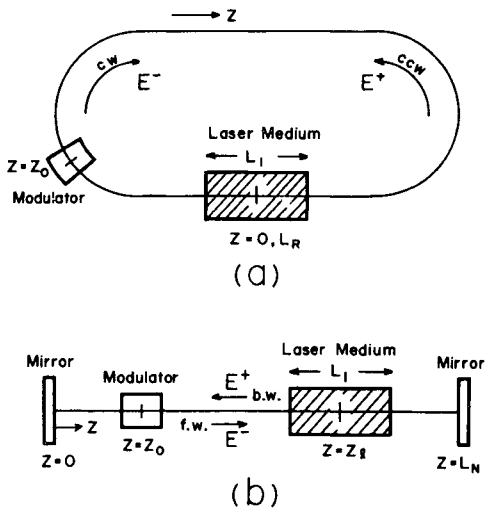

Fig.4.1-1. Configurations of the ring and normal lasers. (a) ring laser. (b) normal laser.

for the ring laser, $L' = 2L_1$ for the normal laser, and L_1 is the length of the laser medium for both lasers. As in the previous chapter, $L = L_R$ or $L = 2L_N$. We assume, for simplicity, that the central cavity-mode is in resonance with the line center ω*. That is

$$\omega\frac{L}{c'} = 2n\pi \ , \qquad (4.1\text{-}46)$$

where n is some large integer, then the boundary conditions become

$$\tilde{E}^{\pm}(0,t) = \tilde{E}^{\pm}(L_R,t) \qquad (4.1\text{-}47)$$

for the ring laser, and

$$\tilde{E}^{+}(0,t) = \tilde{E}^{-}(0,t), \quad \tilde{E}^{-}(L_N,t) = \tilde{E}^{+}(L_N,t) \ , \qquad (4.1\text{-}48)$$

for the normal laser.

---

* The central cavity-mode is specialized at the line center ω indeed, but the actual oscillation frequency may deviate from it or vary with time. Then the complex amplitudes $\tilde{E}^{\pm}(z,t)$ have phase factors which include terms varying with time proportionally.

4.2. Internal Loss-Modulation and Finite Difference Approximation

We treat an internal loss-modulation described by a time-varying transmission coefficient

$$T(t) = 1 - \alpha(1+ \cos\nu_m t) \qquad (4.2\text{-}1)$$

at $z = z_0$, where the modulation frequency ν_m is approximately equal to an integer multiple of the cavity-mode spacing. We solve the non-linear equations (4.1-30~33) with a difference approximation and seek mode-locked solutions which are synchronized with the modulation signal or periodical by itself.

One-round time is divided into l sections whose length is

$$\Delta t = \frac{L}{lv} , \qquad (4.2\text{-}2)$$

where $L = L_R$ or $L = 2L_N$, and v is the average velocity of a mode-locked optical pulse which is determined by the modulation frequency in the presence of the modulation by $v = (\nu_m/2\pi)L$. Here we introduce a detuning parameter

$$\delta = \frac{v}{c'} - 1 , \qquad (4.2\text{-}3)$$

where c' was introduced in the previous section. This parameter is equal to $\Delta\nu/\Delta$ of the previous chapter. Then the spacing $\Delta\tau$ for the normalized time τ (see Eq.(4.1-28)) is given by

$$\Delta\tau = \gamma_\perp \Delta t = \frac{\gamma_\perp L}{lc'(1+\delta)} . \qquad (4.2\text{-}4)$$

To make simple and accurate the difference approximation, we divide the perimeter of the resonator into sections whose length is Δt multiplied by the phase velocity of light, *i.e.*, $\Delta z_m = c\Delta t$ in the laser medium, and $\Delta z_a = c_a \Delta t$ in the free space. Then we find that

$$\Delta x_m = (\gamma_\perp/c)\Delta z_m = \Delta\tau , \qquad (4.2\text{-}5)$$

$$\Delta x_a = (\gamma_\perp / c_a)\Delta z_a = \Delta\tau \ . \qquad (4.2\text{-}6)$$

Even if the length of the laser medium L_1 is exactly an integer (l_m) multiple of Δz_m, the rest of the one-round optical path is not exactly an integer multiple of the spacing Δz_a unless $\delta = 0$. Then we make in the free space p (= 1 or 2) distorted sections of the length $\Delta z'$ so that

$$l'\Delta z_m + (l - l' - p)\Delta z_a + p\Delta z_a' = L \ , \qquad (4.2\text{-}7)$$

where $l' = l_m$ for the ring laser and $l' = 2l_m$ for the normal laser. We find that

$$\Delta z_a' = hc_a\Delta t \ , \quad \Delta x_a' = h\Delta\tau \ , \qquad (4.2\text{-}8)$$

where

$$h = 1 + \frac{l}{p}\,\delta \ . \qquad (4.2\text{-}9)$$

A second-order difference approximation to the basic equations is made in the following sections (see Appendix B). The relative errors of the results are of the order of 1 % .

At first sight, it is questionable that the length of the laser medium varies with the detuning. However it is acceptable as follows. Let us define $\overline{\Delta t}$ by

$$\overline{\Delta t} = \frac{L}{lc'} = (1 + \delta)\Delta t \ ,$$

and

$$\overline{\Delta z_m} = c\overline{\Delta t} \ , \quad \overline{\Delta z_a} = c_a\overline{\Delta t} \ , \quad \overline{\Delta z_a'} = hc_a\overline{\Delta t} \ ,$$

Then

$$l'\overline{\Delta z_m} + (l - l' - p)\overline{\Delta z_a} + p\overline{\Delta z_a'} = (1 + \delta)L \ .$$

That is, the modulation frequency and the length of the laser medium are kept constant and the cavity length is detuned. This is equivalent, for small detunings, to the case in which the cavity

length is kept constant and the modulation frequency is detuned.

4.3. Unidirectional Traveling-Wave Ring Laser

A unidirectional traveling-wave ring laser with a homogeneously broadened line will be the simplest laser system to be investigated. In this section, from the numerical results for this laser mode-locked by internal modulation, a simple investigation is made into the general behavior of the amplitude and phase shift of the mode-locked pulse versus modulation frequency. Self-mode locking (or self-pulsing) phenomenon has been investigated by Tang *et al.* [69] and also by Risken *et al.* [70].

Mode-Locking by Internal Loss-Modulation

The basic equations have been solved for an internally loss-modulated unidirectional ring laser with a finite difference approximation. From the stationary solutions, peak amplitude and phase shift of the mode-locked pulse are plotted versus detuning in Fig.4.3-1.

To begin with, we consider the state in which a mode-locked optical pulse is passing through the modulator at its minimum transmission-loss time, *i.e.*, the pulse phase shift $\beta = 0$ and the circulation of the pulse is synchronized with the modulation signal. Let the detuning for this state be δ_0. The pulse is neither accelerated nor decelerated, but made sharp by the modulation. The time required for the pulse to circulate the resonator is determined by the velocity of the pulse in the laser medium, which is usually lower than the phase velocity. Then the optimum detuning is negative, *i.e.*, $\delta_0 < 0$ (see Eq.(4.2-3)).

If a pulse passes through the modulator before the minimum transmission-loss time, *i.e.*, at a leading phase ($\beta > 0$), it is

decelerated and also decreases in magnitude. On the contrary, if $\beta < 0$, it is accelerated. The acceleration or deceleration increases as $|\beta|$ becomes larger, but it reaches a maximum when $|\beta| = \pi/2$. This mechanism acts usefully in the region $-\pi/2 \leq \beta \leq \pi/2$. Consequently, as δ increases from δ_0, *i.e.*, as the modulation frequency becomes higher, the pulse phase shift β increases negatively within $-\pi/2$ since the pulse should be accelerated by the modulator in order to synchronize with the high modulation frequency. As δ decreases from δ_0, the pulse phase shift β increases positively within $\pi/2$.

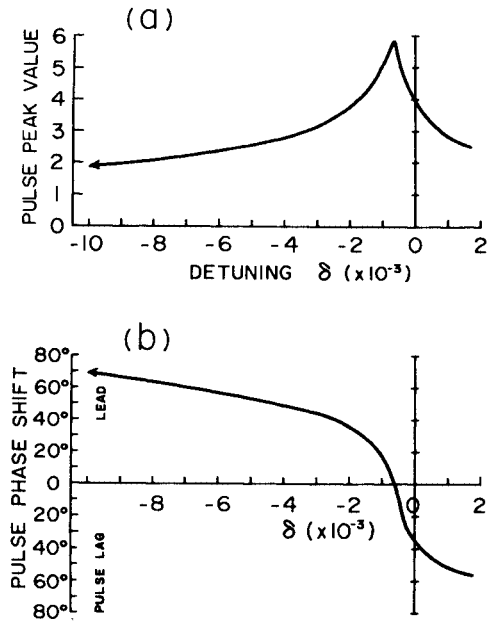

Fig.4.3-1. Peak amplitude and phase shift of the mode-locked pulse versus detuning for an internally loss-modulated unidirectional ring laser. $\gamma_\perp L_R/c' = 10\pi/3$, $\gamma = 0.1$, $k = 0.05$, $\lambda = 6$, $\alpha = 0.1$, $L_1/L_R = 1/10$.

So far, only the transformation caused by the modulation has been considered. Of course a pulse undergoes transformation including amplification from the laser medium. Generally it is decelerated in the laser medium and the deceleration will be minimum at the optimum detuning δ_0 and increase according to the shape and magnitude of the pulse. Therefore the locking curves are not symmetrical, that is, they are expanded for $\delta < \delta_0$ and shrunk for $\delta_0 < \delta$. This characteristic has been also shown from the coupled mode theory in Sec.3.6*B1*.

When the modulation depth α becomes deeper, the variation of the transmission-loss with β becomes larger, and the acceleration and deceleration become larger. Consequently, the locking region becomes wider.

4.4. Bidirectional Traveling-Wave Ring Laser

Various types of CW oscillations, self-mode locking (self-pulsing), and forced locking are investigated by an analytical investigation and a numerical integration of the basic laser equations.

A. CW Oscillation and Self-Mode Locking

It is shown that, for certain choices of laser parameters, there exists an intrinsic instability in the laser equations, *i.e.* a stationary (CW) oscillation is unstable. By a numerical integration of the equations, it is shown next that a buildup of a pulse occurs for these parameters. This is understood as a self-mode locking phenomenon in a laser with a homogeneously broadened line.

A1. Stability of CW Oscillations

The CW (τ and x independent) solutions of the basic equations (4.1-30)~(33) are as follows;

i) No oscillation:

$$E_{cw}^{\pm} = P_{cw}^{\pm} = D_{2cw} = 0 \ , \quad D_{0cw} = \lambda + 1 \ . \tag{4.4-1}$$

ii) Unidirectional CW oscillation:

a) $E_{cw}^{+} = P_{cw}^{+} = \sqrt{2}\exp(i\phi_{cw}^{+}) \ , \quad E_{cw}^{-} = P_{cw}^{-} = D_{2cw} = 0 \ , \quad D_{0cw} = 1 \ .$

b) $E_{cw}^{-} = P_{cw}^{-} = \sqrt{2}\exp(i\phi_{cw}^{-}) \ , \quad E_{cw}^{+} = P_{cw}^{+} = D_{2cw} = 0 \ , \quad D_{0cw} = 1 \ .$

(4.4-2)

iii) Bidirectional CW oscillation:

$$E_{cw}^{+} = P_{cw}^{+} = \sqrt{2/3}\exp(i\phi_{cw}^{+}) \ , \quad E_{cw}^{-} = P_{cw}^{-} = \sqrt{2/3}\exp(i\phi_{cw}^{-}) \ ,$$

$$D_{2cw} = \frac{\lambda}{3}\exp i(\phi_{cw}^{+} - \phi_{cw}^{-}) \ , \quad D_{0cw} = 1 + \frac{\lambda}{3} \ . \tag{4.4-3}$$

Here ϕ_{cw}^{+} and ϕ_{cw}^{-} are arbitrary phases, which can be made zero since the following investigations are independent of them. By a glance at these CW solutions, we can predict that the bidirectional CW

oscillation is always unstable since its total intensity

$$I_B = |E_{cw}^{+}|^2 + |E_{cw}^{-}|^2 = 4/3$$

is lower than that of the unidirectional ones

$$I_u = |E_{cw}^{+}|^2 + |E_{cw}^{-}|^2 = 2 \ .$$

In order to investigate the stability of a CW solution, we linearize Eqs.(4.1-30)~(33) about the CW solution. Therefore,

$$e_r^{\pm} = E_r^{\pm} - E_{cw}^{\pm} \ , \quad e_i^{\pm} = E_i^{\pm} \ , \quad p_r^{\pm} = P_r^{\pm} - P_{cw}^{\pm} \ , \quad p_i^{\pm} = P_i^{\pm} \ ,$$

$$d_0 = D_0 - D_{0cw} \ , \quad d_{2r} = D_{2r} - D_{2cw} \ , \quad d_{2i} = D_{2i} \qquad (4.4\text{-}4)$$

can be treated as small quantities. Here subscripts r and i denote, respectively, the real and imaginary parts of the variables. Substituting these variables into Eq.(4.1-30)~(33) and retaining only the linear terms, we obtain liner partial differential equations. They are solved by the *ansatz*

$$\begin{pmatrix} p_r^{+} \\ p_r^{-} \\ d_0 \\ d_{2r} \\ e_r^{+} \\ e_r^{-} \\ p_i^{+} \\ p_i^{-} \\ d_{2i} \\ e_i^{+} \\ e_i^{-} \end{pmatrix} = \begin{pmatrix} \bar{p}_r^{+} \\ \bar{p}_r^{-} \\ \bar{d}_0 \\ \bar{d}_{2r} \\ \bar{e}_r^{+} \\ \bar{e}_r^{-} \\ \bar{p}_i^{+} \\ \bar{p}_i^{-} \\ \bar{d}_{2i} \\ \bar{e}_i^{+} \\ \bar{e}_i^{-} \end{pmatrix} \exp(\beta\tau + i\alpha x) + \text{c.c.} \qquad (4.4\text{-}5)$$

From the condition for nontrivial solutions, we obtain the characteristic equations for β:

i) no oscillation

$$\beta + \gamma = 0 \ , \qquad (4.4\text{-}6a)$$

$$\beta^2 + (k+1 \pm i\alpha)\beta \pm i\alpha - k\lambda = 0 \ , \qquad (4.4\text{-}6b)$$

ii) unidirectional CW oscillations

$$\beta^3 + (k+\gamma+1 \pm i\alpha)\beta^2 + \{(k+1+\frac{\lambda}{2} \pm i\alpha)\gamma \pm i\alpha\}\beta + (k\lambda \pm \frac{i}{2}\alpha\lambda \pm i\alpha)\gamma = 0, \qquad (4.4\text{-}7a)$$

$$\beta^3 + (k+\gamma+1 \pm i\alpha)\beta^2 + \{(k+1+\lambda \pm i\alpha)\gamma \pm i\alpha\}\beta + (2k\lambda \pm i\alpha\lambda \pm i\alpha)\gamma = 0, \qquad (4.4\text{-}7b)$$

$$\beta^2 + (k+1 \pm i\alpha)\beta \pm i\alpha = 0 \ , \qquad (4.4\text{-}7c)$$

iii) bidirectional CW oscillation

$$\beta + \gamma = 0 \ , \qquad (4.4\text{-}8a)$$

$$\beta^5 + a_1\beta^4 + a_2\beta^3 + a_3\beta^2 + a_4\beta + a_5 = 0 \ , \qquad (4.4\text{-}8b)$$

$$\beta^5 + b_1\beta^4 + b_2\beta^3 + b_3\beta^2 + b_4\beta + b_5 = 0 \ , \qquad (4.4\text{-}8c)$$

where

$$\begin{aligned}
a_1 &= 2(k+1)+\gamma \ , \\
a_2 &= k^2 + 2k(\gamma+1-\frac{\lambda}{3}) + \alpha^2 + (\lambda+2)\gamma + 1 \ , \\
a_3 &= k^2(\gamma - \frac{2}{3}\lambda) + k(\frac{7}{3}\lambda\gamma + 2\gamma - \frac{2}{3}\lambda) + (\gamma+2)\alpha^2 + (1+\lambda)\gamma \ , \\
a_4 &= \frac{4}{3}k\lambda\gamma(k+1-\frac{\lambda}{2}) + \alpha^2(\lambda\gamma + 2\gamma + 1) \ , \\
a_5 &= -\frac{4}{3}k^2\lambda^2\gamma + (\lambda+1)\alpha^2\gamma \ , \\
b_1 &= 2(k+1)+\gamma \ , \\
b_2 &= k^2 + 2k(\gamma+1-\frac{\lambda}{3}) + \alpha^2 + (\frac{\lambda}{3}+2)\gamma + 1 \ , \\
b_3 &= k^2(\gamma - \frac{2}{3}\lambda) + k(\frac{1}{3}\lambda\gamma + 2\gamma - \frac{2}{3}\lambda) + (\gamma+2)\alpha^2 + (1+\frac{\lambda}{3})\gamma \ , \\
b_4 &= \alpha^2(\frac{1}{3}\lambda\gamma + 2\gamma + 1) \ , \\
b_5 &= (\frac{\lambda}{3}+1)\alpha^2\gamma \ .
\end{aligned}$$

A CW solution is stable if for every α the roots of its characteristic equations have negative real parts. They are unstable if one of the roots has a positive real part. Let us investigate the stability condition of each solution.

i) No oscillation: One root of Eq.(6b) has a positive real part for $\alpha = 0$ if $\lambda > 0$, and any root has a negative real part for all α if

$\lambda < 0$. This confirms that the threshold of the laser oscillation is at $\lambda = 0$.

ii) Unidirectional CW oscillation: One root of Eq.(7b) has a positive real part [70] if

$$\lambda > \lambda_c = 4 + 3\gamma + 2\sqrt{4 + 6\gamma + 2\gamma^2} \ , \tag{4.4-9}$$

and

$$\alpha_{1min} < |\alpha| < \alpha_{1max} \ , \tag{4.4-10}$$

where

$$\alpha_{1max,min} = \sqrt{\gamma(3\lambda - \gamma \pm R_1)/2}\,[1 - 2k/(\lambda - 2 - \gamma \pm R_1)], \tag{4.4-11}$$

$$R_1 = \sqrt{\lambda^2 - 2(4 + 3\gamma)\lambda + \gamma^2}.$$

Let us denote this unstable region by Region I. Equation (7a) is obtained from Eq.(7b) if λ is replaced by $\lambda/2$. Thus one root of Eq. (7a) has a positive real part if

$$\lambda > 2\lambda_c \ , \tag{4.4-12}$$

$$\alpha_{2min} < |\alpha| < \alpha_{2max}, \tag{4.4-13}$$

where

$$\alpha_{2max,min} = \sqrt{\gamma(3\lambda/2 - \gamma \pm R_2)/2}\,[1 - 2k/(\lambda/2 - 2 - \gamma \pm R_2)] \ , \tag{4.4-14}$$

$$R_2 = \sqrt{\lambda^2/4 - (4 + 3\gamma)\lambda + \gamma^2} \ .$$

Let us denote this region by Region II. It should be noticed that Eq. (7a) is the characteristic equation for the non-oscillating traveling-wave and Eq.(7b) is for the oscillating traveling-wave. Equation (7c), which is identical with Eq.(6b) if $\lambda = 0$, is for the phase of the oscillating traveling-wave. Its roots have always negative real parts for $\alpha \neq 0$. Only for $\alpha = 0$, one of the roots is equal to zero. Consequently a unidirectional phase-locked pulse oscillation is expected in Region I since the amplitude of the unidirectional CW oscillation becomes unstable there but the phase is stable elsewhere. However this expectation should be limited in the neighborhood of the CW oscillation. Phase-locked pulse oscillations are numerically obtained even far beyond the CW oscillation, which is shown in the following part.

iii) Bidirectional CW oscillation: For $\alpha = 0$, $a_5 < 0$. Thus, at least, one root of Eq.(8b) has a positive real part. Therefore the bidirectional CW oscillation is always unstable. This oscillation corresponds to the CW oscillation of a normal laser (see Sec.4.5*A*), and its instability has been explained by the so-called spatial hole burning effect by Tang *et al.* [55]. Here the spatial hole burning is described by D_2. If D_2 is ignored and made zero, then it can be shown that the basic equations give a stable bidirectional CW solution for certain choices of the parameters.

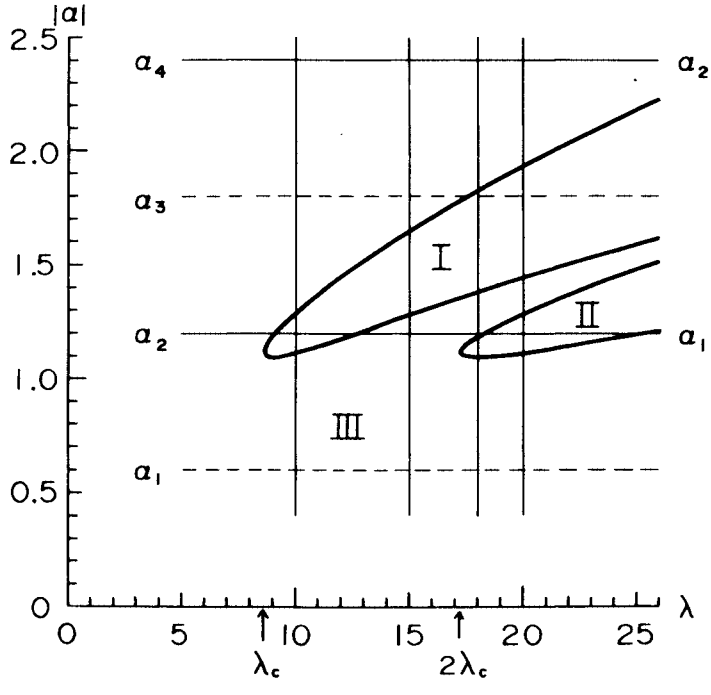

Fig.4.4-1. Stable and unstable regions of the unidirectional CW oscillation. In Region I, the oscillating traveling-wave is unstable; in II, the non-oscillating one is unstable; consequently, in III, the unidirectional CW oscillation is stable. The values of α_n's in the left file are for $\alpha_1 = 2\pi c'/(\gamma_\perp L_R) = 0.6$ and those in the right are for $\alpha_1 = 1.2$. $\gamma = 0.1$, $k = 0.05$ ($\lambda_c = 8.5988$).

Thus we may expect a unidirectional CW oscillation when $0 < \lambda < \lambda_c$, a unidirectional pulse oscillation when $\lambda_c < \lambda < 2\lambda_c$, and a bi-directional pulse oscillation when $2\lambda_c < \lambda$. This is, however, complicated by the periodic boundary condition for α. In a tuned ring or normal laser the fields have to fulfill the periodic boundary conditions (4.1-47,48). Therefore, α takes on only the discrete values

$$\alpha_n = 2n\pi(\frac{c'}{L})/\gamma_\perp = n(\frac{c'}{L})/(\frac{\gamma_\perp}{2\pi}) \ , \qquad n = 0, \pm 1, \pm 2, \ldots \qquad (4.4\text{-}15)$$

which are integer multiples of the ratio of the cavity-mode spacing to the homogeneous line width. Hence, the instability occurs only if one or more α_n lie in the region $\alpha_{min} < |\alpha_n| < \alpha_{max}$, and then, the laser fields have growing off resonance modes at $\omega \pm 2\pi nc'/L$. Stable and unstable regions of the unidirectional CW oscillation on the α-λ plane are shown in Fig.4.4-1.

A2. Numerical Results of Transient Buildup and Final Steady-State of the Pulse

The stability diagram (Fig.4.4-1) tells whether a CW solution is stable or not and also which off resonance mode grows up, if unstable, in the neighborhood of the CW solution. Some examples of the numerically obtained steady-state solutions are shown in Fig.4.4-2. From them it is shown that, if a CW solution is unstable for $\alpha = \alpha_n$, the repetition rate of the final pulse is n times the fundamental mode spacing, *i.e.*, the off resonance modes $\omega \pm m(2\pi n \frac{c'}{L})$ $(m = 1,2,\ldots)$ grow up far beyond the CW solution. For Fig.4.4-2(a), $\lambda = 20$ and $\alpha_1 = 1.2$. The stability diagram tells that, for these parameters, the initially oscillating traveling-wave is stable at a CW oscillation and that the initially non-oscillating one is unstable for only $\alpha = \alpha_1$. Therefore onetraveling-wave remains a quasi-CW oscillation and the other opposite one oscillates at the off resonance modes $\omega \pm 2\pi \frac{c'}{L}$ and has no resonance mode ω. (See also the transient buildup shown

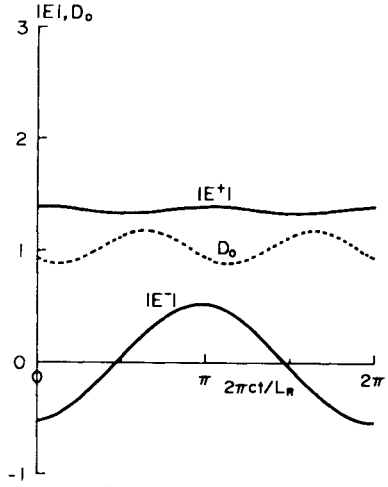

(a) $\lambda = 20$, $\alpha_1 = 1.2$.

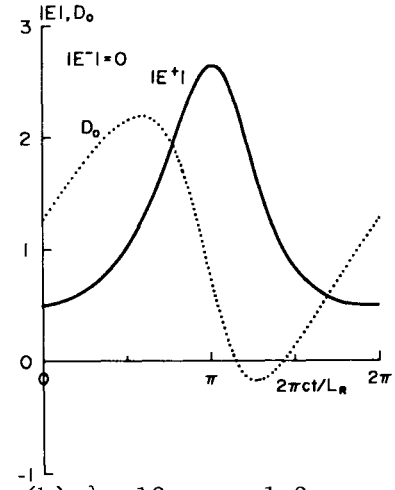

(b) $\lambda = 10$, $\alpha_1 = 1.2$.

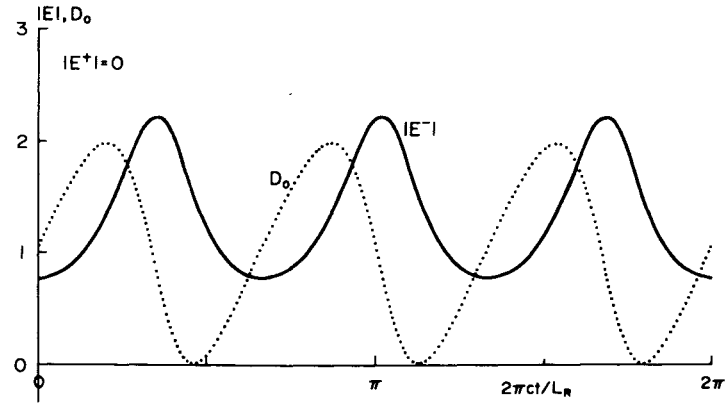

(c) $\lambda = 18$, $\alpha_1 = 0.6$.

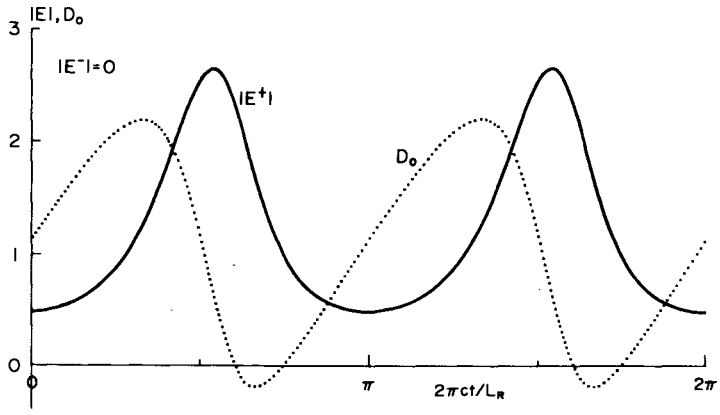

(d) $\lambda = 10$, $\alpha_1 = 0.6$.

Fig.4.4-2. Some steady state solutions at $z = 0$. $\gamma = 0.1$, $k = 0.05$, $\ell_m = 6$, $\ell = 30$ for $\alpha_1 = 1.2$, and $\ell = 60$ for $\alpha_1 = 0.6$.

in Fig.4.4-3(d).) Let us compare Fig.4.4-2(b) with (d). Only α_n's are doubled, *i.e.*, the perimeter of the resonator is halved, and the other parameters are the same. Then the same wave forms as (b) are repeated twice in a period of (d). Viewed in the frequency domain, the every other mode is quenched in (d) and its mode spectrum is identical with those of (b). This multipulse phenomenon is well known in the normal standing-wave He-Ne laser (see Sec.3.4). It will be remarkable that, in the unidirectional solution, the maximum and minimum of the population inversion D_0 is symmetrical about D_{0CW} (=1). This shows that the electric fields of these solutions are not so-called π-pulses [19,20].

In the initial state of the numerical calculations, a small pulse whose normalized amplitude and length are 0.1 and L/l respectively is placed on each traveling-wave in the fully pumped laser medium ($D_0 = \lambda + 1$). The transient buildup of the pulses is shown in Fig.4.4-3. In all the solutions, both traveling-waves grow up equally, in their early round trips, from small pulses receiving the unsaturated gain. After reaching an intermediate state, they proceed to their final steady states. In the latter saturated-gain region, the so-called large signal effects appear. At the beginning of the saturated region, the maxima of the pulses are always about one on the normalized scale. Then it may be said that the normalization constant $(\tilde{E}_{CW})^2 = 3\hbar^2\gamma_\perp\gamma_\parallel\lambda/(8\mu_{12}^2)$ is also a saturation parameter.

When $\lambda = 3$ and $\alpha_1 = 1.2$ (see Fig.4.4-3(a)), since the instability is dominant for $\alpha = \alpha_0$ (=0) in all the transient stage, the electric field grows up, keeping to be almost a CW oscillation, to an intermediate state which is exactly the bidirectional CW solution with an amplitude of $\sqrt{2/3} = 0.816$, and, after staying at this state for a while, proceeds to the final unidirectional CW oscillation without pulsation.

In this section, for simplicity, only the amplitude equations

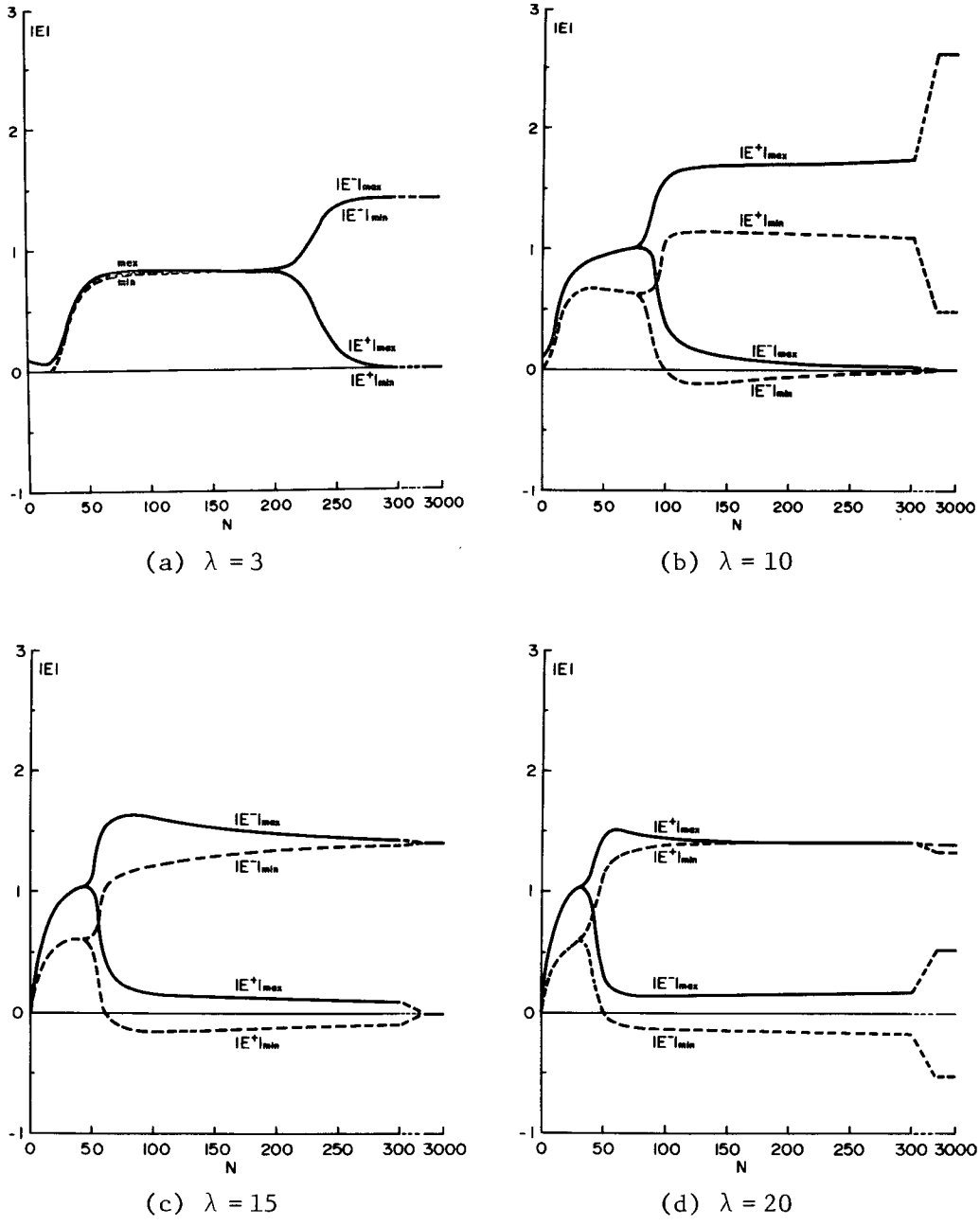

Fig.4.4-3. Examples of the transient buildup of the pulse showed by the evolution of the maximum and minimum of the pulse waveform. N is the number of round trips. $\alpha_1 = 1.2$. The other parameters are identical with those of Fig.4.4-2.

have been solved. It is assumed that $\phi^{\pm} = \psi^{\pm} = \theta = 0$ in Eqs.(4.1-35)~(38). This assumption is allowed since the bidirectional oscillation except π-type locking and the unidirectional oscillation have, always in the steady state, uniform constant phases at which they arrive after a few round trips as shown in Sec.4.5 and [70].

B. Mode Locking by Internal Loss-Modulation

The numerically obtained locking curves are as shown in Fig.4.4-4. The peak amplitude of the mode-locked pulse and its phase shift from the minimum transmission-loss time of the modulator are shown as functions of the detuning δ. The steady state solutions have been independent of the initial conditions.

When the modulator is placed at $z = \pm L_R/4$, mode-locked unidirectional oscillation is obtained about zero detuning ($-1.0 \times 10^{-3} \lesssim \delta \lesssim 2 \times 10^{-3}$), *i.e.*, for high modulation frequencies, and mode-locked bidirectional oscillation is obtained for negative detunings ($\delta \lesssim -1.0 \times 10^{-3}$). In case $z_0 = L_R/2$, the laser makes unidirectional oscillation wherever in the mode-locked region. For other modulator position, it makes an intermediate behavior of the above two extreme ones. Which of the cw and ccw traveling-waves is quenched or survives depends upon the modulator position in the same manner as in the inhomogeneous laser (Sec.3.6). As shown in Fig.4.4-4(b), there is another unidirectional region of large negative detuning. Although this seems mysterious, such a region has been sometimes recognized in a He-Ne ring laser. This will be of minor importance for application. The pulse peak intensity of the unidirectional oscillation can become about five times as large as that of the bidirectional oscillation when $z_0 = \pm L_R/4$. As shown in Sec.3.6, in an inhomogeneous He-Ne ring laser, there exist the mode-locked bidirectional region even when $z_0 = L_R/2$ and the peak intensity of the unidirectional oscillation can become only twice as large as the bidirectional one when $z_0 = \pm L_R/4$. These differences arise from the

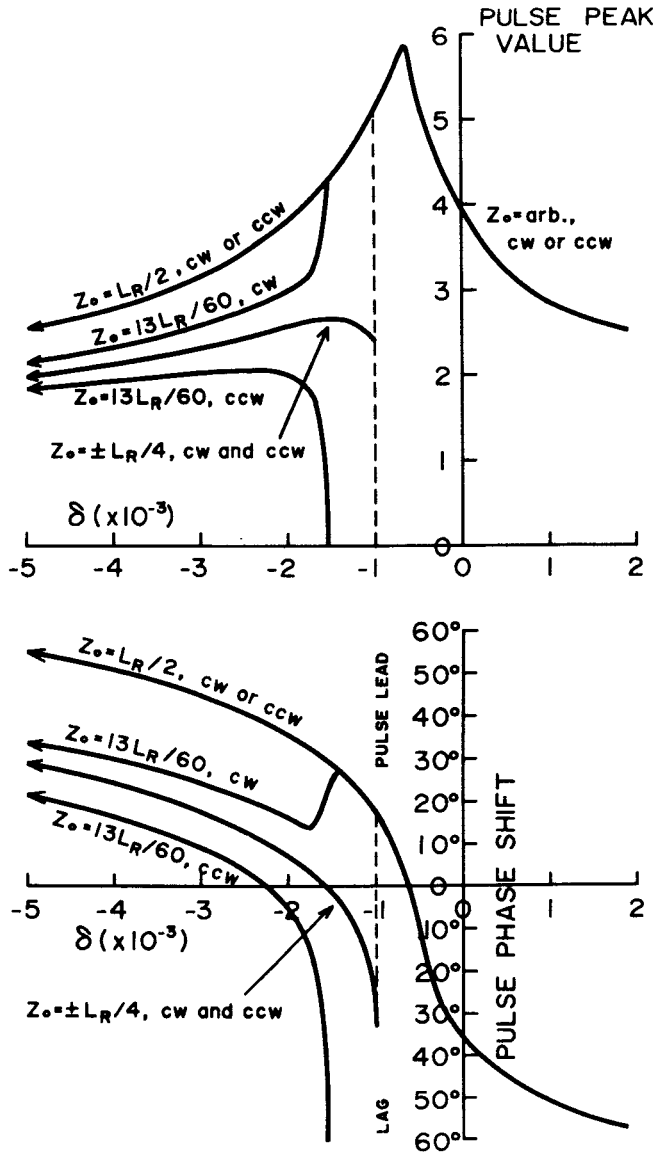

Fig. 4.4-4(a). Locking curves of an internally loss-modulated ring laser near the optimum detunings. $\alpha = 0.1$, $\gamma = 0.1$, $k = 0.05$, $\lambda = 6$, $\gamma_\perp L_R/c' = 10\pi/3$, $l_m = 6$, $l = 60$.

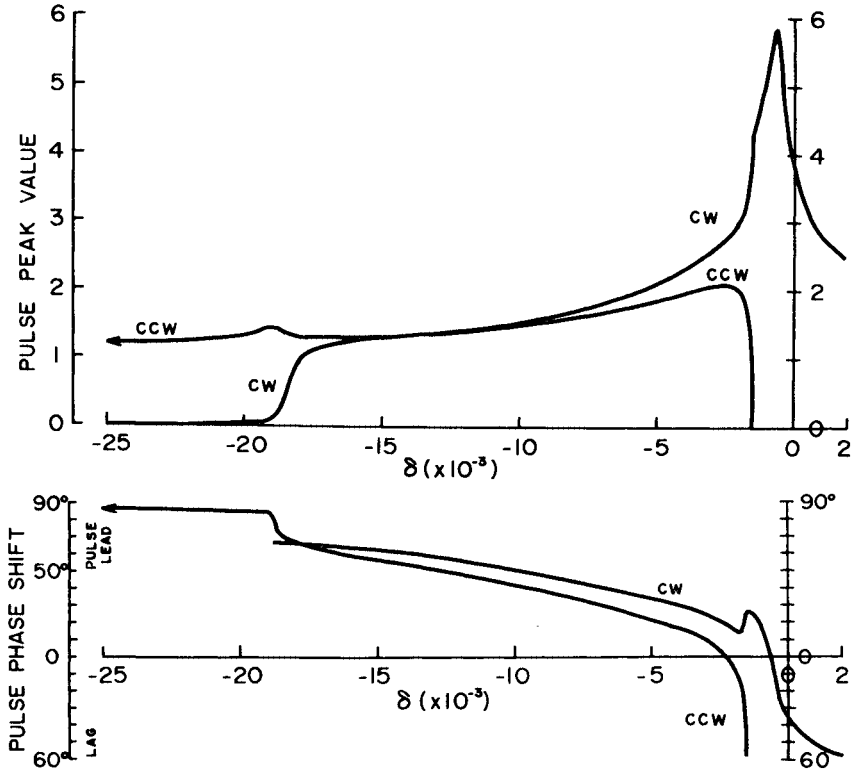

Fig.4.4-4(b). Locking curves of an internally loss-modulated ring laser in the almost whole locking range. $z_0 = 13L_R/60$.

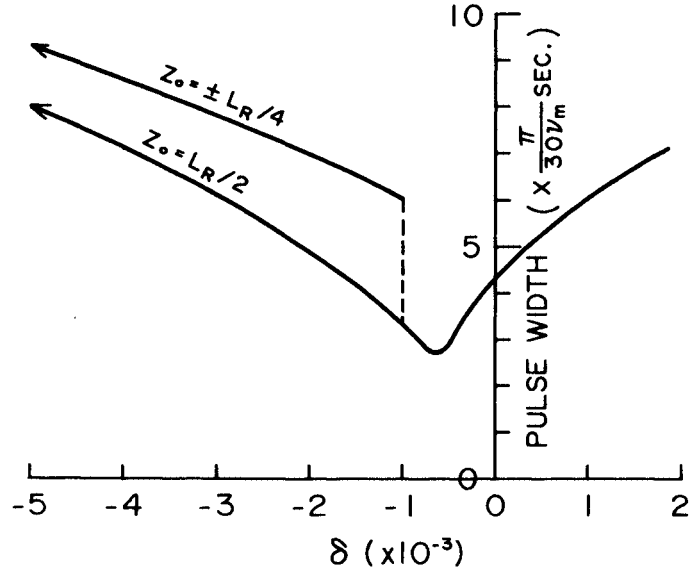

Fig.4.4-5. Pulsewidth (full-width at half-intensity) versus detuning. Parameters are identical with those of Fig.4.4-4.

fact that the oppositely directed two mirror-modes make relatively strong coupling in the medium of a homogeneously broadened line, on the other hand, they make weak coupling in the medium of an inhomogeneously Doppler-broadened line.

The pulsewidth of the unidirectional oscillation becomes about 1/2.3 time the bidirectional one as shown in Fig.4.4-5. Fig.4.4-6

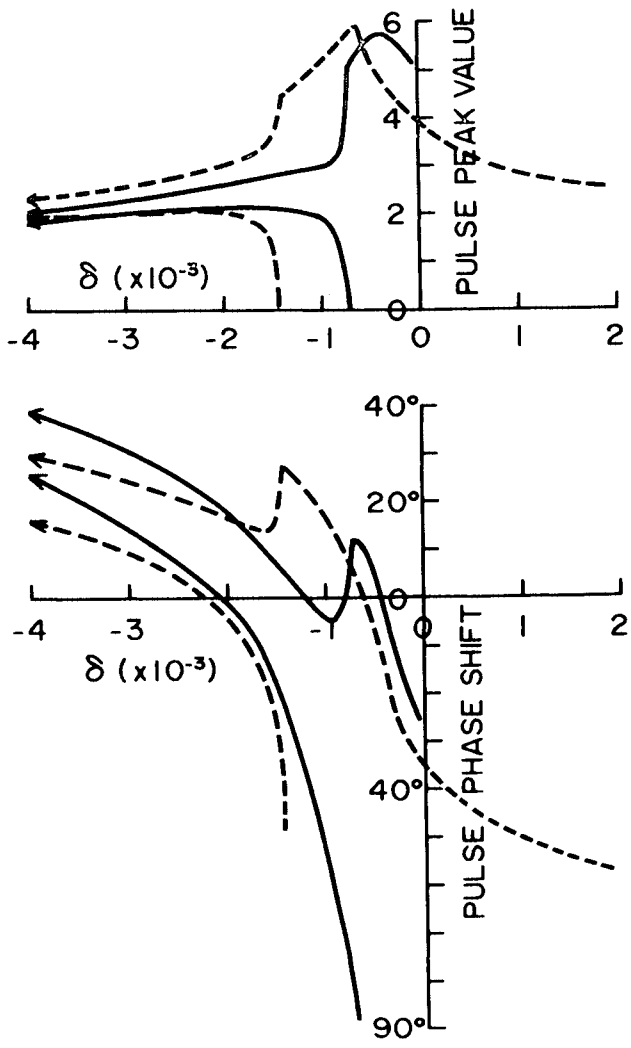

Fig.4.4-6. The α-dependence of the locking curves near the optimum detuning. $z_0 = 13L_R/60$. Solid lines are for $\alpha = 0.05$ and broken lines for $\alpha = 0.1$.

shows that the locking range becomes narrower as α decreases.

Some examples of the steady-state waveforms at the center of the laser medium are shown in Fig.4.4-7. The argument of D_2 is zero and those of $E^{\pm}$ and $P^{\pm}$ are equal to an arbitrary constant in the steady state. This constant is made zero in the figure. The magnitude of the first-order spatial variation of the population inversion D_2 is less than five percent of D_0 even in the bidirectional oscillation because the oppositely traveling pulses hardly overlap each other in the laser medium. Therefore fairly adequate in this case is the expansion of the population inversion D up to the first-order spatial Fourier component (Eq.(4.1-18)). From Fig.4.4-7 it can be seen that the pulses

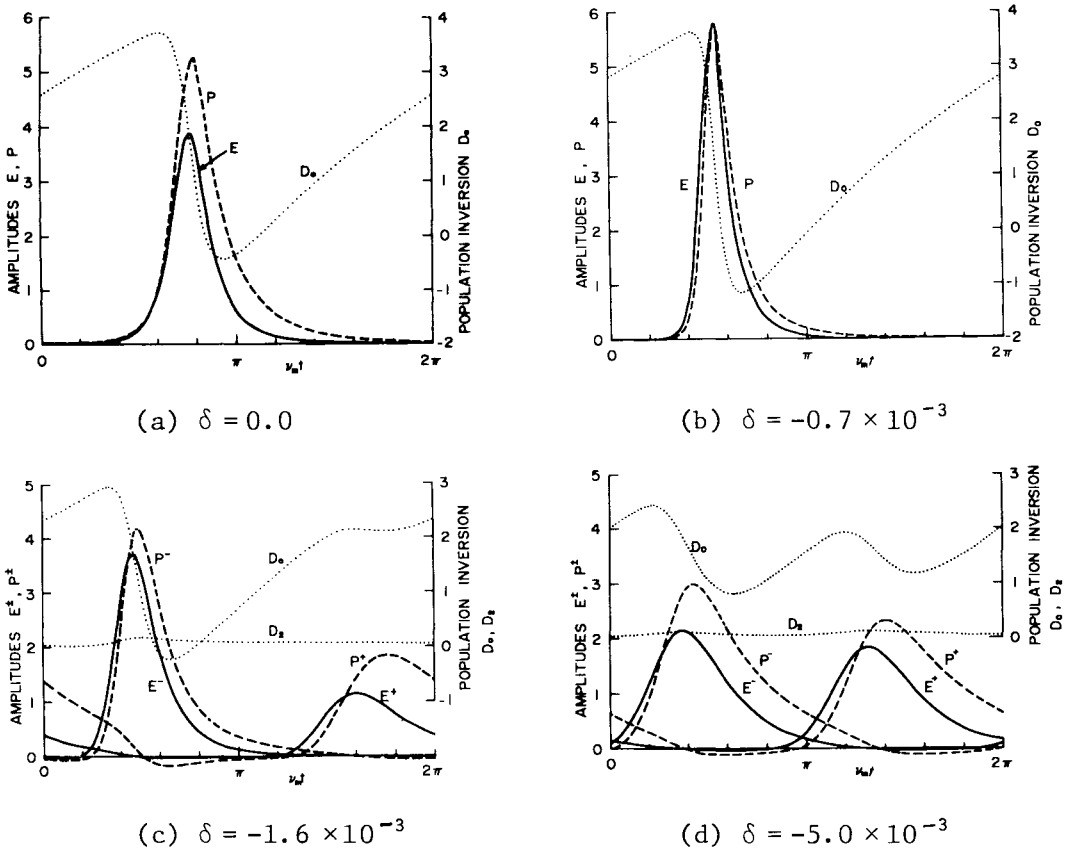

Fig.4.4-7. Examples of the waveforms at the center of the laser medium. $z_0 = 13L_R/60$. The other parameters are identical with those for Fig.4.4-4.

are transformed through the laser medium as if they travel more slowly than the phase velocity of light and that this velocity reduction is minimum at the optimum detuning. In the front part of the pulses $P \simeq E$, but $P > E$ in the hinder part. Therefore, viewed on the coordinate system which is traveling with the phase velocity, the pulses seem to be delayed. (See Eq.(4.1-33).)

It may be explained as follows why unidirectional oscillation is achieved by loss-modulation. When the longitudinal relaxation time $T_1 = 1/\gamma_{\parallel}$ is of the order of the period of the pulse train ($\gamma_{\parallel} L/c' \simeq \pi/3$ in this case), saturation of the active medium effects the pulse shape and pulse propagation nonlinearly; therefore, the velocity of a sharp pulse of the unidirectional oscillation is different from that of two broad pulses of the bidirectional oscillation. Hence only a sharp pulse of the unidirectional oscillation can synchronize with certain modulation frequencies. This explanation shows that unidirectional oscillation is obtainable also in the so-called AM-locking region of the phase-modulation.

Finally, it should be noticed that the bidirectional oscillation of the ring laser corresponds to the oscillation of the normal laser with a Fabry-Perot resonator. Compare, for example, Fig.4.4-4 with Fig.4.5-4(a).

4.5. Normal Standing-Wave Laser

Almost all the conventional laser oscillators are of the standing-wave type. Theoretical investigations have been hardly made on the mode locking phenomena of the normal standing-wave laser with a homogeneously broadened spectral line except those by means of the coupled-mode equations by Statz *et al.*[67]. However there are some interesting phenomena which do not appear in the unidirectional ring laser. In this and the next sections, various types of mode locking phenomena in a normal laser are investigated by a large-signal (time domain) theory.

A. Self-Mode Locking

The bidirectional CW solution for a ring laser Eq.(4.4-3) is also the CW solution for the corresponding normal laser:

$$E_{cw}^{\pm} = P_{cw}^{\pm} = \sqrt{2/3}\,\exp(i\phi),\ D_{2cw} = \frac{\lambda}{3},\ D_{0cw} = 1 + \frac{\lambda}{3}, \qquad (4.5\text{-}1)$$

where ϕ is an arbitrary phase. The boundary condition (4.1-48) imposes a relation upon the amplitudes of the perturbation (4.4-5), but does not alter the characteristic equations (4.4-8). From the stability investigation in Sec.4.4, this CW solution is unstable for any parameter. Hence a mode selector should be inserted into the resonator to obtain a CW oscillation [61].

Statz *et al.* [67] investigated the self-locking phenomena in three and four-mode lasers applying a maximum emission principle to the combination tone terms of the coupled mode equations and obtained the result that "0-type" or "π-type" locking occurs according as the laser medium is placed near one of the end mirrors or in the center of the resonator. They verified this theoretical result experimentally in a ruby laser. Their investigation is restricted near threshold. This section gives a general investigation by the time domain theory

and shows that the above result from the coupled mode theory is indeed restricted near threshold.

In the first place, we classify the types of the mode locking viewing in the time domain. If the envelope of the electric field $|E^{\pm}(t)|$ repeats the same (pulsative) wave form only once in a round trip time, it will be called "0-type". Although the phase of the electric field $\phi^{\pm}(t)$ repeats once, the envelope may repeat twice. It will be called "π-type". The spacing of the oscillating modes is equal to the cavity-mode spacing $c/2L_N$ in these two types. Next we will classify the types where alternate modes are quenched. If both envelope and phase repeat twice, it will be called "quenched 0-type". Similarly it will be called "quenched π-type" if the envelope repeats four times and the phase only twice.

A1. Numerical Results

Dependence of the self-mode locking on the pumping parameter and the cavity length has been investigated in the two configurations of the oscillator; one has the laser medium in the center of the resonator and the other has near one of the end mirrors, *i.e.*, $z_1 = (4/5)L_N$ (see Fig.4.4-1). Parameters are $\gamma = 0.1$, $k = 0.1$, $l = 20 \times 2$, $l_m = 2$. The types of the mode-locked solutions are shown in Fig.4.5-1 as a function of the pumping parameter and the cavity length.

When the laser medium is placed in the center of the cavity (Fig. 4.5-1(a)), "π-type" locking occurs usually, and "0-type" locking occurs only if the cavity is relatively long and also the pumping intensity is relatively high. On the border of the two regions, "0-type" or "π-type" locking occurs depending upon the initial condition. Typical examples of the wave forms are shown in Fig.4.5-2. For simplicity, only the forward traveling-wave is shown. The mode spectrum of the electric field is also shown on the right. As mentioned before, in the "π-type" locking (Fig.4.5-2(a)), the amplitude $|E^{-}|$ makes two cycles, while the phase ϕ^{-} makes only one cycle in a round trip time.

When the laser medium is placed near one of the end mirrors, the types of the mode locking largely depends upon the cavity length and the pumping intensity. "0-type" locking occurs when the cavity length is relatively short and also the pumping intensity is relatively low. As the cavity length or the pumping intensity increases, "π-type", "quenched 0-type", and "quenched π-type" lockings occur in turn. Two typical examples of the wave forms of "quenched 0-type" and "quenched π-type" lockings are shown in Fig.4.5-3.

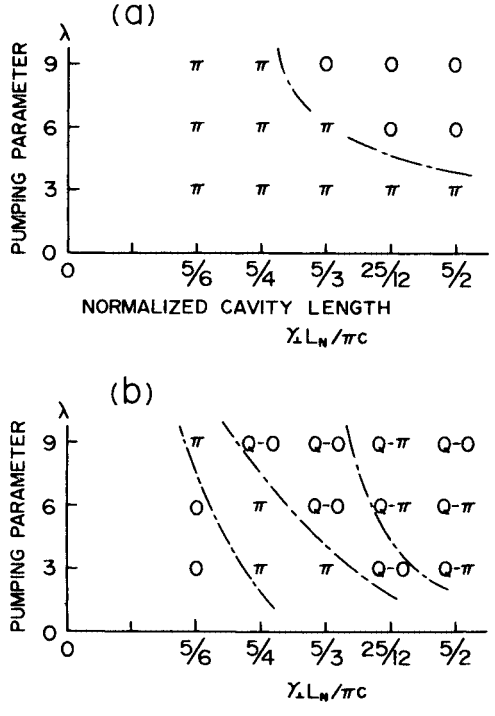

Fig.4.5-1. Dependence of the self-mode locking on the cavity length and the pumping parameter in the normal laser. The laser medium is (a) in the center of the cavity, or (b) near one of the end mirrors. [0]: 0-type, [π]: π-type, [Q-0]: quenched 0-type, [Q-π]: quenched π-type.

A2. A Physical Interpretation

When a certain mode oscillates, a standing-wave pattern appears in the laser medium. The active particles are de-excited at the loops and remain excited at the nodes. Thus the population inversion is spatially modulated. As the spatial cross-relaxation is usually slow in solid state lasers, this spatial modulation persists long enough for some other mode to build up which has, at least, some of its loops at the maxima of the spatially modulated population inversion. When the pumping level is high and, further, the mode spacing ($=c/(2L_N)$) is small, many modes oscillate. Then the electric field makes a sharp pulse. When the laser medium is placed in the center of the cavity (Fig.4.5-1(a)), this sharp pulse makes almost no standing-wave pattern in the laser

medium; therefore the population inversion is depleted spatially uniformly. This is the case with the "0-type" locking. When the pumping level is low or the cavity is short, the pulse will be broad; then a standing-wave pattern arises. To deplete uniformly the population inversion, the standing-wave pattern must move. This is

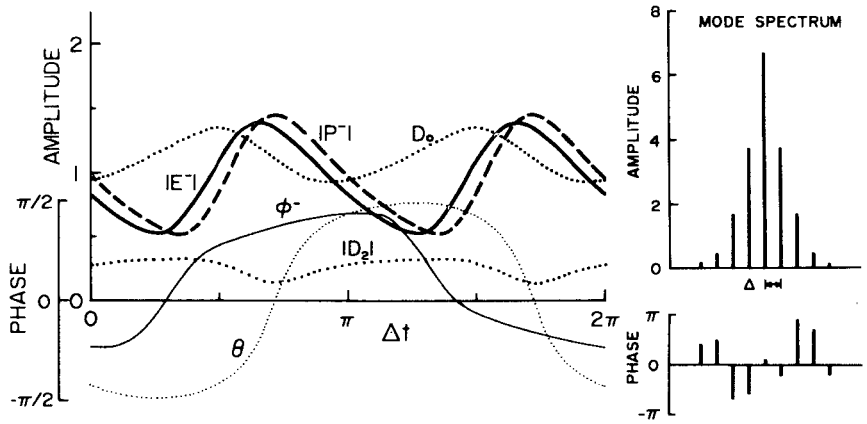

(a) "π-type" locking

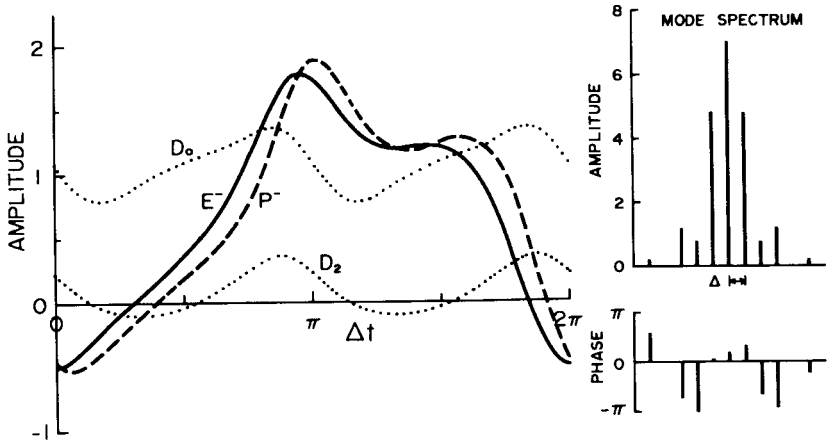

(b) "0-type" locking

Fig.4.5-2. Examples of the wave forms in the center of the laser medium which is placed in the center of the cavity: $z_l = L_N/2$. (a) $\lambda = 3.0$, $\gamma_\perp L_N/(\pi c) = 5/3$. (b) $\lambda = 6.0$, $\gamma_\perp L_N/(\pi c) = 25/12$. Phases ϕ^- and θ are for E^- and D_2, respectively. $\Delta = \pi c/L_N$.

the case with the "π-type" locking. As shown in Fig.4.5-2(a), the phase of D_2 changes from $-\pi/2$ to $\pi/2$ during the first encounter of the two oppositely traveling pulses in the medium and the reverse is the case in the second encounter. That is, the spatial hole burning pattern is shifting back and forth periodically within a quarter of a

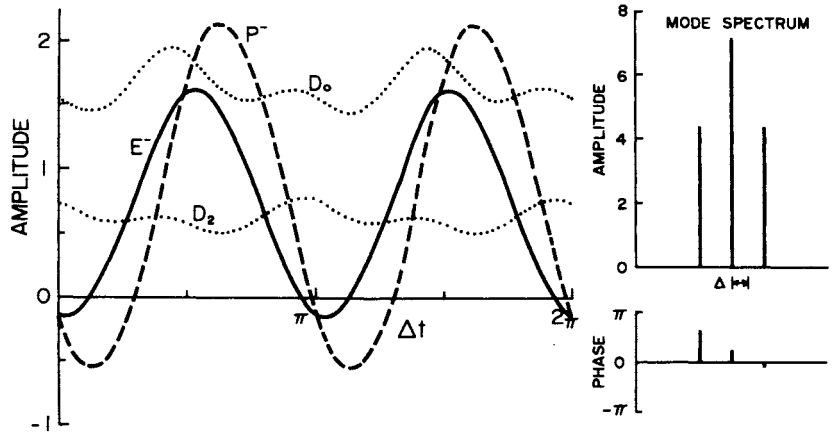

(a) "Quenched 0-type" locking

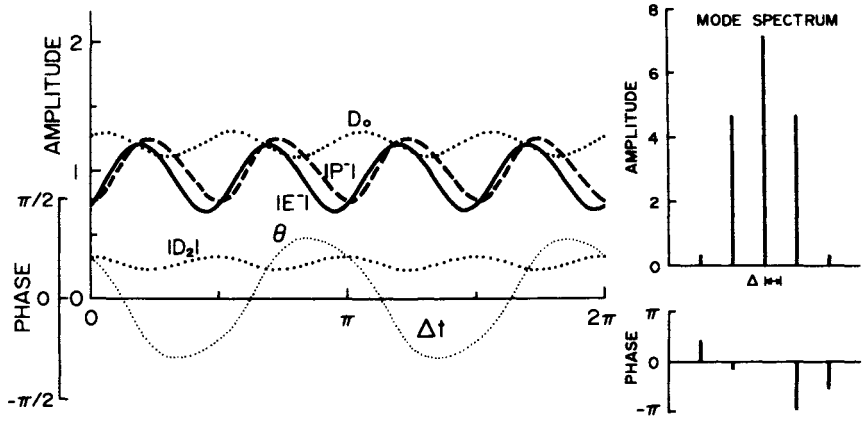

(b) "Quenched π-type" locking

Fig.4.5-3. Examples of the wave forms in the center of the laser medium which is placed near one of the end mirrors: $z_\ell = 4L_M/5$. (a) $\lambda = 6.0$, $\gamma_\perp L_M/(\pi c) = 5/3$. (b) $\lambda = 3.0$, $\gamma_\perp L_M/(\pi c) = 5/2$.

wavelength.

When the laser medium is placed near one of the mirrors, the oppositely traveling-waves incident upon or reflected from the mirror make easily a standing-wave pattern. Thus "0-type" locking readily turns to "π-type" (Fig.4.5-1(b)). As the cavity length and the pumping intensity increase, the population inversion recovers to a higher level. Then double pulsing "quenched 0-type" locking can occur, and, further, finally these pulses split into two sets of "π-type" pulses, *i.e.*, "quenched π-type" locking occurs.

B. Fundamental Mode Locking by Internal Loss-Modulation

Numerical calculations have been made on three oscillator configurations. In Oscillator A, the laser medium is placed in the center, *i.e.*, $z_\ell = L_N/2$ and the modulator at one of the end mirrors, *i.e.*, $z_0 = 0$. In Oscillator B, $z_\ell = L_N/2$ and $z_0 = L_N/6$. In Oscillator C, $z_\ell = 4L_N/5$ and $z_0 = L_N/10$. Parameters are identical with those for the ring laser. (See Fig.4.4-4(a).) Pulse peak amplitudes and phase shifts of the forward (f.w.) traveling-wave E^- and the backward (b.w.) traveling-wave E^+ are plotted versus detuning in Fig.4.5-4. Two examples of the wave forms at the center of the laser medium is also shown in Fig.4.5-5. Phases of the fields $\phi^\pm$, $\psi^\pm$, and θ are equal to a constant and not shown in the figures. It is generally the case with the fundamental mode locking.

In Oscillator A, the pulse peak amplitude has a maximum at $\delta \simeq -3.0 \times 10^{-3}$. This corresponds exactly to the mode-locked bidirectional region of the ring laser with the modulator at $z = L_R/4$ if the value of the detuning for the ring laser is doubled (Figs.4.4-4(a) and 4.4-5). The normal laser is unlocked in the region which corresponds to the mode-locked unidirectional region of the ring laser. As the modulator departs from $z = 0$ or the laser medium departs from $z = L_N/2$, the pulse peak amplitude decreases and becomes a more smooth function of the detuning. Therefore Oscillator A will be of the optimum configuration of the normal laser.

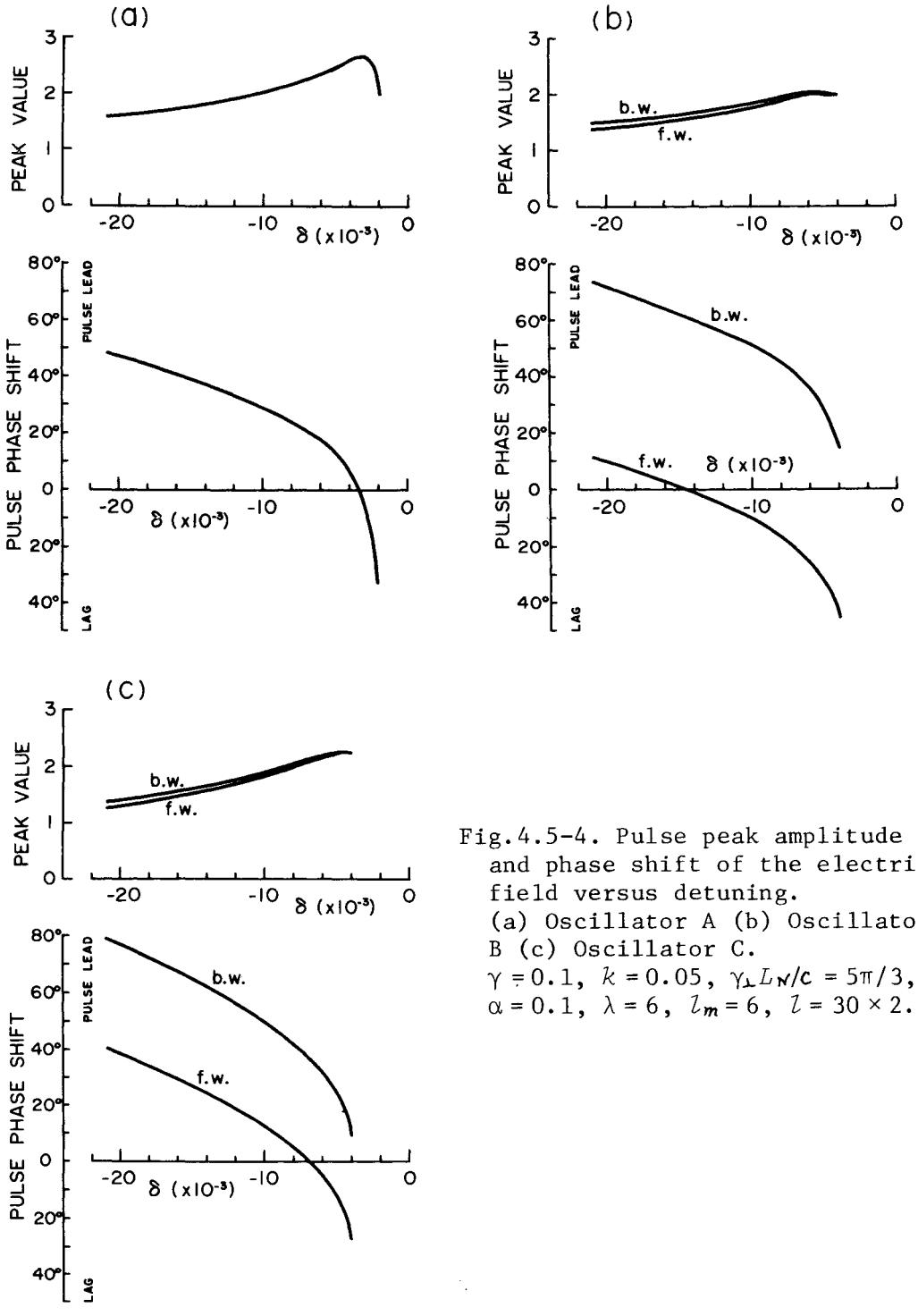

Fig.4.5-4. Pulse peak amplitude and phase shift of the electric field versus detuning.
(a) Oscillator A (b) Oscillator B (c) Oscillator C.
$\gamma = 0.1$, $k = 0.05$, $\gamma_\perp L\kappa/c = 5\pi/3$, $\alpha = 0.1$, $\lambda = 6$, $l_m = 6$, $l = 30 \times 2$.

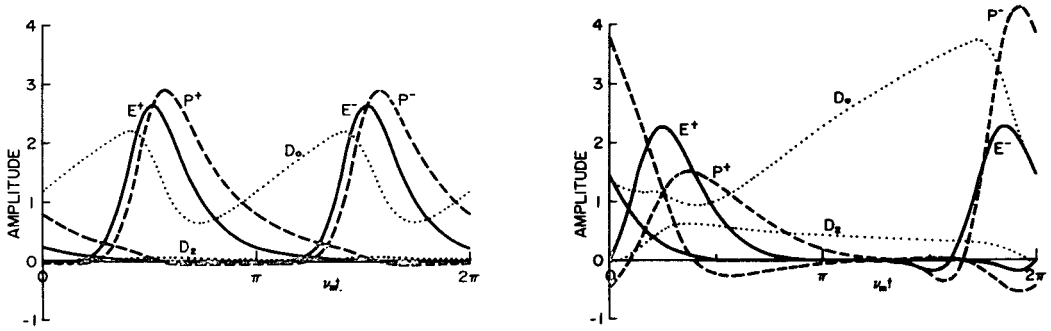

(a) (b)

Fig.4.5-5. Two examples of the numerical solutions.
(a) Oscillator A, $\delta = -3.0 \times 10^{-3}$,
(b) Oscillator C, $\delta = -4.0 \times 10^{-3}$.

C. Second Harmonic Mode-Locking by Internal Loss-Modulation

When a laser oscillator is internally modulated with a frequency equal to a multiple of the cavity-mode spacing, the mode-locked state is expected to have an output of a pulse train whose repetition frequency is also a multiple of the mode spacing. Here second harmonic mode locking is investigated by numerical calculation for two oscillators. In Oscillator A, the laser medium is placed in the center of the resonator ($z_\ell = L_N/2$) and the modulator at $z_0 = L_N/10$. In Oscillator B, $z_\ell = 4L_N/5$ and $z_0 = 0$. Parameters are $\gamma = 0.1$, $k = 0.1$, $\alpha = 0.05$, $\gamma_\perp L_N/c = 5\pi/3$, and $\lambda = 6.0$.

Detuning characteristics of Oscillator A are shown in Fig.4.5-6. Phase shift of 360° in the figure corresponds to two cycles of the modulation signal. This oscillator makes "π-type" or "0-type" locking depending upon the initial condition in the self-mode locked state (Fig.4.5-1(a)). Two types of mode locking occur depending upon the detuning. When the detuning is relatively small ($-9 \times 10^{-3} \lesssim \delta \lesssim -3 \times 10^{-3}$), "π-type" locking occurs; while "0-type" locking occurs when the detuning is large ($-21 \times 10^{-3} \lesssim \delta \lesssim -9 \times 10^{-3}$). The detuning characteristics of "0-type" locking are essentially the same with those of the fundamental mode locking. As the detuning decreases, the

peak amplitude of the pulse increases slowly untile it is finally split into two pulses. This split gives rise to a discontinuous decrease of the pulse peak amplitude and a jump of the pulse phase shift. Two typical examples of the wave forms at the center of the laser medium are shown in Fig.4.5-7 together with their mode spectra. For simplicity, only the forward traveling-wave is shown. The "π-type" pulses are fairly sharp and have many oscillating modes.

When the laser medium is placed apart from the center of the resonator, *i.e.*, in Oscillator B, the locking phenomena are fairly different from the above case. This oscillator makes "quenched 0-type" locking in the self-mode locked state (Fig.4.5-1(b)). In this case,

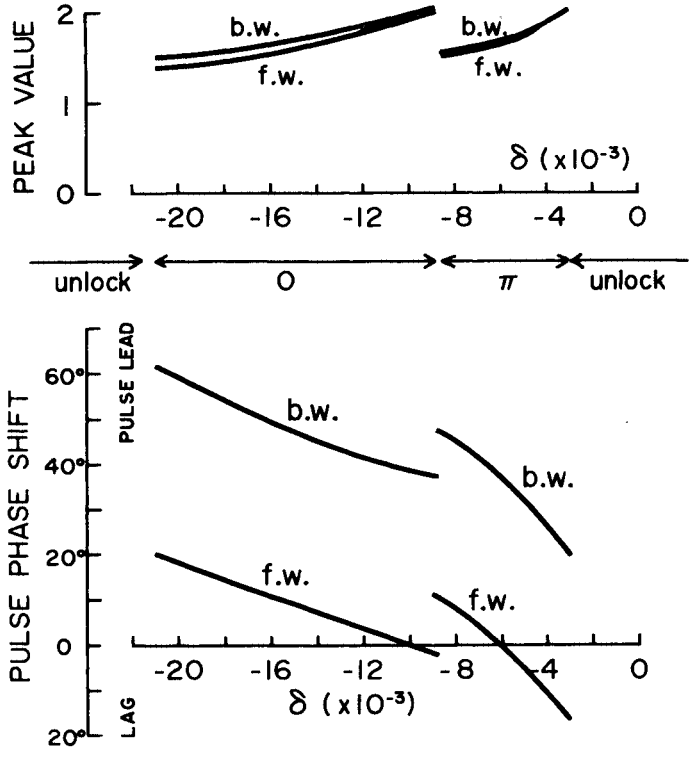

Fig.4.5-6. Detuning characteristics of the second harmonic mode locking for Oscillator A. [0]: "0-type" locking, [π]: "π-type" locking.

double pulsing occurs always independently of the detuning, but the type of the mode-locking varies. Within a narrow range of small detuning, "π-type" locking occurs. As the detuning increases negatively, it changes continuously to "quenched 0-type" locking.

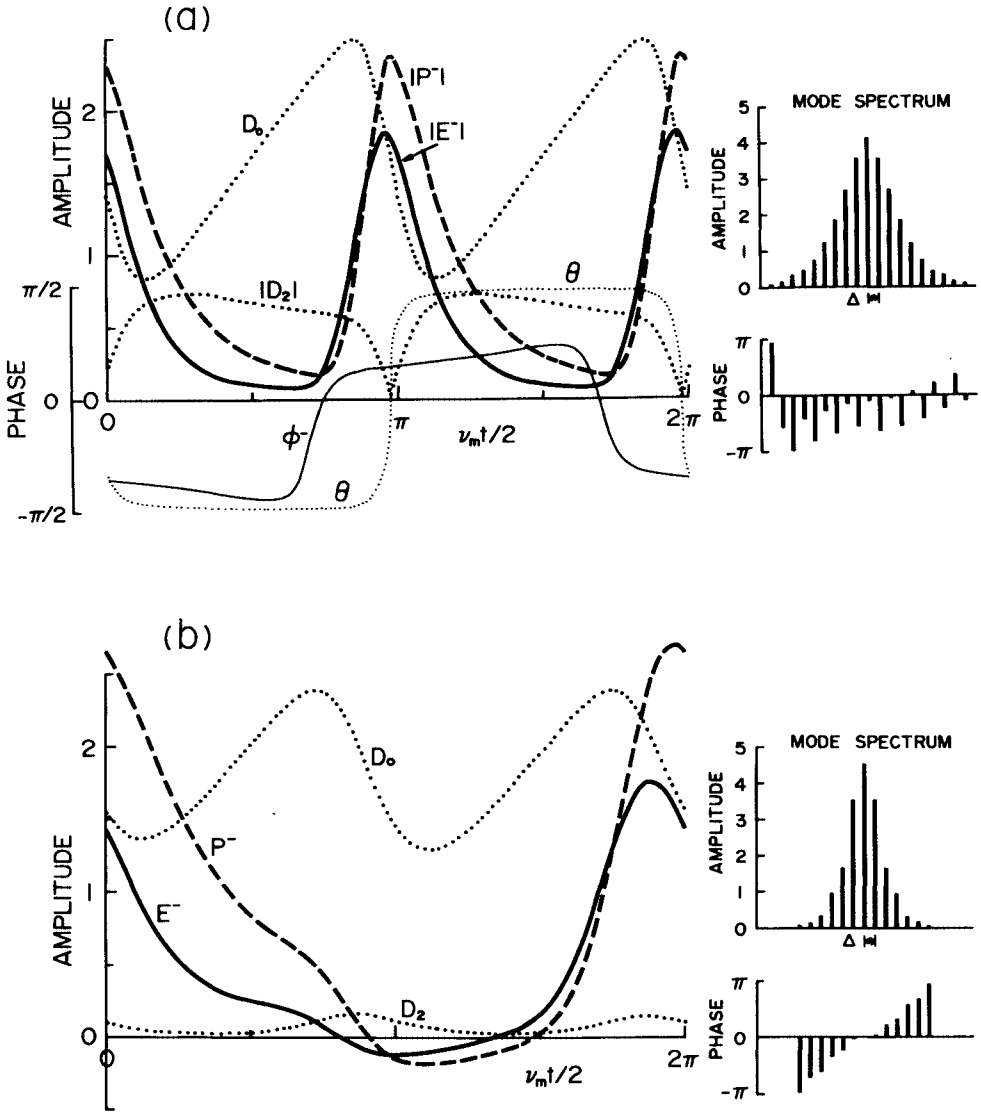

Fig.4.5-7. Two examples of the wave forms at the center of the laser medium for Oscillator A.
(a) "π-type" locking $\delta = -4.0 \times 10^{-3}$,
(b) "0-type" locking $\delta = -12.0 \times 10^{-3}$.

This extends over a relatively wide range where the even modes are suppressed but not necessarily quenched completely. With a further increase of the detuning, "π-type" locking occurs again.

The pulse peak amplitudes of the "π-type" and "quenched 0-type" lockings are as large as that of "0-type" locking. This makes a contrast to an inhomogeneous laser where the pulse peak power of "quenched 0-type" locking is less than half of that of "0-type" locking (Sec.3.4*D*). Therefore the harmonic mode locking will be useful technique for getting a high peak-power and high repetition-rate pulse train from a normal standing-wave laser with a homogeneously broadened spectral line.

Finally we should compare these results with the reported

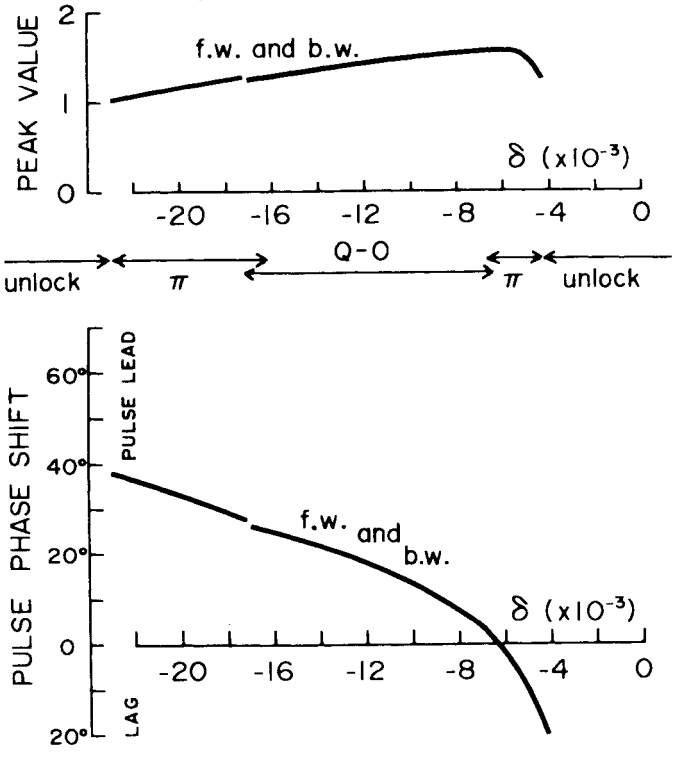

Fig.4.5-8. Detuning characteristics of the second harmonic mode locking for Oscillator B. [π]: "π-type" locking, [Q-0]: "quenched 0-type" locking.

experimental results. There are no available experimental reports of the harmonic mode locking of the homogeneous laser except a report on an internally phase-modulated Nd:YAG laser by Becker *et al.*[81].

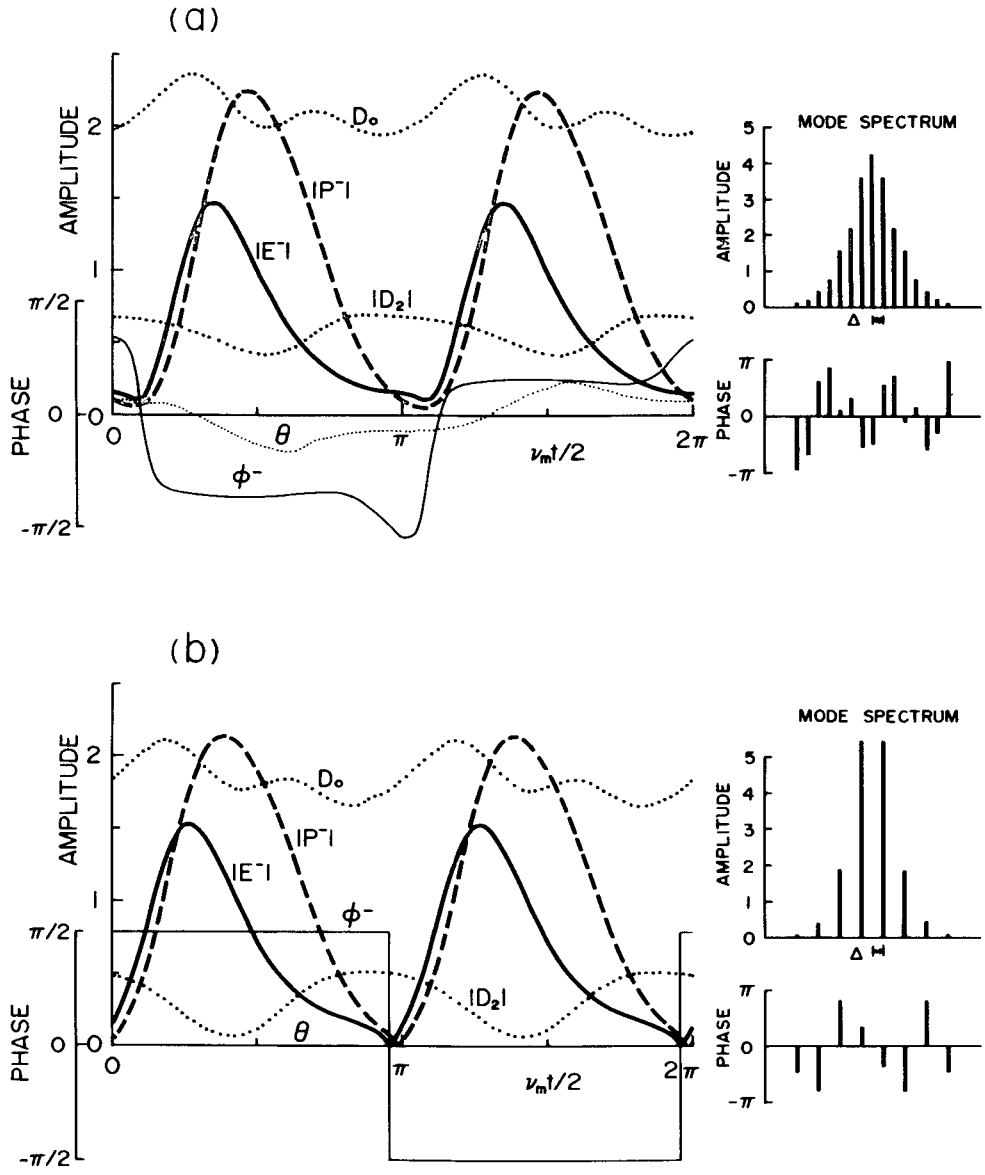

Fig.4.5-9. Two examples of the wave forms at the center of the laser medium for Oscillator B.
(a) "π-type" locking $\delta = -5.0 \times 10^{-3}$,
(b) "quenched 0-type" locking $\delta = -8.0 \times 10^{-3}$.

According to their report on the second harmonic mode locking, every adjacent axial mode was oscillating when the laser rod was located near the center of the resonator but only every other mode was oscillating when the rod was located at the end of the resonator. In either case, the repetition rate of the mode-locked pulse is equal to the modulation frequency. In other words, "π-type" locking occured in the former case and "quenched 0-type" locking in the latter case. Any quantitative observation was not reported in their paper. Their results qualitatively agree with the theoretical results of this section within a certain range of detuning ($-8.6 \times 10^{-3} \lesssim \delta \lesssim -6.5 \times 10^{-3}$).

CHAPTER 5

CONCLUSION

This thesis comprises a general study of the mode locking and mode competition phenomena in lasers on the basis of the equations of bidirectional traveling-wave ring lasers. A summary of the results is as follows.

Inhomogeneous Lasers

Theoretical investigations by the coupled mode theory and detailed experiments were made on He-Ne lasers with an inhomogeneously Doppler-broadened line.

1) Basic equations were derived for a general bidirectional multimode ring laser. These include as special cases Lamb's basic equations for a normal standing-wave laser and Aronowitz's equations for a bidirectional single-mode ring laser. The theoretical investigations were made on the basis of these basic equations.

2) Mode competition of a normal three-mode laser was investigated analytically. An experiment was made on the mode competition and mode locking in a multimode He-Ne laser. Its result was explained qualitatively by the analytical results. Usually, in the experiment, "0-type" or "quenched 0-type" locking occured according as the cavity-length was short or long.

3) The basic equations were solved numerically for the normal three-mode laser with the results that "0-type" locking occurs usually and that "π-type" locking occurs only if a relatively short laser tube is placed in the center of the cavity.

4) It was theoretically derived that, when a normal multimode laser is internally loss-modulated with double the mode spacing, "0-type"

fundamental mode locking occurs in the center of the locking range and "quenched 0-type" second harmonic mode locking occurs on the lower frequency side or on both sides. This result was verified quantitatively in an experiment on a He-Ne laser.

5) The basic equations were solved numerically for a unidirectional three-mode ring laser with the result that, unlike the normal laser, "0-type" or "π-type" locking occurs according as the mode spacing is larger or smaller than a certain value. This result was verified qualitatively in an experiment on a unidirectional He-Ne ring laser with a Faraday isolator.

6) An investigation was made on the self-locking between the oppositely traveling (OT) waves peculiar to the ring laser in a simple bidirectional two-mode ring laser with the result that the OT pulses encounter at $z = \pm L_R/4$ independently of the mode spacing, which agrees with experiments in multimode He-Ne ring lasers.

7) Mode locking and competition between the OT waves of an internally loss-modulated bidirectional ring laser were investigated analytically and numerically in the two-mode operation, numerically in the five-mode operation, and experimentally in a He-Ne ring laser. A summary of the results is as follows. a) Mode-locked unidirectional oscillation occurs in a higher-frequency part of the locking range and bidirectional one in the lower part. b) Pulse peak intensity of the unidirectional oscillation is higher than twice the bidirectional one. Pulse width becomes narrowest in the unidirectional locking range. c) The direction of the unidirectional oscillation is controlled by the position of the modulator. It is bistable when the modulator is placed at $z = \pm L_R/4$. d) Crossing point of the OT pulses are pulled towards the modulator. e) An additional external mirror makes the unidirectional oscillation more stable or changes its direction depending upon the position of the mirror.

Homogeneous Lasers

Theoretical investigations were made on lasers with a homogeneously broadened line by the time domain theory.

1) Basic equations were derived for a bidirectional ring laser. The spatial pulsation of the population inversion was taken into account by its first-order Fourier component. Investigations on the homogeneous laser in the time domain had been limitted to the self-mode locking and forced locking with zero detuning of the unidirectional ring laser. The following results were obtained from the numerical solutions of these basic equations.

2) Detuning characteristics of the forced locking of an internally loss-modulated unidirectional ring laser were calculated. Its general behavior was explained qualitatively viewed in the time domain.

3) Stability of all the CW solutions for a bidirectional ring laser was investigated analytically. Bidirectional CW oscillation proved unstable necessarily. Consequently, the stability criteria were reduced to those for the unidirectional CW oscillation by Risken *et al.*

4) Self-mode locked pulse oscillations were investigated. From the numerical solutions, it was confirmed that the number of the pulses in a round of the resonator is given by the order n of the parameter α_n which gives, at least, a root with a positive real part of the characteristic equations.

5) Detuning characteristics of an internally loss-modulated bidirectional ring laser were numerically obtained. They are qualitatively similar to those of the inhomogeneous laser except that unidirectional oscillation occurs all over the locking range when the modulator is placed about $z = L_R/2$. Pulse peak power in the unidirectional region becomes about five times as large as that in the bidirectional region, and further, the pulse width becomes less than a half. These results show that the competition between the OT waves are strong in the homogeneous laser.

6) Self-mode locked solutions of a normal laser were calculated to

investigate their dependence on the pumping parameter, the cavity-length, and the position of the laser medium in the cavity. Statz *et al.* had derived, from the coupled-mode equations, the result that "π-type" or "0-type" locking occurs according as the laser medium is placed in the center of the cavity or near one of the end mirrors. This result proved to be limited to a case in which the pumping parameter and the cavity-length are relatively small.

7) It was confirmed that the fundamental mode locking of an internally loss-modulated normal laser corresponds exactly to the bidirectional mode-locked region of the corresponding ring laser. The normal laser is unlocked with the corresponding modulation frequency to the unidirectional mode-locked region of the ring laser.

8) Second harmonic mode locking of an internally loss-modulated normal laser was calculated as a function of the modulation frequency and the position of the laser medium. Depending upon these two factors, "0-type", "π-type", "quenched 0-type", or "quenched π-type" locking occurs. Their peak power is comparable to that of the fundamental mode locking. Dependence of the results on the position of the laser medium is consistent with the experiment in a Nd:YAG laser by Becker *et al.*

Concluding Remarks

The ring resonator had not been used in the usual laser oscillators, although it has been used in the laser gyroscope. Recently, with the development of various kinds of high power lasers and tunable dye lasers, ring lasers were given attention and investigated for its strength against the optical damage, spectral purity, transverse mode purity, and mode locking characteristics. Since the advantages of the ring laser are exhibited in its unidirectional oscillation, the mode-locked unidirectional oscillation investigated in this thesis will be useful in this respect.

In this thesis, the longitudinal relaxation time is of the order

of the one round trip time of the resonator and about ten times as long as the transverse one. This condition corresponds to He-Ne laser. Solid state lasers have a very fast transverse relaxation rate and a considerably slow longitudinal relaxation rate. Both rates are very fast in dye lasers. A contrivance is needed to obtain numerical solutions of the basic equations for these lasers. We are now getting the result that these lasers also make mode-locked unidirectional oscillation like He-Ne laser with the aid of a saturable absorber.

ACKNOWLEDGMENT

The author would like to acknowledge the continuing guidance and encouragement of Professor Jun-ichi Ikenoue. He also wishes to express his thanks to Professor Kiyoshi Fukui (now he is with Okayama University) for drawing his attention to this problem. The author also wishes to thank the members of Professor Ikenoue's research group Takashi Hamada, Yôichi Ito, Hiromitsu Kato, Hakuro Mori, Yoshihiro Kawata, Saburo Shinmyo, and Hiroshi Saka for their considerable assistance.

The study on a He-Ne ring laser mode-locked by internal loss-modulation presented in Sec.3.6*B* was partially supported by the Grant-in-Aid for Scientific Research from the Ministry of Education in 1971.

APPENDIX A

Equilibrium States and Their Stability Conditions for Three-Mode Operation (Sec.3.4*B*)

One-Mode Oscillations

Equilibrium States $\mathbf{X}_o$	Stability Conditions
$(\alpha_1/\beta_1,\ 0,\ 0)$	$A_{21} < 0\ ,\quad A_{31} < 0$
$(0,\ \alpha_2/\beta_2,\ 0)$	$A_{32} < 0\quad A_{12} < 0$
$(0,\ 0,\ \alpha_3/\beta_3)$	$A_{13} < 0\quad A_{23} < 0$

Here $A_{ij} = \alpha_i \beta_j - \theta_{ij}\, \alpha_j$.

Two-Mode Oscillations

Equilibrium States $\mathbf{X}_o$	Stability Conditions
$(A_{12}/C_{12},\ A_{21}/C_{21},\ 0)$	$S_3 < 0,\ A_{12} > 0,\ A_{21} > 0,\ C_{12} > 0$
$(A_{13}/C_{13},\ 0,\ A_{31}/C_{31})$	$S_2 < 0,\ A_{31} > 0,\ A_{13} > 0,\ C_{31} > 0$
$(0,\ A_{23}/C_{23},\ A_{32}/C_{32})$	$S_1 < 0,\ A_{23} > 0,\ A_{32} > 0,\ C_{23} > 0$

Here $C_{ij} = C_{ji} = \beta_i \beta_j - \theta_{ij}\, \theta_{ji}$,

$$S_i = \alpha_i C_{jk} - \theta_{ij} A_{jk} - \theta_{ik} A_{kj} \quad (i \neq j \neq k) \ .$$

Three-Mode Oscillation

Equilibrium State: $\mathbf{X}_0 = (\Delta_1/\Delta,\ \Delta_2/\Delta,\ \Delta_3/\Delta)$.

Stability Condition:

$$\Delta_1 > 0,\quad \Delta_2 > 0,\quad \Delta_3 > 0,\quad \Delta > 0,$$

$$(\beta_1\beta_2 - \theta_{12}\theta_{21})X_{10}X_{20} + (\beta_2\beta_3 - \theta_{23}\theta_{32})X_{20}X_{30}$$

$$+ (\beta_3\beta_1 - \theta_{31}\theta_{13})X_{30}X_{10} > 0 \ ,$$

$$\beta_1\{(\beta_1\beta_2 - \theta_{12}\theta_{21})X_{20} + (\beta_1\beta_3 - \theta_{13}\theta_{31})X_{30}\}X_{10}^2$$

$$+ \beta_2\{(\beta_2\beta_3 - \theta_{23}\theta_{32})X_{30} + (\beta_2\beta_1 - \theta_{21}\theta_{12})X_{10}\}X_{20}^2$$

$$+ \beta_3\{(\beta_3\beta_1 - \theta_{31}\theta_{13})X_{10} + (\beta_3\beta_2 - \theta_{32}\theta_{23})X_{20}\}X_{30}^2$$

$$+ (2\beta_1\beta_2\beta_3 - \theta_{12}\theta_{23}\theta_{31} - \theta_{32}\theta_{21}\theta_{13})X_{10}X_{20}X_{30} > 0 \ ,$$

where

$$\Delta_1 = \begin{vmatrix} \alpha_1 & \theta_{12} & \theta_{13} \\ \alpha_2 & \beta_2 & \theta_{23} \\ \alpha_3 & \theta_{32} & \beta_3 \end{vmatrix} \ , \quad \Delta_2 = \begin{vmatrix} \beta_1 & \alpha_1 & \theta_{13} \\ \theta_{21} & \alpha_2 & \theta_{23} \\ \theta_{31} & \alpha_3 & \beta_3 \end{vmatrix} \ , \quad \Delta_3 = \begin{vmatrix} \beta_1 & \theta_{12} & \alpha_1 \\ \theta_{21} & \beta_2 & \alpha_2 \\ \theta_{31} & \theta_{32} & \alpha_3 \end{vmatrix} \ ,$$

$$\Delta = \begin{vmatrix} \beta_1 & \theta_{12} & \theta_{13} \\ \theta_{21} & \beta_2 & \theta_{23} \\ \theta_{31} & \theta_{32} & \beta_3 \end{vmatrix} .$$

APPENDIX B

Finite Difference Approximation to the Partial Differential Equations (4.1-30~33)

A second-order finite difference approximation has been made. The difference equations solved by numerical calculations are as follows. Here m and n indicate mth grid point of the x-axis and nth grid point of the τ-axis respectively.

In the Laser Medium

$$E^+(m,n+1) = b_1E^+(m,n) + b_2E^+(m+1,n) + b_3P^+(m,n) + b_4P^+(m+1,n)$$

$$+ b_5[E^+(m,n)D_0(m,n) - E^-(m,n)D_2(m,n)] \quad , \tag{B-1}$$

$$E^-(m,n+1) = b_1E^-(m,n) + b_2E^-(m-1,n) + b_3P^-(m,n) + b_4P^-(m-1,n)$$
$$+ b_5[E^-(m,n)D_0(m,n) - E^+(m,n)\{D_2(m,n)\}^*] \quad , \tag{B-2}$$

$$P^+(m,n+1) = c_1P^+(m,n) + c_2E^+(m,n) + D_0(m,n)H^+(m,n) - D_2(m,n)H^-(m,n)$$
$$+ c_6[E^+(m,n)R(m,n) + \frac{1}{2}E^-(m,n)M(m,n)] \quad , \tag{B-3}$$

$$P^-(m,n+1) = c_1P^-(m,n) + c_2E^-(m,n) + D_0(m,n)H^-(m,n) - \{D_2(m,n)\}^*H^+(m,n)$$
$$+ c_6[E^-(m,n)R(m,n) + \frac{1}{2}E^+(m,n)\{M(m,n)\}^*] \quad , \tag{B-4}$$

$$D_0(m,n+1) = d_1 + d_2D_0(m,n)$$
$$+ d_3 \cdot \mathrm{Re}[\{P^+(m,n)\}^*H^+(m,n) + \{P^-(m,n)\}^*H^-(m,n)]$$
$$+ d_4[D_0(m,n)K(m,n) - 2\mathrm{Re}\{D_2(m,n)N(m,n)\}] \quad , \tag{B-5}$$

$$D_2(m,n+1) = d_2D_2(m,n) - \frac{1}{2}d_3[P^+(m,n)\{H^-(m,n)\}^* + \{P^-(m,n)\}^*H^+(m,n)]$$
$$+ d_5[D_2(m,n)K(m,n) - 2D_0(m,n)\{N(m,n)\}^*] \quad , \tag{B-6}$$

where

$$H^{\pm}(m,n) = c_3E^{\pm}(m,n) + c_4E^{\pm}(m\pm1,n) + c_5P^{\pm}(m,n) \quad ,$$

$$N(m,n) = \{E^+(m,n)\}^*E^-(m,n) \quad ,$$

$$M(m,n) = E^+(m,n)\{P^-(m,n)\}^* + \{E^-(m,n)\}^*P^+(m,n) \quad ,$$

$$R(m,n) = \mathrm{Re}[E^+(m,n)\{P^+(m,n)\}^* + E^-(m,n)\{P^-(m,n)\}^*] \quad ,$$

$$K(m,n) = |E^+(m,n)|^2 + |E^-(m,n)|^2 \quad , \tag{B-7}$$

$$b_1 = k^2(\Delta\tau)^2/2 \quad , \qquad b_2 = 1 - k\Delta\tau \quad ,$$
$$b_3 = k\Delta\tau\{1 - (1+k)\Delta\tau\}/2 \quad , \qquad b_4 = k\Delta\tau/2 \quad ,$$
$$b_5 = k(\Delta\tau)^2/2 \quad , \qquad c_1 = 1 - \Delta\tau + (\Delta\tau)^2/2 \quad ,$$
$$c_2 = \gamma(\lambda+1)(\Delta\tau)^2/2 \quad , \qquad c_3 = \Delta\tau\{1 - (1+k+\gamma)\Delta\tau\}/2 \quad ,$$
$$c_4 = \Delta\tau/2 \quad , \qquad c_5 = b_5 \quad ,$$
$$c_6 = -\lambda\gamma(\Delta\tau)^2/4 \quad , \qquad d_1 = \gamma(\lambda+1)(1 - \gamma\Delta\tau/2)\Delta\tau \quad ,$$
$$d_2 = 1 - \gamma\Delta\tau + \gamma^2(\Delta\tau)^2/2 \quad , \qquad d_3 = -\lambda\gamma/2 \quad ,$$
$$d_4 = c_6 \quad , \qquad d_5 = c_6/2 \quad . \tag{B-8}$$

At the Incidence Points to the Laser Medium

1) Equation (B-2) is replaced by

$$E^{-}(m_1,n+1) = E^{-}(m_1-1,n)$$

at m_1, and

2) Equation (B-1) is replaced by

$$E^{+}(m_2,n+1) = E^{+}(m_2+1,n)$$

at m_2. The other equations are unchanged.

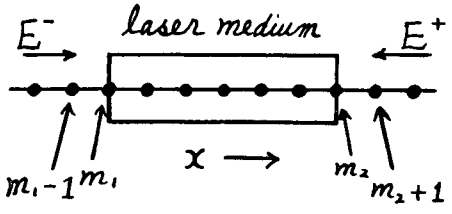

In the Free Space

$$E^{\pm}(m,n+1) = E^{\pm}(m\pm1,n) \quad . \tag{B-9}$$

In the Distorted Sections

Usually one distorted section is sufficient, *i.e.*, $p = 1$.

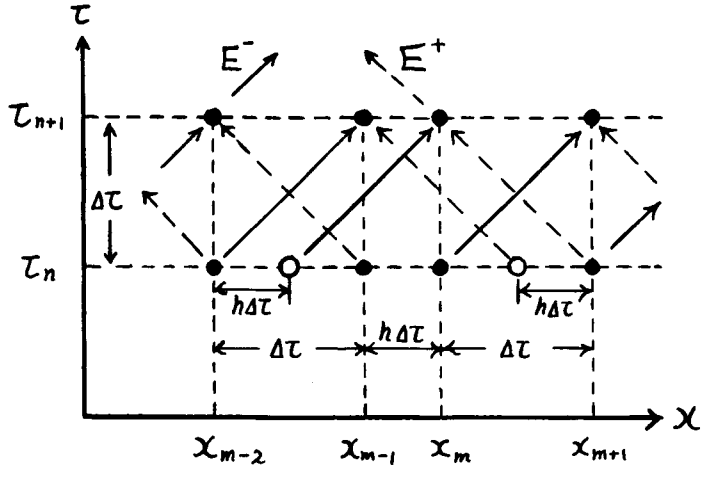

Let $\overline{x_{m-1}\, x_m}$ be the distorted section, then, using the three-point Lagrangian interpolation formula,

$$E^{+}(m-1,n+1) = E^{+}(m,n) + \frac{1-h}{1+h}\{E^{+}(m+1,n) - E^{+}(m-1,n)\} \quad ,$$

$$E^{-}(m,n+1) = E^{-}(m-1,n) + \frac{1-h}{1+h}\{E^{-}(m-2,n) - E^{-}(m,n)\} \quad . \tag{B-10}$$

BIBLIOGRAPHY

Gas Lasers and Inhomogeneous Broadening

Basic Theory

[1] W.E.Lamb.Jr.,"Theory of an optical maser," *Phys.Rev.*, 134 (1964) A1429.

[2] a. T.Miyashita and J.Ikenoue,"4モード・リング・レーザの基礎方程式" 輻射科学研究会 Jan. 1970.
b. T.Miyashita, H.Mori, and J.Ikenoue,"Theory of a multimode ring laser," *Japan.J.Appl.Phys.* 10 (1971) 1051.

Single-Mode Operation

[3] R.A.McFarlane, W.R.Bennett,Jr., and W.E.Lamb Jr.,"Single mode tuning dip in the power output of an He-Ne optical maser," *Appl. Phys.Letters* 2 (1963) 189.

[4] a. R.H.Cordover *et al.*,"Isotope shift measurement for 6328Å He-Ne laser transition," *ibid.* 7 (1965) 322.
b. A.Szöke and A.Javan,"Isotope shift and saturation behavior of the 1.15μ transition of Ne," *Phys.Rev.Letters* 10 (1963) 521.

[5] a. B.J.Feldman and M.S.Feld,"Theory of a high-intensity gas laser," *Phys.Rev.A* 1 (1970) 1375.
b. S.Stenholm and W.E.Lamb,Jr.,"Semiclassical theory of a high-intensity laser," *Phys.Rev.* 181 (1969) 618.
c. A.Icsevgi and W.E.Lamb,Jr.,"Propagation of light pulses in laser amplifier," *ibid.* 185 (1969) 517.

[6] F.Aronowitz,"Effects of radiation trapping on mode competition and dispersion in the ring laser," *Appl.Opt.* 11 (1972) 2146.

[7] P.W.Smith,"The effect of cross relaxation on the behavior of gas laser oscillators," *IEEE J.Quantum Electron.* QE-8 (1972) 704.

Mode Competition

[8] W.R.Bennett,Jr.,"Hole burning effects in a He-Ne optical maser," *Phys.Rev.* 126 (1962) 580.

[9] R.A.McFarlane,"Frequency pushing and frequency pulling in a He-Ne gas optical maser," *ibid.* 135 (1964) A543.

[10] R.L.Fork and M.A.Pollack,"Mode competition and collision effects in gaseous optical maser," *ibid.* 139 (1965) A1408.

[11] G.W.Hong,"Mode-coupling effects in mode-selection experiments," *J.Appl.Phys.* 39 (1968) 4754.

[12] a. K.Fukui, T.Miyashita, and J.Ikenoue, "3モード・レーザの安定解およびモード競合" 電気四学会連合大会 1534 April 1967.
b. K.Fukui, T.Miyashita, Y.Ito, and J.Ikenoue, "3,4モード・レーザの安定解" 輻射科学研究会 Feb. 1967.
c. ——, "3,4モード・レーザの安定解について" 量子エレクトロニクス研究会 QE67-5 June 1967.

Self-Locking

[13] T.Uchida and A.Ueki,"Self-locking of gas lasers," *IEEE J.Quantum Electron.* QE-3 (1967) 17.

[14] F.R.Nash,"Observations of spontaneous phase locking of TEM_{00q} modes at 0.63μ," *ibid.* QE-3 (1967) 189.

[15] R.E.McClure,"Mode locking behavior of gas lasers in long cavities," *Appl.Phys.Letters* 7 (1965) 148.

[16] M.H.Crowell,"Characteristics of mode-coupled lasers," *IEEE J. Quantum Electron.* QE-1 (1965) 12.

[17] O.L.Gaddy and E.M.Schaefer,"Self-locking of modes in the Argon ion laser," *Appl.Phys.Letters* 9 (1966) 281.

[18] P.W.Smith,"The self-pulsing laser oscillator," *IEEE J.Quantum Electron.* QE-3 (1967) 627.

[19] A.G.Fox and P.W.Smith,"Mode-locked laser and the 180° pulse," *Phys.Rev.Letters* 18 (1967) 826.

[20] J.A.Armstrong and E.Courtens,"Exact solution of a π-pulse problem," *IEEE J.Quantum Electron.* QE-4 (1968) 411.

[21] M.Sargent III,"Mode locking according to the Lamb theory," *ibid.* QE-4 (1968) 346.

[22] A.Bambini and P.Burlamacchi,"Stability conditions for mode-locked gas lasers," *ibid.* QE-4 (1968) 101.

[23] D.G.C.Jones,"Self-locking of three modes in the He-Ne laser," *Appl.Phys.Letters* 13 (1968) 301.

[24] J.A.Carruthers and T.Bieber,"Pulse velocity in a self-locked He-Ne laser," *Proc. IEEE* 57 (1969) 426.

[25] R.L.Fork, L.E.Hargrove, and M.A.Pollack,"Population pulsations and lifetimes in He-Ne lasers," *Appl.Phys.Letters* 5 (1964) 5.

[26] P.W.Smith,"Phase locking of laser modes by continuous cavity length variation," *ibid.* 10 (1967) 51.

Mode Locking by Internal Modulation

[27] L.E.Hargrove, R.L.Fork, and M.A.Pollack,"Locking of He-Ne laser modes induced by synchronous intracavity modulation," *ibid.* 5 (1964) 4.

[28] E.O.Ammann, B.J.McMurtry, and M.K.Oshman,"Detailed experiments on Helium-Neon FM lasers," *IEEE J.Quantum Electron.* QE-1 (1965) 263.

[29] T.Uchida,"Dynamic behavior of gas lasers," *ibid.* QE-3 (1967) 7.

[30] G.W.Hong and J.R.Whinnery,"Switching of phase-locked states in the intracavity phase-modulated He-Ne laser," *ibid.* QE-5 (1969) 367.

[31] C.M.Ferrar,"Controllable phase-locked frequency splitting in two-frequency lasers," *ibid.* QE-7 (1971) 373.

[32] a. M.DiDomenico,Jr.,"Small-signal analysis of internal (coupling-type) modulation of lasers," *J.Appl.Phys.* 35 (1964) 2870.
b. A.Yariv,"Internal modulation in multimode laser oscillators," *ibid.* 36 (1965) 388.
c. ———,"Parametric interaction of optical masers," *IEEE J. Quantum Electron.* QE-2 (1966) 30.

[33] a. S.E.Harris and O.P.McDuff,"Theory of FM laser oscillation," *ibid.* QE-1 (1965) 245.
b. O.P.McDuff and S.E.Harris,"Nonlinear theory of the internally loss-modulated laser," *ibid.* QE-3 (1967) 101.
[34] J.Hirano and T.Kimura,"Multiple mode locking of lasers," *ibid.* QE-5 (1969) 219.
[35] a. T.Miyashita, Y.Ito, and J.Ikenoue,"基本モード間隔の2倍の周波数での強制AMモード同期" 電子通信学会 全国大会 620 Sept. 1969.
b. ——,"——" 輻射科学研究会 Sept. 1969.
c. T.Miyashita and J.Ikenoue,"Phase-locking of the gas laser loss-modulated with double the mode spacing," *Japan. J. Appl. Phys.* 9 (1970) 717.

Ring Laser

[36] a. S.A.Collins,"Analysis of optical resonators involving focusing elements," *Appl.Opt.* 3 (1964) 1263.
b. S.A.Collins,Jr. and D.T.M.Davis,Jr.,"Modes in a triangular ring optical resonator," *ibid.* 3 (1964) 1314.
c. S.N.Bagaev *et al.*,"The polarization of radiation and the frequency characteristics of ring lasers with a triangular resonator," *Opt.Spectr. U.S.S.R.* (1966) 768.
d. I.M.Karzhenevich *et al.*,"Selection of the principal transverse mode in a ring resonator," *Soviet J.Quantum Electron.* 1 (1972) 637.
e. L.S.Watkins and R.C.Smith,"Operation of a circularly polarized ring laser," *IEEE J.Quantum Electron.* QE-7 (1971) 59.
[37] a. W.M.Macek *et al.*,"Ring laser rotation rate sensor," *Proc. Symposium on Optical Masers* (Polytechnic, New York, 1963) p.199
b. ——,"The ring laser," *Proc. Symposium on Modern Optics* (Polytechnic, New York, 1967) p.389.
c. J.Killpatrick,"The laser gyro," *IEEE Spectrum* 44 Oct. 1967.
[38] F.Aronowitz,"Theory of a traveling-wave optical maser," *Phys.Rev.* 139 (1965) A635.
[39] T.J.Hutchings *et al.*,"Amplitude and frequency characteristics of a ring laser," *ibid.* 152 (1966) 467.
[40] F.Aronowitz,"Single-isotope laser gyro," *Appl.Opt.*11 (1972) 405.
[41] K.Takata,"Stability of traveling wave oscillation with arbitrary intensity in ring lasers," *Japan.J.Appl.Phys.* 11 (1972) 699.
[42] P.W.Smith,"Stabilized single-frequency out put from a long ring laser," *IEEE J.Quantum Electron.* QE-4 (1968) 485.
[43] W.W.Rigrod and T.J.Bridges,"Bistable traveling-wave oscillation of ion ring laser," *ibid.* QE-1 (1965) 298.
[44] a. S.N.Bagaev *et al.*"Spectral characteristics of a gas laser with traveling wave," *JETP Letters* 1 (1965) 114.
b. G.Marowsky,"A tunable flashlamp-pumped dye laser of extremely narrow bandwidth," *IEEE J.Quantum Electron.* 9 (1973) 245.
c. R.J.Freiberg *et al.*,"Unidirectional unstable ring lasers," *Appl. Opt.* 12 (1973) 1140.
[45] V.I.Chernen'kii,"Anisotropic optical traveling-wave resonator,"

Soviet J.Quantum Electron. 1 (1972) 472.
[46] B.K.Garside,"Mode spectra in ring and normal lasers," *IEEE J. Quantum Electron.* QE-4 (1968) 940.
[47] T.Miyashita, H.Mori, and J.Ikenoue, "リング・レーザ" における単方向進行波発振の自己同期現象" 量子エレクトロニクス研究会 QE70-52 Feb. 1971.
[48] a. F.Aronowitz and R.J.Collins,"Mode coupling due to back-scattering in a He-Ne traveling-wave ring laser," *Appl.Phys. Letters* 9 (1966) 55.
b. H.de Lang,"Derivation of the relation between two weakly coupled nonlinear optical oscillators," *ibid.* 9 (1966) 205.
c. E.M.Belenov *et al.*,"Interaction of traveling waves in a ring laser," *JETP Letters* 3 (1966) 54.
[49] a. T.Miyashita and J.Ikenoue, "リング・レーザの強制AMモード同期" 電気四学会連合大会 1509 April 1970.
b. ——,"Phase-locking of the internally loss-modulated ring laser," *Japan.J.Appl.Phys.* 9 (1970) 720.
[50] N.Buholz and M.Chodorow,"Acoustic wave amplitude modulation of a multimode ring laser," *IEEE J.Quantum Electron.* QE-3 (1967) 454.
[51] S.I.Wax,"Phase modulation of a ring laser gyro-Part I: Theory," *ibid.* QE-8 (1972) 343.
b. —— and M.Chodorow,"——Part II: Experimental results," *ibid.* QE-8 (1972) 352.
[52] a. T.Miyashita and J.Ikenoue, "強制AM同期によるリング・レーザの単一方向発振" 電子通信学会全国大会 627 Aug. 1970.
b. ——,"Unidirectional oscillation of the internally loss-modulated ring laser," *Japan.J.Appl.Phys.* 9 (1970) 1547.
c. ——, "双方向進行波発振リング・レーザのモード同期現象" 量子エレクトロニクス研究会 QE71-53 Jan. 1972.
[53] a. ——, "リング・レーザの強制AM同期II" 電子通信学会全国大会 759 April 1971.
b. ——, "He-Neリング・レーザの強制AM同期IV" 電気関係学会関西支部連合大会 G10-15 Oct. 1973.

Solid State Lasers and Homogeneous Broadening

Multimode Oscillation

[54] B.J.McMurtry and A.E.Siegman,"Photomixing experiments with a ruby optical maser and a traveling-wave microwave phototube," *Appl.Opt.* 1 (1962) 51.
[55] a. C.L.Tang, H.Statz, and G.DeMars,"Regular spiking and single-mode operation of ruby laser," *Appl.Phys.Letters* 2 (1963) 222.
b. K.Simoda,"Amplitude and frequency variations in ruby optical masers," *Proc. Symposium on Optical Masers* (Polytechnic, New, York, 1963) p.95.
c. C.L.Tang, H.Statz and G.DeMars,"Spectral output and spiking

behavior of solid state laser," *J.Appl.Phys.* 34 (1963) 2289.
d. C.L.Tang *et al.*,"Spectral properties of a single-mode ruby laser: Evidence of homogeneous broadening of the zero-phonon lines in solids," *Phys.Rev.* 136 (1964) A1.
e. V.Evtuhov,"The effect of spatial modulation of pump light on the longitudinal-mode spectra of ruby lasers," *Appl.Phys. Letters* 6 (1965) 141.
f. T.Kimura *et al.*,"Spatial hole-burning effects in a Nd^{3+}:YAG laser," *IEEE J.Quantum Electron.* QE-7 (1971) 225.
[56] S.Singh,R.G.Smith, and M.DiDomenico,Jr.,"Axial modes of a ruby laser with external reflectors," *Proc. IEEE* 53 (1965) 507.
[57] T.Deutch,"Mode-locking effects in an internally modulated ruby laser," *Appl.Phys.Letters* 7 (1965) 80.
[58] W.J.Witteman,"Mode competition in lasers with homogeneous line broadening," *IEEE J.Quantum Electron.* QE-5 (1969) 92.
[59] M.Hercher, M.Young, and C.B.Smoyer,"Traveling-wave ruby laser with a passive optical isolator," *J.Appl.Phys.* 36 (1965) 3351.
[60] a. J.E.Geusic and H.E.D.Scovil,"A unidirectional traveling-wave optical maser," *BellSystem Tech.J.* 41 (1962) 1372.
b. A.L.Mikaeliane *et al.*,"Q-switched unidirectional ring laser," *IEEE J.Quantum Electron.* QE-5 (1969) 617.

Single-Mode (CW) Oscillation
[61] a. M.Hercher,"Single-mode operation of a Q-switched ruby laser," *Appl.Phys.Letters* 7 (1965) 39.
b. D.Roess,"Single-mode operation of a room-temperature cw ruby laser," *ibid.* 8 (1966) 109.
c. H.G.Danielmeyer,"Stabilized efficient single-frequency Nd:YAG laser," *IEEE J.Quantum Electron.* QE-6 (1970) 101.
d. W.Culshaw and J.Kannelaud,"Two-component-mode filters for optimum single-frequency operation of Nd:YAG lasers," *ibid.* QE-7 (1971) 381.
[62] A.L.Mikae'lyan *et al.*,"Single-mode ruby laser with a ring resonator," *Soviet J.Quantum Electron.* 1 (1971) 100.
[63] a. B.L.Zhelnov *et al.*,"Stimulated traveling-wave radiation in lasers," *Soviet Phys. Solid State* 7 (1965) 2816.
b. J.A.White,"Stability of traveling waves in lasers," *Phys.Rev.* 137 (1965) A1651.

Self-Locking (Self-Pulsing)
[64] a. M.DiDomenico,Jr. *et al.*,"Generation of ultrashort optical pulses by mode locking the YAlG:Nd laser," *Appl.Phys. Letters* 8 (1966) 180.
b. A.R.Clobes and M.J.Brinza,"Passive mode locking of a pulsed Nd:YAG laser," *ibid.* 14 (1969) 287.
[65] a. H.W.Mocker and R.J.Collins,"Mode competition and self-locking effects in a Q-switched ruby laser," *ibid.* 7 (1965) 270.
b. A.J.DeMaria, D.A.Stetser,and H.Heynau,"Self-mode-locking of lasers with saturable absorbers," *ibid.* 8 (1966) 174.

c. M.E.Mack,"Mode locking the ruby laser," *IEEE J.Quantum Electron.* QE-4 (1968) 1015.
[66] a. R.Cubeddu *et al.*,"Picosecond pulses, TEM_{00} mode, mode-locked ruby laser," *ibid.* QE-5 (1969) 470.
b. R.Polloni,"Single-transverse-mode mode-locked ruby laser," *ibid.* QE-8 (1972) 428.
[67] a. H.Statz and C.L.Tang,"Phase locking of modes in lasers," *J. Appl.Phys.* 36 (1965) 3923.
b. H.Statz, G.A.DeMars, and C.L.Tang,"Self-locking of modes in lasers," *ibid.* 38 (1967) 2212.
c. C.L.Tang and H.Statz,"Maximum-emission principle and phase locking in multimode lasers," *ibid.* 38 (1967) 2963.
d. H.Statz,"On the condition for self-locking of modes in lasers," *ibid.* 38 (1967) 4648.
e. H.Statz and M.Bass,"Locking in multimode solid-state lasers," *ibid.* 40 (1969) 377.
[68] R.R.Cubeddu and O.Svelto,"Theory of laser self-locking in the presence of host dispersion," *IEEE J.Quantum Electron.* QE-5 (1965) 495.
b. J.T.Boyd,"Threshold for spontaneous mode locking in Q-switched lasers," *ibid.* QE-7 575.
[69] C.L.Tang and H.Statz,"Large-signal effects in self-locked lasers," *J.Appl.Phys.* 39 (1968) 34.
[70] H.Risken and K.Nummedal,"Self-pulsing in lasers," *ibid.* 39 (1968) 4662.

Mode Locking (Pulsation) by Internal Modulation
[71] A.J.DeMaria *et al.*,"Mode locking of a Nd^{3+}-doped glass laser," *Appl.Phys.Letters* 8 (1966) 22.
[72] K.Gürs,"Modulation and mode locking of the continuous ruby laser," *IEEE J.Quantum Electron.* QE-3 (1967) 175.
[73] H.Haken and M.Pauthier,"Nonlinear theory of multimode operation in loss modulated lasers," *ibid.* QE-4 (1968) 454.
[74] T.J.Nelson,"A coupled-mode analysis of mode locking in homogeneously broadened lasers," *ibid.* QE-8 (1972) 29.
[75] a. D.J.Kuizenga and A.E.Siegman,"FM and AM mode locking of the homogeneous laser - Part I: Theory," *ibid.* QE-6 (1970) 694.
b. ———," ——— Part II: Experimental results in a Nd:YAG laser with internal FM modulation," *ibid.* QE-6 (1970) 709.
[76] a. A.E.Siegman and D.J.Kuizenga,"Modulator frequency detuning effects in the FM mode-locked laser," *ibid.* QE-6 (1970) 803.
b. D.J.Kuizenga and A.E.Siegman,"FM-laser operation of the Nd: YAG laser," *ibid.* QE-6 (1970) 673.
[77] J.B.Gunn,"Spectrum and width of mode-locked laser pulses," *ibid.* QE-5 (1969) 513.
[78] a. Y.Cho and Y.Matsuo, "レーザの強制モードロッキング"における非線形性" 量子エレクトロニクス研究会 QE71-57 Feb. 1972.
b. Y.Cho and H.Geffers,"Nonlinear resonance effects in loss-modulated lasers," *Opt. Comm.* 4 (1971) 29.

[79] a. T.Miyashita, Y.Kawata, S.Shinmyo, and J.Ikenoue, "リング・レーザの強制AM同期 III" 電子通信学会全国大会 869 March 1973.
b. T.Miyashita and J.Ikenoue,"High-Peak power and short pulses from a ring laser mode-locked by internal modulation," *IEEE J. Quantum Electron.* QE-10 (1974) March (to be published).
c. T.Miyashita and J.Ikenoue, "強制AM同期によるリング・レーザの単方向進行波発振 — 均一なスペクトルの拡がりの場合 —" 量子エレクトロニクス研究会 QE73-15 July 1973.
[80] a. K.Otsuka, "YAGレーザのモード同期について" 量子エレクトロニクス研究会 QE72-32 July 1972.
b. ————,"Separation of mode-locked states in the intracavity phase-modulated Nd^{3+}:YAG laser," *IEEE J.Quantum Electron.* QE-8 (1972) 496.
[81] M.F.Becker, D.J.Kuizenga, and A.E.Siegman,"Harmonic mode locking of the Nd:YAG laser," *ibid.* QE-8 (1972) 687.

Basic Theory of Locking Phenomena in Conventional Oscillators
[82] a. R.Adler,"A study of locking phenomena in oscillators," *Proc. IRE* 34 (1946) 351.
b. C.C.Cutler,"The regenerative pulse generator," *ibid.* 43 (1955) 140.
c. D.W.Fraser,"Synchronization of oscillators by periodically interrupted waves," *ibid.* 45 (1957) 1256.
d.L.J.Paciorek,"Injection locking of oscillators," *Proc. IEEE* 53 (1965) 1723.

Optical Modulator
[83] T.Uchida,"Direct modulation of gas lasers," *IEEE J.Quantum Electron.* QE-1 (1965) 336.

Scanning Fabry-Perot Interferometer (Optical Spectrum Analyzer)
[84] R.L.Fork *et al.*,"A scanning spherical mirror interferometer for Spectral analysis of laser radiation," *Appl.Opt.* 3 (1964) 1471.

Quantum Theory
[85] a. P.A.M.Dirac,"The principles of quantum mechanics," fourth edition (Oxford University Press, London, 1958).
b. W.H.Louisell,"Radiation and noise in quantum electronics," (McGraw-Hill, New York, 1964).